Design of an Induction Heating Domestic Water Heater and a Device for Scheduling Its Operation

A dissertation in fulfilment
of the requirements of the Masters degree in Technology (Mtech)
in the Faculty of Engineering

of the Cape Peninsula University of Technology

By

Grant Manuel

Supervisor Prof MTE Khan
Degree of confidentiality: none

Declaration

Hereby I, Grant Manuel, declare that this dissertation entitled **"Design of an Induction Heating Domestic Water heater System"** is my own original work and that all sources have been accurately reported and acknowledged, and that this document has not previously in its entirety or in part been submitted at any university in order to obtain an academic qualification.

Grant Manuel

2009/01/29

Design of an Induction Heating Domestic Water Heater System

Grant Manuel

Keywords and phrases

- Crucible
- Geyser management
- High frequency inverter
- Intelligent control
- Induction heating
- Water heating

Abstract

A study was conducted in order to explore means by which the high running cost of water heating may be reduced. This study was divided up into two sections. The first section dealt with how the running cost due to water heaters may be reduced simply by using a suitable control method. A controller was used to switch on and off the water heater. An algorithm was derived in order to determine when an appropriate time to turn off the geyser was. The algorithm consisted of two parts, termed static and dynamic factors, static factors being the influences that do not change and dynamic factors being the influence that is subjected most frequently to change. These two instances were solved using Fuzzy logic and crisp set theory. Test were conducted in order to investigate whether adequate control of the geyser would result in an energy saving. It is methods such as this that is necessary to reduce peak period demand. Test result showed that there was a significant reduction with regards to running cost when the algorithm together with the controller was used to control the geyser.

The second part of the study investigated an alternative water heating method. One by which water may be heated by means of the process of induction heating. The paper discusses how an optimum induction heating model for the purposes of induction heating may be developed. The operation of this process starts with the incoming 220V single phase 50Hz supply found in most domestic homes is transformed into a high frequency in the order of 20kHz. This high frequency is used to induce current in a crucible that is directly immersed into water. The crucible will begin to heat up due to the resistivity of the material opposition to this induced current. Heat would be produced rather rapidly and will cause the water to heat up as well. Test using this method showed that this method had not been much more effective than existing water heating methods using resistive elements. However this form of water heating would be more advisable in large plants where large capacities of heated water would be required. This method could also be used in the heating up of corrosive fluids. With efficient inverter topologies and low loss switching devices, currently not available, it would be possible in the future to have induction water heating methods match the efficacy of existing electric water heating methods.

Final recommendations were made on cost effective methods by which the high running cost of water heaters may be reduced.

LIST OF ILLUSTRATIONS

FIGURE 1-1 GEYSER THERMOSTAT 2
FIGURE 1-2: THE RIPPLE SIGNAL GENERATOR INSTALLED IN A SUBSTATION (LJ GROBLER & C.A. VAN DER MERWE, 2004) 6
FIGURE 1-3 RESISTIVE ELEMENTS 7
FIGURE 1-4: SOLAR POWERED WATER HEATER 11
FIGURE 3-1: MACRO LEVEL CONTROL IMPLEMENTED BY THE SUPPLY AUTHORITY 16
FIGURE 3-2: FLOW METER INSTALLED TO MEASURE LIQUID FLOW FROM A STORAGE TANK 18
FIGURE 3-3: BLOCK DIAGRAM OF A SUCCESSIVE APPROXIMATION ADC (TL FLOYD, 1997, PG 670) 20
FIGURE 3-4: TSUNAMI MP11 BSU/SU (PROXIM WIRELESS, 2007, [PG 1]) 22
FIGURE 3-5: BSU/SU COMMUNICATION (PROXIM WIRELESS, 2007, [PG 65]) 22
FIGURE 3-6: (A) SOLID STATE RELAY (B) ELECTRICAL CONTACTOR 23
FIGURE 3-7: (A) AVERAGE WEEKDAY GEYSER DEMAND PROFILE 25
FIGURE 3-8 CRISP AND FUZZY SET THEORY EXAMPLE (J JANTZEN, 2006, PG 5) 27
FIGURE 3-9: EXAMPLE OF A CRISP/FUZZY SET ALGORITHIM 27
FIGURE 3-10 MICRO LEVEL GEYSER MANAGEMENT SYSTEM CONTROL ALGORITHM 28
FIGURE 3-11: AN MPC (MULTI PURPOSE CONTROLLER) USED TO CONTROL A GEYSER 29
FIGURE 3-12 GRAPHICAL USER INTERFACE FOR THE GEYSER MANAGEMENT SYSTEM 29
FIGURE 3-13 WEEKDAY GEYSER ON TIME (DAY 1) 31
FIGURE 3-14 WEEKDAY GEYSER ON TIME (DAY 2) 31
FIGURE 3-15 GEYSER MANAGEMENT SYSTEM (DAY 1) 32
FIGURE 3-16 GEYSER MANAGEMENT SYSTEM (DAY 2) 32
FIGURE 4-1: SEQUENCE OF TRANSFORMATION (H MILEAF, 1999, P 97) 34
FIGURE 4-2: SKIN EFFECT 36
FIGURE 4-3: SQUARE WAVE CONSISTING OF MULTIPLE SINE WAVES 36
FIGURE 4-4: RF POWER SUPPLY CIRCUIT 39
FIGURE 4-5: INVERTER TOPOLOGIES (I KHAN, 2000, P 19) 40
FIGURE 4-6 VOLTAGE FED FULL BRIDGE INVERTER 42
FIGURE 4-7: LOW SIDE (A) AND HIGH SIDE (B) SWITCHES 43
FIGURE 4-8: FAST FOURIER ANALYSIS OF A VOLTAGE FED FULL BRIDGE INVERTER 44
FIGURE 4-9: SIMULATED WAVE FORM OF AN H-BRIDGE INVERTER 45
FIGURE 4-10: SWITCHING LOSSES OF SOLID STATE SWITCHES 46
FIGURE 4-11: FREQUENCY AND OUTPUT POWER COMPARISONS OF HIGH SPEED DEVICES (MOHAN, UNDERLAND & ROBBINS, 2003, P27) 47
FIGURE 4-12: CONSTRUCTION OF AN N CHANNEL IGBT (J DODGE, 2002) 48
FIGURE 4-13: HELICAL SPRING TYPE COIL 53
FIGURE 4-14: FLAT TYPE COIL 54
FIGURE 5-1 B-H CURVE FOR IRON AND STEEL 58
FIGURE 6-1: SINGLE AND THREE PHASE VARIABLE TRANSFORMERS 61
FIGURE 6-2 PI TYPE FILTER 64
FIGURE 6-3 SIMPLE SINGLE PHASE RECTIFIER 64
FIGURE 6-4 OUTPUT WAVE FORM (VOLTAGE) OF A SINGLE PHASE RECTIFIER 65
FIGURE 6-5 THREE PHASE BRIDGE RECTIFIER 66
FIGURE 6-6 OUTPUT WAVE FORM (VOLTAGE) OF A THREE PHASE RECTIFIER 66
FIGURE 6-7 CAPACITOR BANK USED TO DECREASE THE RIPPLE VOLTAGE 69
FIGURE 6-8 RECTIFIER STAGE TESTING: RIPPLE VOLTAGE 70
FIGURE 6-9: H BRIDGE CIRCUIT USING TWO IR2110 DRIVERS 72
FIGURE 6-10: THE SEMIKRON STACK INVERTER 72
FIGURE 6-11 SKM100GB123D IGBT MODULES (SEMIKRON, 2005) 73
FIGURE 6-12: HYBRID DUAL MOSFET/IGBT DRIVER (SEMIKRON, 2006, PG 5/6) 74
FIGURE 6-13: ILLUSTRATION OF A SKHI 61 SEMIKRON STACK 76
FIGURE 6-14 STAINLESS STEEL CRUCIBLE 77
FIGURE 6-15 METAL CRUCIBLE WITH COIL AND INSULATION 77
FIGURE 6-16: COIL MEASURED USING A HEWLETT PACKARD LCR MATER 79

FIGURE 6-17 FFT SIMULATION RESULTS OF SERIES TANK CIRCUIT 80
FIGURE 6-18 POWER SIMULATION WAVEFORMS OF TANK CIRCUIT 80
FIGURE 6-19: OUTLAY OF CONTROLLER BOARD 81
FIGURE 6-20: PWM SIGNAL 82
FIGURE 6-21 GUI OF CONTROLLER 83
FIGURE 7-1 BOILING KETTLE TEST 1(2KW) 87
FIGURE 7-2 BOILING KETTLE TEST 2 (2KW) 87
FIGURE 7-3 BOILING KETTLE TEST 1/2/3/AVG (2KW) 88
FIGURE 7-4 BOILING WATER TEST 1 (3KW ELEMENT) 88
FIGURE 7-5 BOILING WATER TEST 1/2/3/AVG (3KW ELEMENT) 89
FIGURE 7-6: RESISTOR LOAD TESTING OF THE SKHI 22A SEMIKRON STACK INVERTER USING A SINGLE PHASE SUPPLY 90
FIGURE 7-7: RESISTOR LOAD TESTING OF THE SKHI 61 SEMIKRON STACK INVERTER USING A SINGLE PHASE SUPPLY 90
FIGURE 7-8 RESISTOR UNDER TEST 91
FIGURE 7-9 PWM MEASURED ACROSS LOAD RESISTOR 91
FIGURE 7-10 COIL USED TO HEAT A COKE CAN 93
FIGURE 7-11 FFT ANALYSIS CONDUCTED ON NEW "ELEMENT" 93
FIGURE 7-12 FFT ANALYSIS CONDUCTED ON NEW "ELEMENT" USING SCMI MEASURING SOFTWARE 94
FIGURE 7-13 OUTPUT WAVE FORM ACROSS THE LOAD WHEN NOT AT RESONANCE 94
FIGURE 7-14 IWH TEST 1 95
FIGURE 7-15 IWH AVERAGE TEST RESULTS OF FOUR TEST CONDUCTED 95

LIST OF TABLES

TABLE 1-1 RESULTS OF THE ETU GEYSER BLANKET RESEARCH PROJECT (A HARRIS, M KILFOIL AND E-A UKEN, 2008, PG 141) 5
TABLE 5-1 SPECIFIC HEAT CAPACITIES OF MATERIALS (ENGINEERINGTOOLBOX, 2008) 56
TABLE 5-2 PERMEABILITY OF MATERIALS TABLE 5-3: MATERIAL RESISTIVITY 56
TABLE 7-1 TEST RESULT SUMMARY 96

List of Abbreviations

A	Amps
ADC	analogue to digital converter
BJT	bipolar junction transistor
°C	degrees Celsius
DAC	digital to analogue converter
DSM	demand side management
ESR	equivalent series resistance
FET	field effect transistor
FFT	fast Fourier transforms
GUI	graphical user interface
IH	Induction heating
IWH	induction water heater
J	Joules
V	Volts
MSB	most significant bit
PIV	Peak inverse voltage
LSB	least significant bit
W	Watts
HWC	Hot water cylinder
l	litres

Table of Contents

Chapter 1 Problem analysis ____ *1*

1.1 The Geyser Control ____ 1

1.2 Resistive Elements ____ 6

1.3 Evaluating Current Trends Aimed At Reducing High Energy Consumption Caused By Geysers ____ 9

1.4 Summary of the Problem Analysis ____ 11

Chapter 2 Introduction to the Research Study ____ *12*

2.1 Intelligent Load Control ____ 12

2.2 Water Heating By Means of Induction Heating ____ 12

2.3 Research Methodology ____ 13

2.4 Research Objectives and Scope ____ 14

Chapter 3 Geyser Load Control ____ *16*

3.1 Introduction ____ 16

3.2 Macro Level Geyser Management System ____ 17

3.2.1 Gathering Information about the Consumer ____ 17

A) Flow Measurement ____ 17

B) Temperature Measurement ____ 18

C) Analogue to Digital Conversion ____ 19

D) Smart Sensors ____ 21

3.2.2 The Communication Medium ____ 21

3.2.3 Control Hardware ____ 23

3.2.4 Factoring In Static and Dynamic Factors within an Algorithm ____ 24

3.3 Micro Level Geyser Management System ____ 28

3.3.1 Derivation of the Smart Algorithm ____ 28

3.3.2 Hardware ____ 29

3.3.3 Testing ____ 30

Chapter 4 Induction Heating ____ *33*

4.1 Introduction to Induction Heating ____ 33

4.2 Skin Effect ____ 35

4.3 The Fundamental Frequency ____ 36

4.4 Power Supplies ____ 37

4.4.1 The full bridge Rectifier and filter circuit ____ 41

4.4.2 The Full Bridge Inverter ____ 42

4.5 High Speed Switching ____ 45

4.6 Efficiency Calculations (Factors affecting the concept design) ____ 49

4.6.1 Coupling Efficiency ____ 49

4.6.2 Electrical efficiency ____ 50

4.7 Tank Circuits ____ 51

4.8 Coil Design ____ 53

4.8.1 Helical spring type ____ 53

4.8.2 Flat type ____ 54

Chapter 5 Crucible Properties and Water Heating Principles 55
5.1 Comparing Metals 55
5.2 Permeability and Resistivity of Metals 57
5.3 Thermal Conductivity 58
5.4 Principles of Water Heating 59
Chapter 6 System Design 61
6.1 Introduction 61
6.2 Step down Transformer 61
6.3 Rectification 62
6.3.1 Single Phase Rectifier 62
6.3.2 Three Phase Rectifier 65
6.3.3 Practical Build of a Rectifier 67
6.4 Inverter Overview 70
6.4.1 The H Bridge Inverter Based Upon the IR2110 Driver 71
6.4.2 The H Bridge Inverter Based Upon the SKHI 22A Driver 72
6.4.3 The H Bridge Inverter Based Upon the SKHI 61 Drivers 76
6.5 The Element Design 77
6.6 Tank Topology 79
6.7 Control Board Design 81
6.8 Temperature Sensing and Data Logging 83
Chapter 7 Testing and Conclusion 85
7.1 Resistive Element Testing 85
7.2 Inverter and Crucible Testing 90
7.2.1 Inverter Testing Using a Resistive Load 90
7.2.2 Inverter Testing Using an LC Tank Circuit 92
7.3 Induction Water Heater Testing 95
7.4 Conclusion/Recommendation 97
References 98

Appendices A: IR211A application note
Appendices B: Controller Board schèmatic
Appendices C: SKPC PCB by Semikron
Appendices D: SKHI21A module data sheet
Appendices E: SKHI 61
Appendices F: SMT16030 digital temperature sensor
Appendices G: CD4504B Cmos hex level shifter

Acknowledgements

The author would like to thank the following people and organisations for there support.

Firstly, my family for there support. My parents Peter George and Rosalind Manuel. Special thanks also go out to my brothers Peter John and Theodore Manuel for always being there. My grandparents, Isaacs and Manuel family.

The staff at the Stanley group (Blick SA). The directors and managers, especially Leslie Steenkamp, John Powell, Marius Heydeman, Jeff Muvango, Peter Moloi, Francois van de Berg, service and projects teams.

A special thanks to my supervisor, Prof MTE Khan from whom I have learnt great many things. His research assistant Fizzel, who have assisted me in this project.

The congregation at Good Hope Christian centre (Ottery) and AFM (Athlone). Chris, in the machines lab at the University of Cape Town. Thank you for all your help.

The institutions that have all equipped me this far with an abundance of knowledge, namely:

- Westlake Technical College (N1-N3)
- Western Province Technical College (N4-N6)
- Cape Technikon (S1-S4, Btech)
- Cape Peninsula University of Technology (Mtech)
- South African Institute of Electrical Engineers

The following professionals for their contribution:

Prof Uken (DUE conference)

Prof Beute (DUE conference)

The following publishers:

Crown publications

EEpublishers

Chapter 1 Problem analysis

Heated water is regarded as an essential in the domestic home for the purpose of cooking, cleaning and washing. In South Africa the most common form of water heating is by means of an electrical element immersed in a storage tank being controlled by a thermostat. Electric water heating is more preferential in South Africa because the country lacks a distribution network for the distribution of natural gas. Water heating by means of a combustible gas is preferred in many other countries that have a distribution network since this kind of water heating proves to be cheaper than the alternative resistive element heating. Local water heating by means of gas is done by means of gas storage tanks. The liability is that the consumer suffers the inconvenience of having to disconnect the storage tank refill the tank and reconnect the tank. Instantaneous water heaters have also been introduced recently to the market. But many consumers still view instantaneous water heaters as a novelty. Both electrical suppliers and consumers have realised the high cost of electric storage heaters, commonly referred to as geysers and many have undertaken to try and reduce the high running cost. A number of factors contribute to the high running cost of geysers, one of which is the geyser control mechanism found in most homes.

1.1 The Geyser Control

Common geyser control mechanisms are thermostats which consist of a metal rod which expands when heated and opens a set of contacts once a set temperature has been reached. This simple control mechanism does present a problem. The metal rod cools down as the water cools down and therefore the contacts close, connecting the electric element to the source (fig1-1). This commits the geyser to an endless cycle of heating and cooling and reheating once the temperature in the tank reaches a certain lower temperature. During weekday business hours, many house occupants are not at home and therefore hot water is not required during this time. Municipalities have attempted to solve this problem by means of ripple control. The consumer's supply to the geyser is connected to a special controller that receives a signal to turn off and on the consumer's geysers.

This is usually done in groups where municipalities would shut down a certain amount of geysers for a specified time. In the past, carefully constructed algorithms were used to determine the appropriate time to switch on and off a group of consumer geysers. The object is to be able to control a group of geysers with emphasis on placing minimum liability on the consumer. The problem is that it is not always possible to consider the needs of the individual consumer over the needs of a group of consumers.

Another problem mentioned prior was the problem of cooling taking place inside the storage tank which forces the thermostat to switch on the element in order to reheat the water. The water inside the tank cools down due to a phenomenon best described by the laws of thermodynamics. A body strives to be in thermal equilibrium with its environment that it finds itself within. Ice caps melt as it moves away from the poles due to the fact that the surrounding environment is at a higher temperature.

Most geysers are found inside the roof spaces of houses. At night, the ambient temperature outside the storage tank is much lower than the temperature of the water found inside the tank and because of this, there is a loss of thermal energy or heat loss. During the day, the temperature inside the roof is higher and therefore heat loss is lower during the day. Heat loss as it relates to geysers is referred to as Q_{losses}.

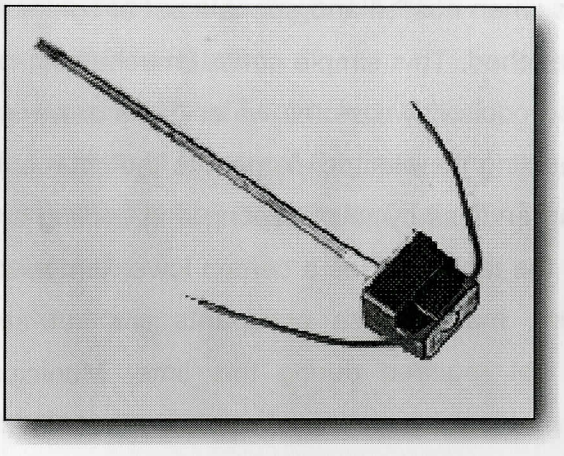


Figure 1-1 Geyser Thermostat

Q_{losses} may be calculated by taking into account the dimensions of the storage tank. This is calculated by the following formulae (B F Grobbelaar & J Wheeler, 2006, pg 100):

$$Q_{losses} = \frac{T_h - T_{ambient}}{\frac{\Delta x}{k} - \frac{1}{h}} \qquad (1\text{-}1)$$

Where:

Q_{losses} *: Heat loss in W/m²*

T_h *: The water temperature inside the cylinder in °C*

$T_{ambient}$ *: Air temperature outside the cylinder in °C*

Δx = thickness of insulation layer in m

k = thermal conductivity in W/m.K

h = surface heat transfer coefficient in W/m2.K

A paper presented at the international conference for the domestic use of energy, Mr GJ Delport (2005) presented the following data that may be used in order to calculate heat loss. The calculations were conducted using the following assumptions:

- The cost of electricity 35c/kwh
- A horizontal type 150 litre cylinder was used

Losses were calculated as follows:

Losses (70 °C) = heat loss (W/m²) x Area of cylinder x hours in a day
= 62.89 x 1.677 x 24
=2.531 kWh

For 58 °C = heat loss (W/m²) x Area of cylinder x hours in a day
= 47.79 x 1.677 x 24
=1.924 kWh

It can be concluded by evaluating the previous formulae that a lower temperature setting on the geyser control mechanism would result in less heat loss and therefore less power being used since the geyser commits to fewer reheating cycles. Hence better utilisation of power. Electrical suppliers have suggested that consumers lower the temperature settings on thermostats in order to save energy and reduce cost. Here the responsibility of saving energy rest upon the consumer. Another method to reduce heat loss as suggested by the countries main supplier of electricity, namely Eskom, is the use of thermal insulation. By encapsulating a geyser in thermal insulation, heat loss is reduced. A major initiative was implemented by Eskom under the DSM (demand side management) program, where consumer geysers were fitted with geyser blankets. This project was referred to as the Geezer duvet program and was met with great success.

Test conducted by the Energy Technology Unit (ETU), shows typical energy savings that may be expected when insulating geysers and water distribution pipes. What was also observed was that a significant amount of energy was saved with the utilization of lagging pipes. However, this also increased the cut in time. The ideal energy saving result of around 27% was achieved when using lagging pipes and a geyser blanket. Methods such as these may lead to heat losses reduction of up to 53% (J Delport, 2005, pg 139).

The solutions mentioned beforehand can be divided into solutions that may be implemented by the consumer to reduce cost or by the supplier to save energy. Suppliers target loads brought on by the domestic sector since it is this sector that is responsible for the highest percentage of peak period demand. Ripple control is preferential with emphasis on the supplier since load control may be done in such a manner that the peak period demand is reduced.

Table 1-1 Results of the ETU Geyser Blanket Research Project (A Harris, M Kilfoil and E-A Uken, 2008, Pg 141)

	No lagging	Pipes lagged	Geyser covered	GB + pipes lagged
Standing losses (kWh/day)	2.3	2.0	1.8	1.68
Savings %	N/A	13.04	21.74	26.97
Cut-in time hh:mm:ss	06:14:20	07:20:39	08:12:59	09:22:11

An example of where a supplier/distributor such as Eskom and the municipality intervene in order to save energy resources would be the use of ripple signal generators. This is a common form of geyser control adopted by many distributors and is preferred because it gives the supplier control over the consumer load during peak period demands. Especially the residential load. This technology was used in earlier years for the control of street lighting.

An example of the implementation of ripple control would be by the Breede Valley municipality where the highest implementation of ripple voltage (66kv) may be found (LJ Grobler & C.A. Van de Merwe, 2004). Here switch off times were established by means of a fuzzy logic algorithm which accounted for factors such as the quantity of consumer geysers and the time of day.

Thus far solutions aimed at reducing the running cost of geysers were mainly aimed at the inadequate control of current thermostats and heat loss. None of these widely used solutions were aimed at evaluating the type of heating topology used.

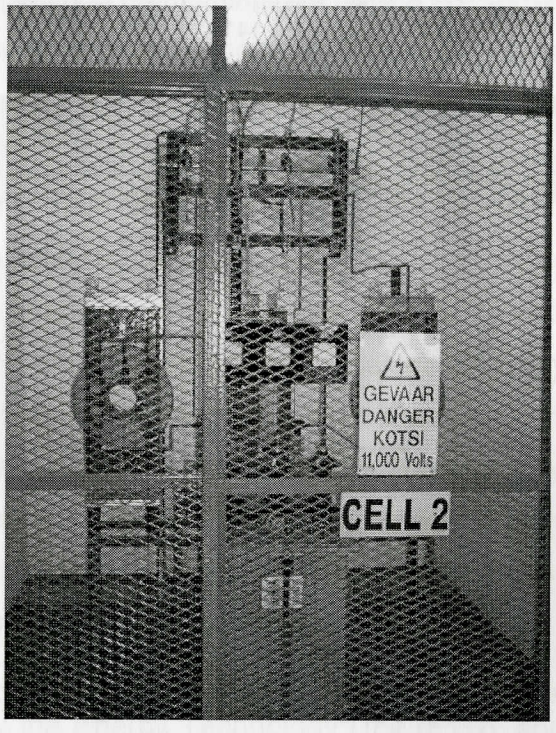


Figure 1-2: The Ripple Signal Generator Installed In a Substation (LJ Grobler & C.A. Van Der Merwe, 2004)

1.2 Resistive Elements

Resistive elements are relatively simple devices consisting of a resistive tube inserted within a thin metal sheath or tube. The connecting terminals protrude out of hexagonal fixture used to connect the element to its source (fig 1-3). This kind of element was immersed directly in water and therefore heat loss is minimised because the heating element had direct contact with the end substance. In electric stoves, heat losses occur because the heat has first to be transferred to the metal that the pot is made out of and then the contents of the pot. Resistive elements are cheap devices and are sold locally at around R90.00 ($12.00). Thermostats cost around R60.00 ($8.00). If losses were ignored, the power dissipated by the resistive element would equal the equivalent heat energy produced. This is calculated according to the following:

$$P = I \cdot V \qquad (1\text{-}2)$$

Or alternatively:

$$P = I^2 \cdot R \qquad (1\text{-}3)$$

The total resistance of a resistive element is calculated by taking into account the area of the resistive tube, length and resistivity of the material used. This may be calculated by using the following equation (standard formulae for resistivity):

$$R = \frac{\rho l}{A} \qquad (1\text{-}4)$$

Where:

R: total resistance (Ω)

ρ *: Resistivity of the material (Ω)*

l : Length (m)

A *: Area* (m^2)

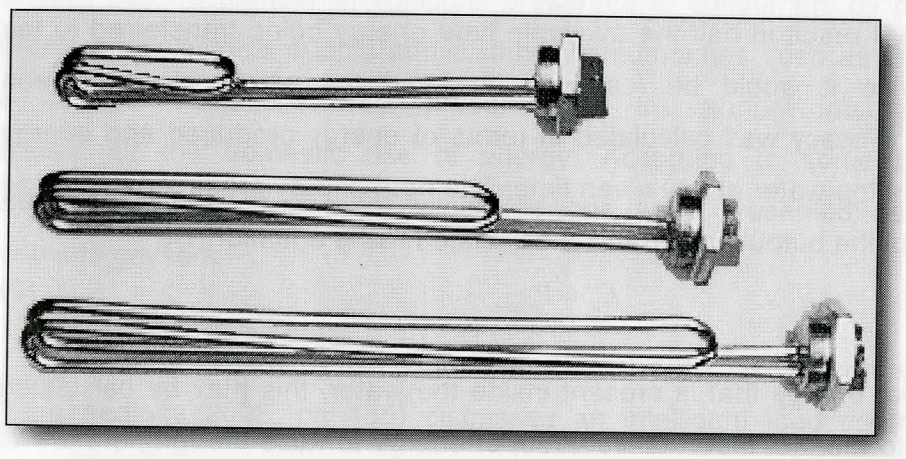


Figure 1-3 Resistive Elements

The total resistance of an element has direct bearing on the total power used and hence electrical power converted to heat energy. This is proven by combining equation 1-3 and 1-4.

$$P = I^2 \cdot \frac{\rho l}{A} \qquad (1\text{-}5)$$

In terms of energy, the general formula is formulated as follows:

$$E = Pt \qquad (1\text{-}6)$$

Where:

E = Energy (given in joules)

t = time (in seconds)

The main concern of this study was not feasibility but rather efficiency and efficacy. Resistive elements can be measured according to these descriptions and therefore it is important to be able to define these terms. Efficiency may be described as the total amount of power that is the resultant after a process whereby power is inserted. This is formulated by:

$$\eta = \frac{P_{out}}{P_{in}} \qquad (1\text{-}7)$$

$$P_{out} = P_{in} - losses \qquad (1\text{-}8)$$

$$\eta = \frac{P_{out}}{P_{in}} \qquad (1\text{-}9)$$

Efficacy relates to how much of this output power is effectively converted to do work, which in this case is heat. An element that is immersed half way into the water will result in half the available heat energy being transferred to the water. Hence it would be less effective had the whole element been immersed. Efficacy was calculated in terms of energy produced and energy found inside the water at any given time. The heat energy produced serves as a function of the output power and is calculated using equation 1-6.

$$E_o = P_{output} \cdot t \qquad (1\text{-}10)$$

For the heat energy that is present inside the water, this may be calculated according to the fact that it takes 4180j of energy to raise the temperature of water by one degree.

Example on calculating the efficacy of an element:

If it took 10 minutes to boil 1.2l of water from an initial room temperature of 25°C using a 5kw resistive element, the *efficacy* would be calculated by:
(Using equation 1-10 to calculate)

$$t = 10 \times 60 = 600s$$

$$E_o = 5000 \times 600\, j = 3000kj$$

The boiling temperature of water is 100°C. Therefore the change in temperature would be calculated by:

$$\Delta c = 100°C - 25°C$$

$$= 75$$

The equivalent heat energy found within the storage tank would therefore be:

$$E_{tank} = 4180 * 75$$

$$= 313.5kj$$

Therefore the efficacy of the process would be:

$$\eta = \frac{E_{tank}}{E_o} = 313.5/3000 = 10.45\%$$

In this manner the efficacy may be calculated.

1.3 Evaluating Current Trends Aimed At Reducing High Energy Consumption Caused By Geysers

There have been a number of solutions presented to consumers by private institutions and electrical supply and distribution authorities such as Eskom. Some of these solutions were presented at the annual international conference for the domestic use of energy. According to some of the conference proceedings, the following solutions were presented as it is applicable to geysers.

- A paper presented by PA Gouws and Ho Hanger (DUE conference proceedings 2008, pg 135) discusses an intelligent load control by means of Demandwise. A device used to switch off the consumers geyser during peak periods of the day and maintains a constant water temperature of 40°C during the day. The device would activate the geyser before the time that hot water was required. This paper did not present an in depth evaluation of determining the time when hot water was required. However it did make the conclusion that a total average energy saving of 5% was achievable. This paper reiterates the fact that running cost may be reduced significantly if the geyser was controlled in a more adequate method in comparison with existing methods.

- Another paper presented at the DUE conference by A Harris, M Kilfoil and E-A Uken under a paper entitled "Options for residential water heating", concluded that the only way that cost may be reduced due to water heating inside the home, was if less water was used or heat loss was reduced. A number of solutions were introduced by these authors, of which one solution included a dual element system. A dual element system consisted of two heating elements in a single apparatus. One element was controlled by a thermostat set to be five degrees higher than the other. When the hot water was used, the element with the higher set temperature would go into operation. When the water inside the tank reached approximately eight litres, the second element would operate. This type of heating method reduced the maximum demand and resulted in a minimum energy saving of 40kWh per month per consumer. Further recommendations included the use of digital thermostats. This was because many times these devices had added features which included the following

I. Loss of water from the HWC to the point of consumption as a result of leaks
II. Defective resistive heating elements
III. Faulty metering (energy metering systems)
IV. Earth leakages

Solar energy is preferred by many since it takes the load off the supplier and presents consumers with low maintenance and minimum running cost. South Africa receives a very high amount of annual solar energy. This clean source of energy carries the burden of having a very high cost of installation. This is due to expensive solar panels and inverters. Manufacturers of these devices have tried to justify the short term cost matched against the long term savings. A saving of up to 70% can be the resultant of using solar energy. There are two types of solar water heaters. The first is the passive type which uses gravity or rather the relative position of the storage tank in order to circulate water. The second is the active type which requires a pump to circulate water.



Figure 1-4: Solar Powered Water Heater

The operation of a solar water heater follows that solar radiation is gathered by means of a solar collector which converts this energy to heat which in turn is used to heat water. A problem experienced by many consumers was that during days of very little sun shine, there may not be enough heated water available. Thus far water heating by means of solar energy has not received significant credit. This was due to financial, technical and political reasons (A Harris, M Kilfoil and E-A Uken, 2008, pg 141).

1.4 Summary of the Problem Analysis

Two problems were identified thus far by independent consultants and energy suppliers. The first was the inadequate setup of the geyser controls. The solutions that were discussed involved controlling the geyser in a more intelligent manner. The second problem was heat loss. An ideal solution may preside in a heating topology that consists of the following:

- An intelligent control device or smart controller that places minimum liability on the consumer and supplier

- The utilisation of smart element designs such as the dual element

Chapter 2 Introduction to the Research Study

It was previously suggested how the running cost of water heating may be reduced if more controllable heating topologies were evaluated and better control methods were utilised. This study was divided into two sections. The first was developing an adequate control mechanism that may be used to control the geyser. The second was to explore what may be a water heating alternative, namely water heating by means of induction heating.

2.1 Intelligent Load Control

Controlling a geyser is seamlessly achievable by means of low cost solid state relays or contactors. What may not seem as seamless, is the appropriate time to switch on or off a geyser. From a supplier or electrical distributor point of view, it is easier to control geysers in large groups rather than individual consumers. Electrical suppliers control geysers in such a way as to reduce maximum peak period demand. This objective is different to the consumers objective. The consumer wants to save money by not having to utilise electricity when it is not needed. It becomes difficult to satisfy the objectives of both the supplier and consumer and still take into account factors such as heat loss, time of the day and time of the year. The first part of the study only evaluated how the consumer may control his own hot water load through cleverly formulated algorithms and controllers. Some of the hardware needed was also studied such as temperature sensors which are vital in controlling geysers.

2.2 Water Heating By Means of Induction Heating

A few chose to explore other avenues of water heating other than by means of resistive elements. This is because many assume that this form of water heating may be the most efficient and effective kind there is. Many justify the short term cost and not the long term cost of geyser elements and thermostats. This study was aimed at finding an alternative form of water heating, where the long term cost savings derived from more effective use of energy would justify the high short term cost. Other forms of heating methods that were evaluated briefly included the following:

- Plasma Heating
- Conduction Heating
- Induction heating
- Electric Arc Heating
- Infrared Radiation Heating
- Dielectric Hysteresis Heating
- Electron Beam Heating

Not all these methods were appropriate for heating water. Induction heating was chosen primarily because this method of heating was not new to the domestic home. Induction heating was used in the home before, for the purposes of cooking. Induction heating is a fast, localised and effective form of heating. This study investigated the energy saving potential that this heating method may have if introduced in the home as a water heating method.

2.3 Research Methodology

For the intelligent load control part of the study, formulating an algorithm was done using data loggers to obtain an idea of consumer habits with regards to hot water consumption. Then various mathematical methods were investigated which were capable of dynamically controlling the hot water load based upon highly dynamic variables. Finally the hardware was designed. The aim was to introduce a method by which only the consumer may control his hot water energy consumption. But this did not hamper the study from exploring how a supply authority may also use a dynamic algorithm to control groups of consumer geysers. When a supply authority control geysers from a central point, the communication infrastructure needed to achieve this must also be evaluated. With regards to the second part of the study, the principles surrounding induction heating were first investigated. Research materials included journals, accredited published papers and informal discussions with induction heating furnace manufacturers. This study was conducted at the Cape Peninsula University of Technology, were a prototype induction heating furnace for purposes of metal smelting was built before by Mr Irshaad Khan.

In the earlier stages of this project, many of Mr Khan's previous designs were used.

Progress and findings were show cased in various publications and international conferences which included the following:

- A publication in the Quantum journal, Aug 2007, page 5. The title of this publication was "New technology for domestic water heating"
- A publication inside the Energize, March 2008, page 52. The title of this publication was "Intelligent load control using crisp and fuzzy set algorithms"
- A publication inside the Vector, April 2008, page 69. The title of this publication was "Intelligent load control using crisp and fuzzy set algorithms"
- Conference proceedings of the domestic use of energy conference held at the Eastern blvd hotel (2008). The title of this presentation was *load control based upon fuzzy and crisp set theory.*
- Proceedings of the industrial and commercial use of energy conference held at the Mount Nelson hotel (2008). The title of this presentation was "*The design of an induction heating based water heater system*".

The essential part of an induction heater was the RF or high frequency power supply which was built using simulation models based upon software packages such as Psim. Test equipment included spectrum analysers, oscilloscopes, temperature data loggers and pc based software tools.

2.4 Research Objectives and Scope

The research study had two focal areas and hence the objectives and scope of this project were divided amongst the two studies. These were:

a) Geyser control

The main objective here was to formulate a control method which was capable of controlling any load, especially the load that stems from water heating in such a way that energy is not used by the system when it was not required. Another requirement was that the consumer did not suffer any form of liability due to control of the geyser unit. The target for this form of control

was on a micro level, meaning one or very few consumers, although macro (many consumers) level was also investigated.

b) Induction water heater (IWH)

This part of the project involved the design of an induction heater and tank circuit which was modelled to take the form of a new type of heating element. The objective was to build and test a high frequency power supply, design an element and heat water to a temperature of 60°C. A conclusion would be based upon comparative test conducted between the conventional water heating method and the proposed one. The comparison was done according to efficiency and efficacy and not necessarily financial or production feasibility.

Chapter 3 Geyser Load Control

3.1 Introduction

The strategy for which a load control algorithm is developed is influenced greatly by the amount and type of consumers that would be affected by it, programmable timers and controllers which have been termed in the past as geyser gadgets impact the individual consumer (Calmeyer JE and Britz EA, 2005). This form of control is referred to as micro load management, since only the individual is being affected. The consumer knows when he will be requiring hot water and therefore micro level control is easily implemented because no high level algorithms are necessary to control the load. However this is not the case with macro level load control which is usually the kind implemented by municipalities and distributors of electrical power. Ripple control is an example of how a supply authority controls the consumption of many consumers (Fig 3.1). Macro level control is not easily implemented because the needs of the individual consumer is disregarded for purposes of fulfilling the needs of a group of consumers. Another aspect of macro level control is the communication medium in which the control is done. Ripple control uses the consumer's source voltage to carry a signal used to control the geyser. The problem with this is that this form of communication medium only allows for one way information, from the supplier to the consumer only. A two way communication medium allows communication to take place between the supplier to the consumer and visa versa.

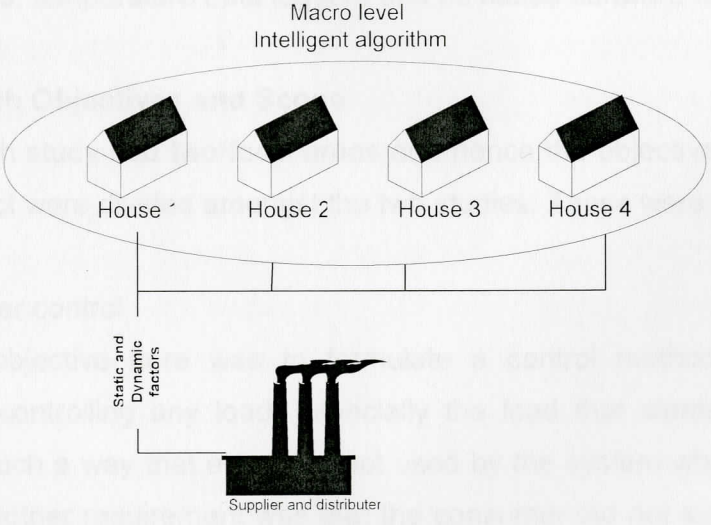


Figure 3-1: Macro Level Control Implemented By the Supply Authority

Two way communications allows the supplier to perfect his load control methods by gathering information about the consumer. Such as the appropriate time to switch off a group of consumers. Two forms of geyser management systems were investigated during the course of this study. The first was a practical micro level geyser management system and the second was a theoretical model for a macro level geyser management system which may be implemented by a supply authority.

3.2 Macro Level Geyser Management System

3.2.1 Gathering Information about the Consumer

Programmable timers and controllers may not be adequate to be implemented on a macro level simply because they do not take into account the ever changing needs of the consumer on a day to day basis. Before the supply authority controls the load of many consumers, he needs to acquire knowledge about the consumer's use of that load. Primarily the supplier needs to take into account when the geyser is being used regularly and at what temperature is hot water required. For a large group of consumers, a sample may be used to represent the majority consumers. Of course the greater the amount of samples, the more accurate the data. The time of use of a geyser represents a dynamic factor because this is an ever changing boundary. The temperature at which water is required represents less of a dynamic factor and may be referred to as a static factor. The required temperature of heated water is expected to be around 60°C. The information with regards to the use of hot water may be gathered using flow meters and for the temperature requirement, temperature sensors may be used.

A) Flow Measurement

Liquid flow is used to measure the amount of water taken from the storage tank. Water flows from the storage tank by means of distribution tanks whenever it is required and therefore by measuring the volume extracted from the tank, information pertaining to how much water was used and at what time it was used, may be gathered. Volume flow rate can be measured using various flow measurement techniques which include the following (A.S Morris, pg 321):

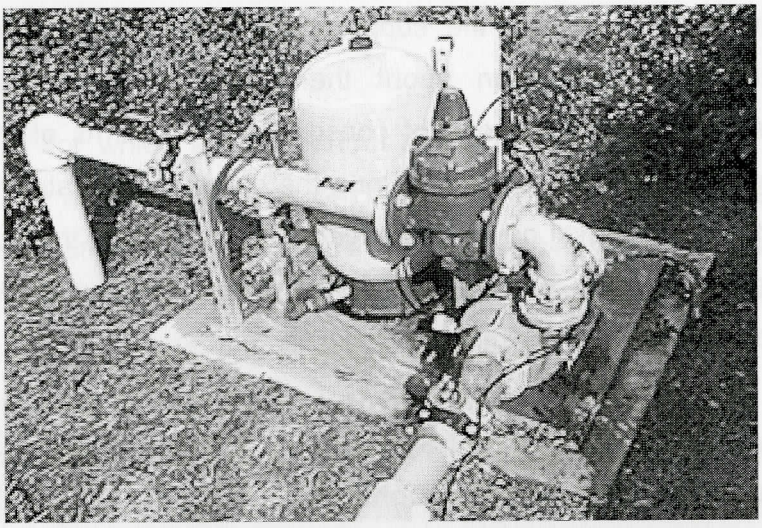


Figure 3-2: Flow Meter Installed To Measure Liquid Flow From A Storage Tank

- Differential pressure meters
- Variable area flow meters
- Positive displacement flow meters
- Turbine meters
- Electromagnetic flow meters
- Vortex shedding flow meters
- Ultrasonic flow meters

B) Temperature Measurement

Thermostats consist of a metal rod that expands and opens a set of contacts at a set temperature. This is merely used to control the temperature of the water inside the tank, but does not offer the consumer any information with regards to the temperature of the liquid inside the tank at any time. Depending on the required accuracy, resolution and output quantity, temperature sensors are fairly low cost and freely available. Most popular are temperatures based upon the sensitivity of a semiconductor device (AS Morris, 2005, p272). Generally semiconductors such as diodes and integrated circuits are highly dissectible to temperature changes and it is these characteristics that make them ideal for temperature measurement. Specifically inside smart sensors where the output is provided with a digital quantity making it easier to interface with a microcontroller. Their inaccuracy lies within the region of ±0.5%. These devices have a limited range from about -50°C to +150°C.

C) Analogue to Digital Conversion

Not all sensors produce outputs in the form of digital logic. For this reason Analogue to digital converters are used to convert an analogue quantity into a digital value. A digital signal or quantity may be defined as one or two specific voltage levels, whereas analogue signal is defined by a voltage that varies between some maximum and minimum level. This voltage may even be bipolar *(sometimes expressed as negative values)*. A/D converters are vital when using communication means that only support digital infrastructures. The advantage of many of today's microcontrollers is that they offer onboard A/D conversion usually at a ten bit resolution. This conversion is made to conform to a number system that is a multiple of the power of two (*32, 64,128...*). Each digital number count will correspond to being contained by one of the equal voltage divisions of the analogue signal. Resolution plays a major role here, since this defines the smallest change of an analogue signal that can be represented by two consecutive digital numbers (*one and zero: binary*) (Horowitch & Hill, 1989). For a temperature sensor where the voltage varies between 0v and +5v, an eight bit A/D converter is used. The resolution is calculated by:

$$\frac{\Delta voltage}{no.of.bits \rightarrow decimal} = \frac{5}{255} = 19.61mV$$

This would mean that the analogue signal would have to change by 19,61mV to result in a change in the digital value. Between these changes lies dead space which is defined as the range of different input values over which there is no change in the output value (AS Moris, 2005 , p 23). The most common type of analogue to digital converter is one that is also employed by most microprocessors. This is the successive approximation type. This type of ADC has the shortest conversion time (*excluding the flash type*) (TL Floyd, 1997, p 670). This type of device consists of a DAC, SAR and comparator (fig 6.2). The operation of this type of ADC begins with each output of the DAC being enabled one at a time, starting with the most significant bit. The comparator produces an output as an indication of whether the analogue input is greater or less than the DAC.

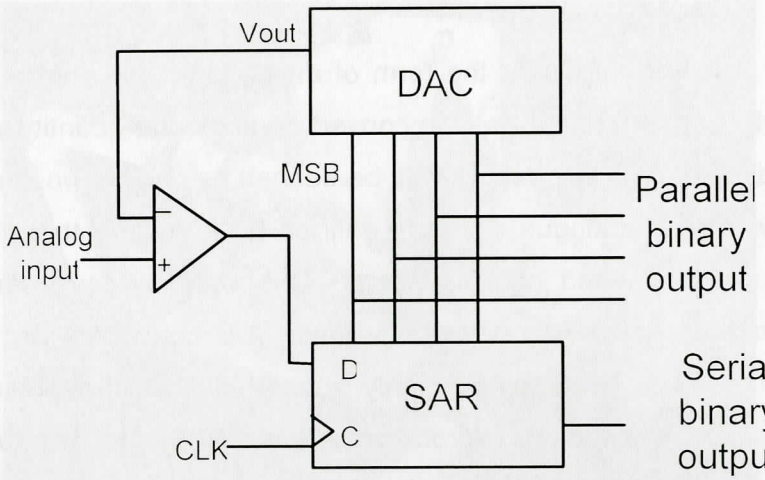


Figure 3-3: Block Diagram of a Successive Approximation ADC (TL Floyd, 1997, Pg 670)

If the output of the comparator indicates that the associated register is less than the output of the DAC, then the register is reset resulting in zero logic. After all the bits have been compared, the conversion cycle is complete. The microcontroller used with this study (Microchip 18f452 and similar devices) has a successive approximation ADC onboard the device. The ADC is interfaced with, using special function registers. Most devices in this family consist of a 10 bit resolution ADC. There are certain steps required to obtain a conversion from an analogue value to a digital one (*Microchip microprocessors*). By default, all ports allocated to the ADC are digital inputs. These have to be configured to be analogue inputs. This is done by writing to the associated registers. The reference voltage is also determined. This can be an external reference off a port pin or a reference to the microcontrollers operating voltage.

The conversion clock is also setup and it serves as a clock for the conversion process. This stage is concluded by turning on the ADC module. A certain amount of acquisition time is required after this module is made active. Now that the ADC is configured, it is ready for use. The conversion starts by activating a bit in the associated register. Once again a certain amount of acquisition time is required after which the result of this conversion is obtainable by the associated registers. Microprocessors with onboard ADC's have proven to be feasible when a low resolution ADC solution is required.

However these devices are still subjected to acquisition time and a resolution of between eight and ten bits. Higher resolution in the order of sixteen bits and lower acquisition time are available on dedicated ADC devices.

D) Smart Sensors

Analogue sensors need instrumentation amplifiers and analogue to digital converters in order to produce a digital equivalent quantity of the measured quantity signal. It has become more feasible for manufacturers to combine all the necessary parts in one. These are termed smart sensors.

3.2.2 The Communication Medium

The communication medium plays a very important role as the link between the consumer and supplier. Often, the communication medium that is required for effective macro level control is compromised by the cost of the communication medium. Ripple control is cheap since it uses the consumer power lines to control the geyser but does not allow two way communications. According to a report presented by Prof Nico Beute & Johan Delport (2005), two way radio communications were used in the past for geyser management systems with great success. The problem was that many of these two way radios operated inside the unlicensed frequency bands which have become seriously congested in recent years. Manufacturers have tried to address the problem of congested frequency bands by setting up stringent protocols that are able to filter out unwanted signals.

However the use of these protocols increase overheads on data packets and reduce bandwidth. Two way radio communication provides the only feasible option that suppliers of electrical power may have since investing into costly communication infrastructures is not the business of electrical suppliers. Other communication mediums include fibre optics, which is impractical from a supplier point of view since this presents the biggest cost and installation time. Fortunately with the development of computer networks, new technology that support TCP and UDP protocols have provided many with cheaper and rich bandwidth telecommunication systems.

Below is Tsunami MP.11 radio (Proxim wireless, ver2.3) that was used to establish a wide area communication network for purposes of a surveillance system. This may also be used for a Macro level geyser management system.

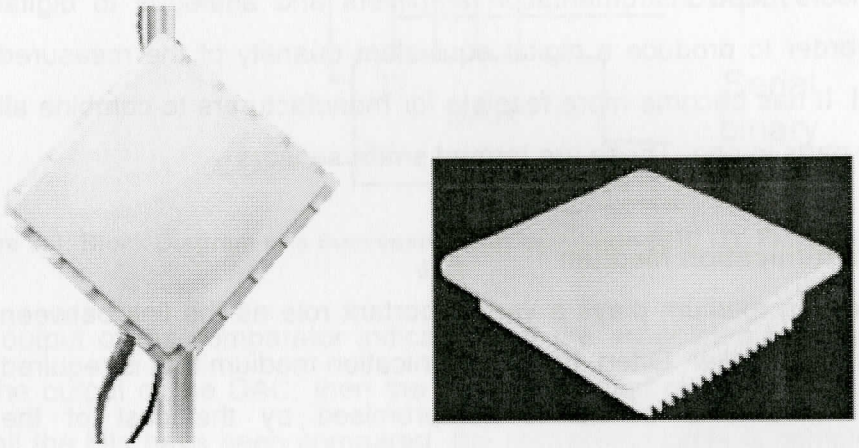


Figure 3-4: Tsunami MP11 BSU/SU (Proxim Wireless, 2007, [Pg 1])

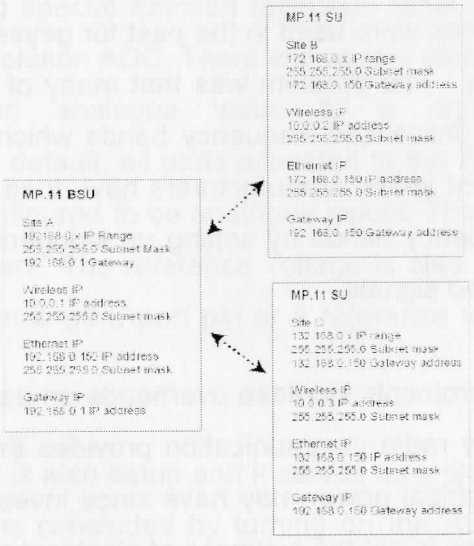


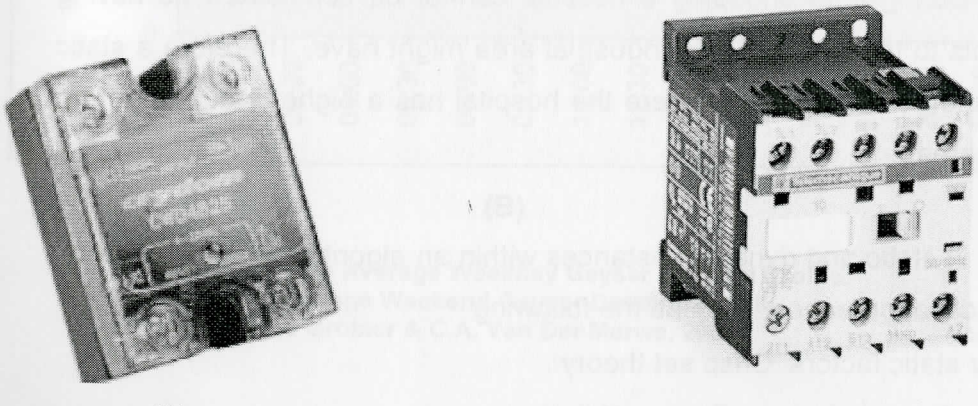
Figure 3-5: BSU/SU Communication (Proxim Wireless, 2007, [Pg 65])

The communication stream is established by many subscribers (MP.11 subscriber units SU) linking to a central station (Base station/ BSU) is shown above (Fig 3-4). An IP address is programmed for both the wireless and Ethernet network.

Many microcontrollers such as Microchip's 18F97J60 offers a free TCP/IP stack aboard their devices which may easily be used to implement this form of communication infrastructure.

3.2.3 Control Hardware

The control hardware centres around a microprocessor which is used to interpret data coming from a central point in order to switch on and off the source voltage to the geyser. Examples of switching devices include solid state relays (Fig 3.6), Thyristors, and contactors. Opto-isolators and similar devices provide isolation between the output signal derived from the microcontroller and the load for which it is used to control. These devices require a small amount of switching current in order to control the load. Microcontrollers usually require signal drivers that are used to switch on and off switching devices. Programmable logic devices such as Microcontrollers and field programmable gate arrays (FPGAs) are used to control these switching devices. Today's medium range low cost PLDs, offer built in peripherals that support analogue to digital conversion and communication protocols such as SPI,I2C, Ethernet and USB. The advantage of microcontrollers having built in communication peripherals is that additional cost due to dedicated devices is reduced.



(A) (B)

Figure 3-6: (A) Solid State Relay (B) Electrical Contactor

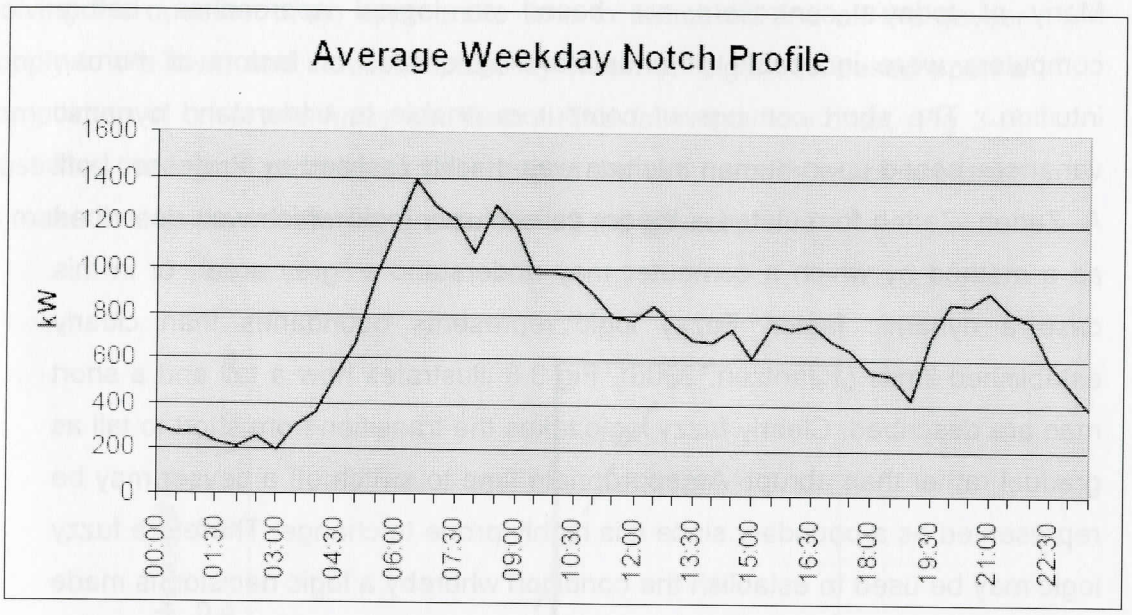
3.2.4 Factoring In Static and Dynamic Factors within an Algorithm

There are a number of factors that have to be taken in consideration when developing a geyser management system for a wide metropolitan area or for many users. The main objective on the consumer side is to reduce cost without having to compromise on his lifestyle. The energy supplier just wants to reduce peak period demand or the amount of load drawn from the supply. All factors that must be considered may be classed into what is termed as static and dynamic factors. Instances are classed as static factors when they do not change or do not change as easily. For example, in the case of a geyser management system, peak period demand times represent a static entity, since this rarely changes. Fig 3.7 represents a series of notch test conducted on 1446 geyser units. Here it is proven that peak period demand is experienced between 06h00 AM to 09h00 AM during a weekday (fig 3.7 a) and 06h30 to 09h30 over weekends (fig 3.7 b). Other examples of dynamic factors are the type of season or time of day. During summer months, consumers require less electricity to heat their houses than during winter months. This represents an entity that dynamically changes.

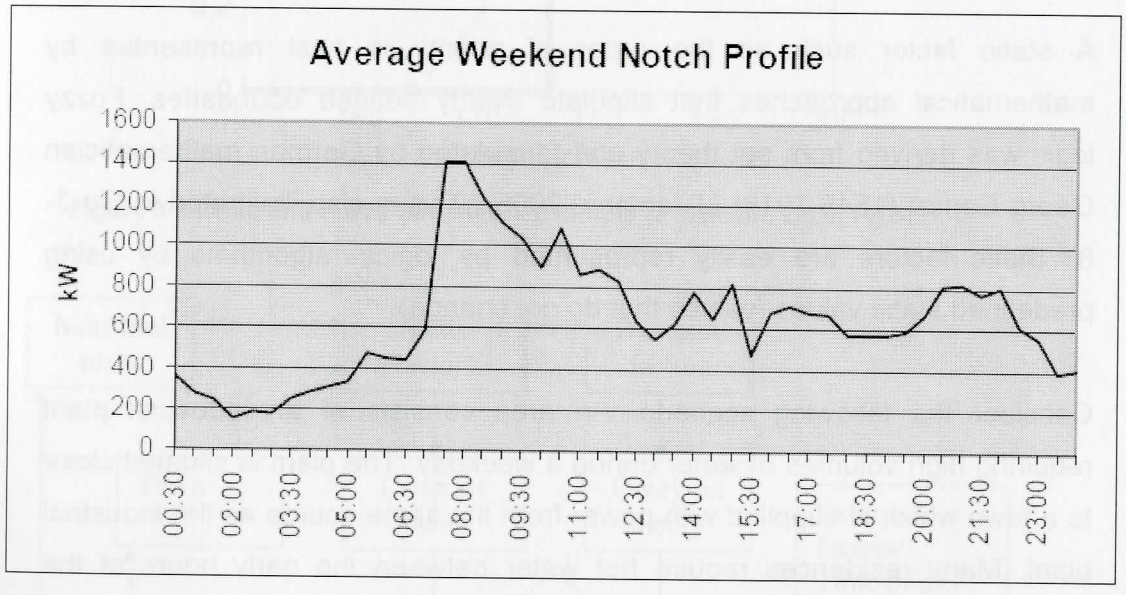
A static entity represents instances that cannot easily be predicted, such as the exact amount of geyser units that would be on for a specified time or even the order of importance that some consumers may have over others, example. During load shedding a hospital cannot be considered as having equal rights to the supply as an industrial area might have. Therefore a static factor would be the instance where the hospital has a higher status than the industrial area.

Factoring in static and dynamic instances within an algorithm is achievable by using logical approaches, such as the following

- For static factors: Crisp set theory
- For dynamic factors: Fuzzy set theory



(A)



(B)

Figure 3-7: (A) Average Weekday Geyser Demand Profile
(B) Average Weekend Geyser Demand Profile
(LJ Grobler & C.A. Van Der Merwe, 2004)

Many of today's controllers are based on logical approaches, before computers were incapable of understanding entities or factors of human intuition. The short comings of computers unable to understand dynamic variances based upon human intuition was quickly realised by Professor Lotfi A. Zadeh. Zadeh formulated a theory called fuzzy logic which was described as a method by which a computer may understand a "grey area", or in this case a dynamic factor. Fuzzy logic represents boundaries than clearly established limits (J.Jantzen, 2006). Fig 3.8 illustrates how a tall and a short man are described. Clearly fuzzy logic takes the transition from short to tall as gradual rather than abrupt. An appropriate time to switch off a geyser may be represented as a boundary since it is highly prone to change. Therefore fuzzy logic may be used to establish the condition whereby a logic decision is made to turn on and off the geyser.

A static factor such as the order of priority is best represented by mathematical approaches that stipulate clearly defined boundaries. Fuzzy logic was derived from set theory and formulated by German mathematician Georg Cantor (1845-1918) (J.Jantzen, 2006). This is also illustrated in Fig 3-8. Static factors are easily represented by logical algorithms by using predefined static values (values that do not change).

Consider the following scenario. An area consists of an industrial plant requiring high volumes of water during a weekday. The plant is situated close to a town which is supplied with power from the same source as the industrial plant. Many residences require hot water between the early hours of the morning as they prepare for work and in the late evenings as occupants arrive from work. A static factor would be the order of priority. The residents of the town have a higher priority during peak periods experienced in the mornings and as the residents of the town arrive from work than the industrial plant. However during the day the industrial plant has priority. This type of instance represents a static factor that may be solved within an algorithm using set theory. But there is a problem that this static factor may be subjected to dynamic influences. The time that the town residences leave and arrive from work is ever changing.

Solving the question of an appropriate time to switch on and off the geyser supply to the town and industrial plant lay within an algorithm based upon a compilation of crisp and fuzzy set theory. The following flow chart (Fig 3-9) illustrates the logical processors based upon the two theories which are used to make a decision weather to turn on and off the geyser.

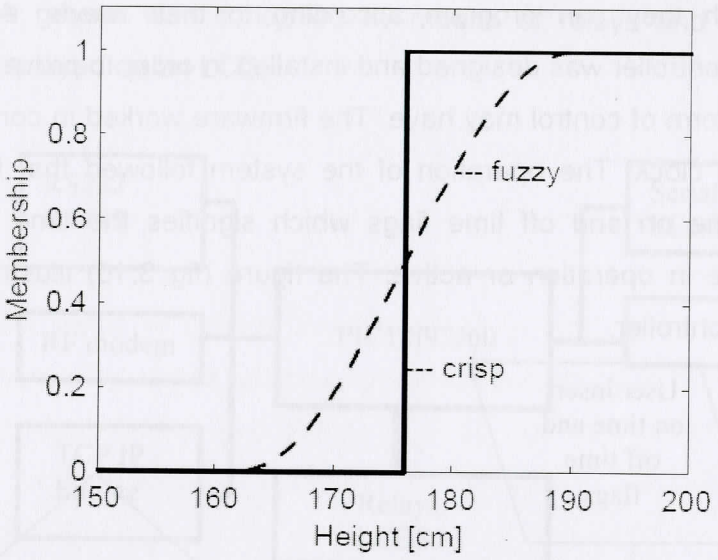


Figure 3-8 Crisp and Fuzzy Set Theory Example (J Jantzen, 2006, Pg 5)

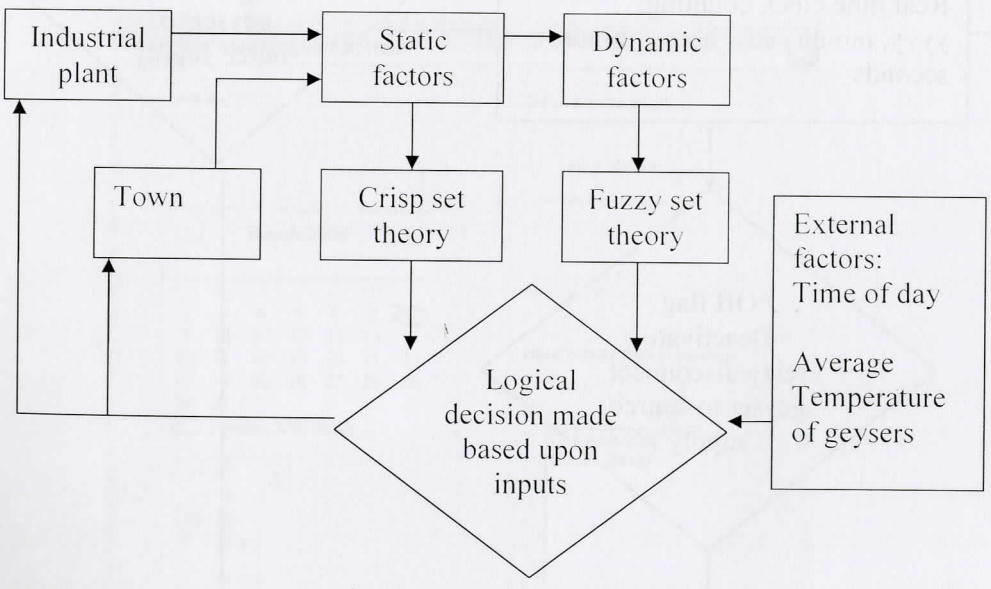


Figure 3-9: Example of a Crisp/Fuzzy Set Algorithim

3.3 Micro Level Geyser Management System

3.3.1 Derivation of the Smart Algorithm

A geyser management system was developed for a single household (micro level power consumption management). Micro level energy management systems are easily implemented since this type of control does not require carefully derived algorithms. Household occupants use programmable controllers which they can program according to their needs. A simple programmable controller was designed and installed in order to prove the cost saving that this form of control may have. The firmware worked in conjunction with a real time clock. The operation of the system followed that the user would programme on and off time flags which signifies the time that the geyser would be in operation or active. The figure (fig 3.10) illustrates the process of the controller.

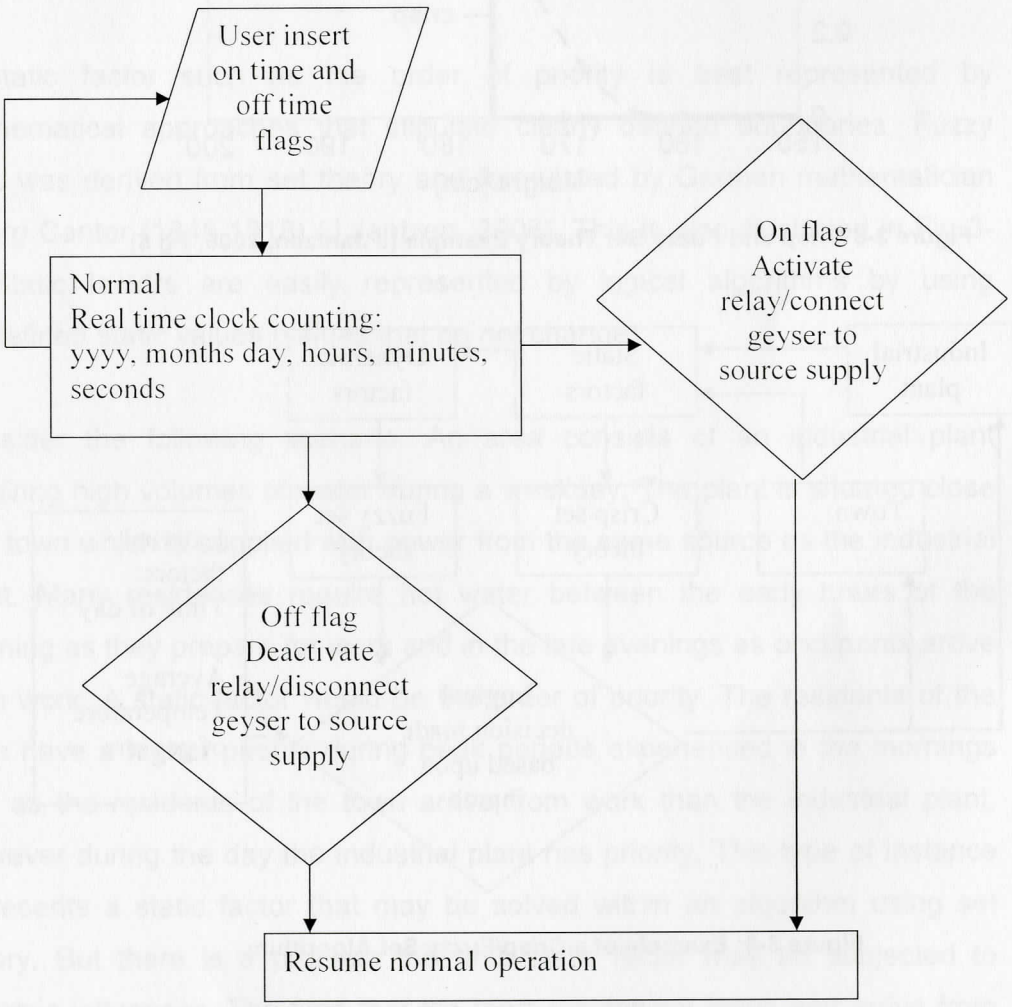


Figure 3-10 Micro Level Geyser Management System Control Algorithm

3.3.2 Hardware

The algorithm was loaded upon a MPC (multi purpose controller) supplied by Stanley security solutions. The basic layout of the controller is illustrated in fig 3-11. A Microchip PIC 18F97J60 was used with an onboard real time clock. All on and off switching flags were stored inside a serial eeprom. These flags were set by means of software (Fig 3-12) that connected to the MPC through Ethernet. The geyser was controlled by means of relays and the current status was displayed on an LCD.

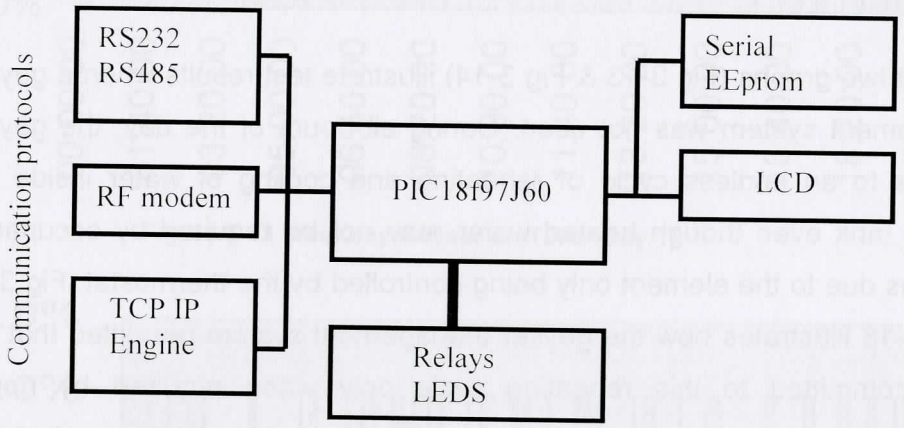


Figure 3-11: An MPC (Multi Purpose Controller) Used To Control a Geyser

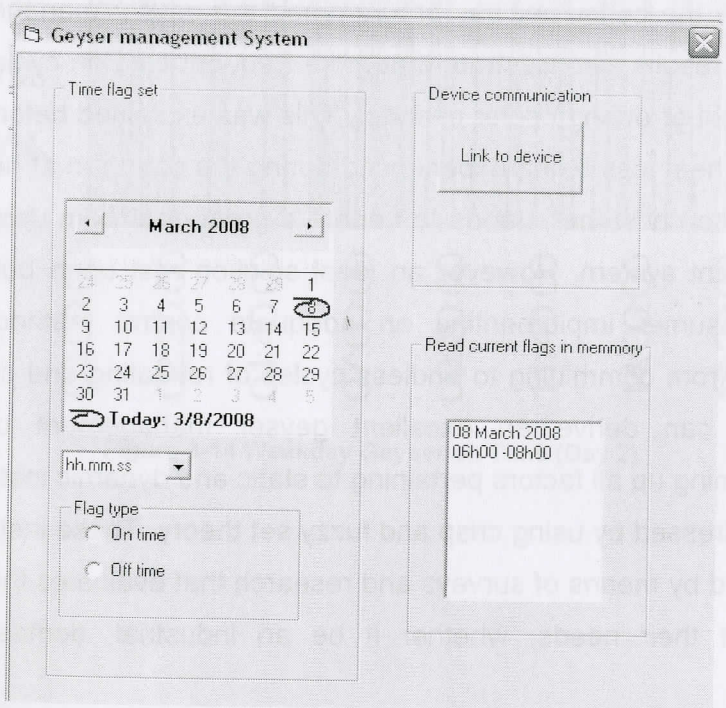


Figure 3-12 Graphical User Interface for the Geyser Management System

3.3.3 Testing

Several test were conducted for the purposes of a proof of concept of geyser management system. Fig3-12 to Fig3-15 shows the results of these tests. The geyser element was connected to a thermostat and then to the source through a relay that was controlled by the MPC. A temperature data logger was used to log the temperature of the water coming from the tank and the real time clock was used to create a time stamp together with a record of when the geyser element was drawing current from the supply. Tests were conducted on a geyser situated in a household (residential area).

The first two graphs (Fig 3-13 & Fig 3-14) illustrate test results when a geyser management system was not used. During all hours of the day, the geyser commits to an endless cycle of reheating and cooling of water inside the storage tank even though heated water may not be required by occupants. This was due to the element only being controlled by the thermostat. Fig 3-15 & Fig 3-16 illustrates how the geyser management system permitted that the water committed to this reheating cycle only when required by house occupants. Savings when using the geyser management system resulted in a cost saving of approximately R1.25 a day. However this saving is still dependent on how the consumer has programmed the geyser management system. The tests results also illustrate that more frequent time on cycles are experienced at night or during cooler periods. This was explained before that this is due to less heat loss being experienced during the day than at night. It was proven that the consumer stands to benefit a great deal from using the geyser management system. However an ideal solution rest upon both the supplier and consumer implementing an adequate control method that prevents geysers from committing to endless cycles of reheating and cooling water. Suppliers can derive an excellent geyser management control algorithm by summing up all factors pertaining to static and dynamic instances which may be addressed by using crisp and fuzzy set theory. These instances may be determined by means of surveys and research that evaluates the type of consumer and their needs, whether it be an industrial, domestic or commercial entity,

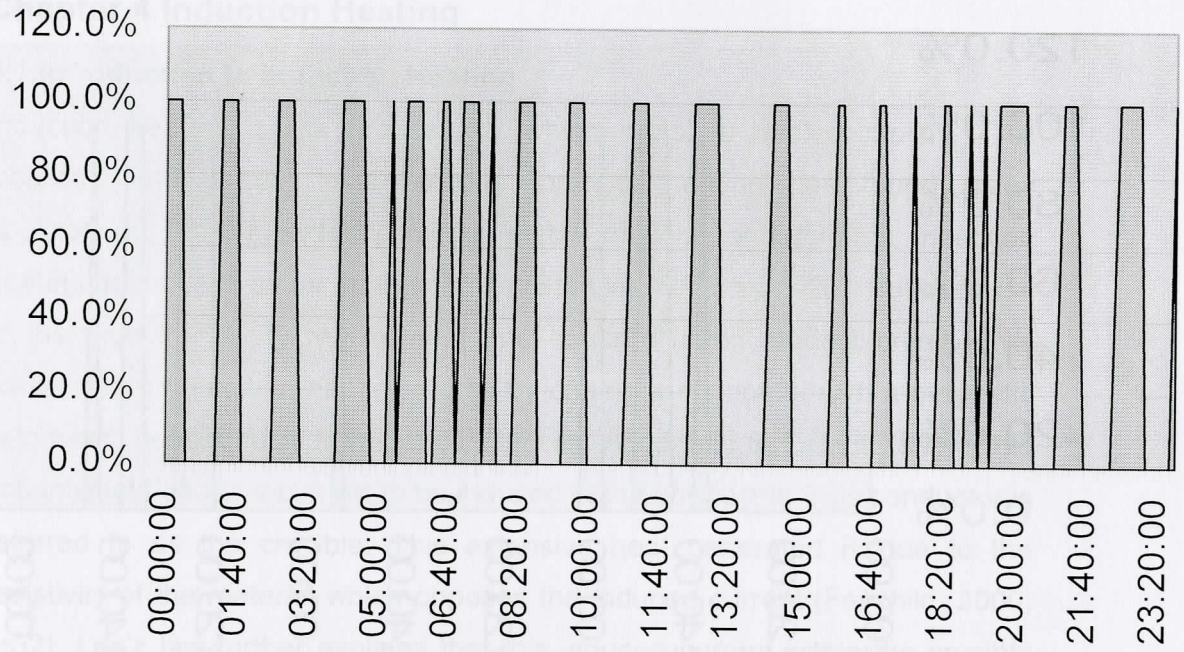


Figure 3-13 Weekday Geyser on Time (Day 1)



Figure 3-14 Weekday Geyser on Time (Day 2)

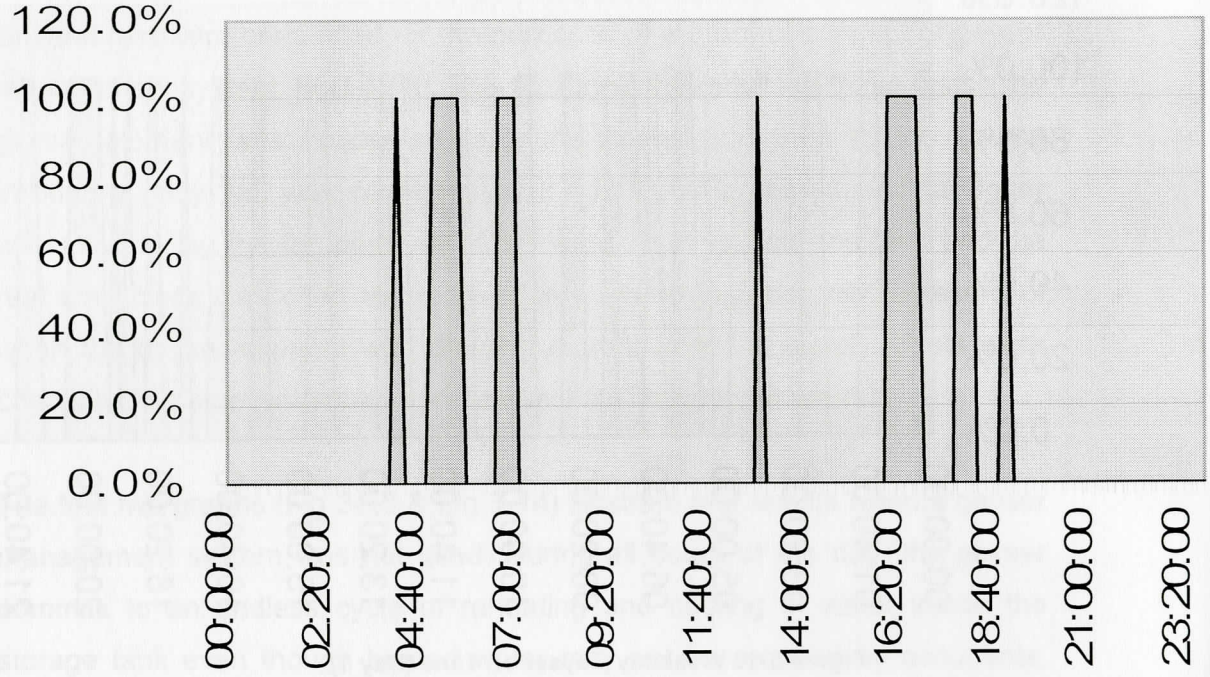


Figure 3-15 Geyser Management System (Day 1)

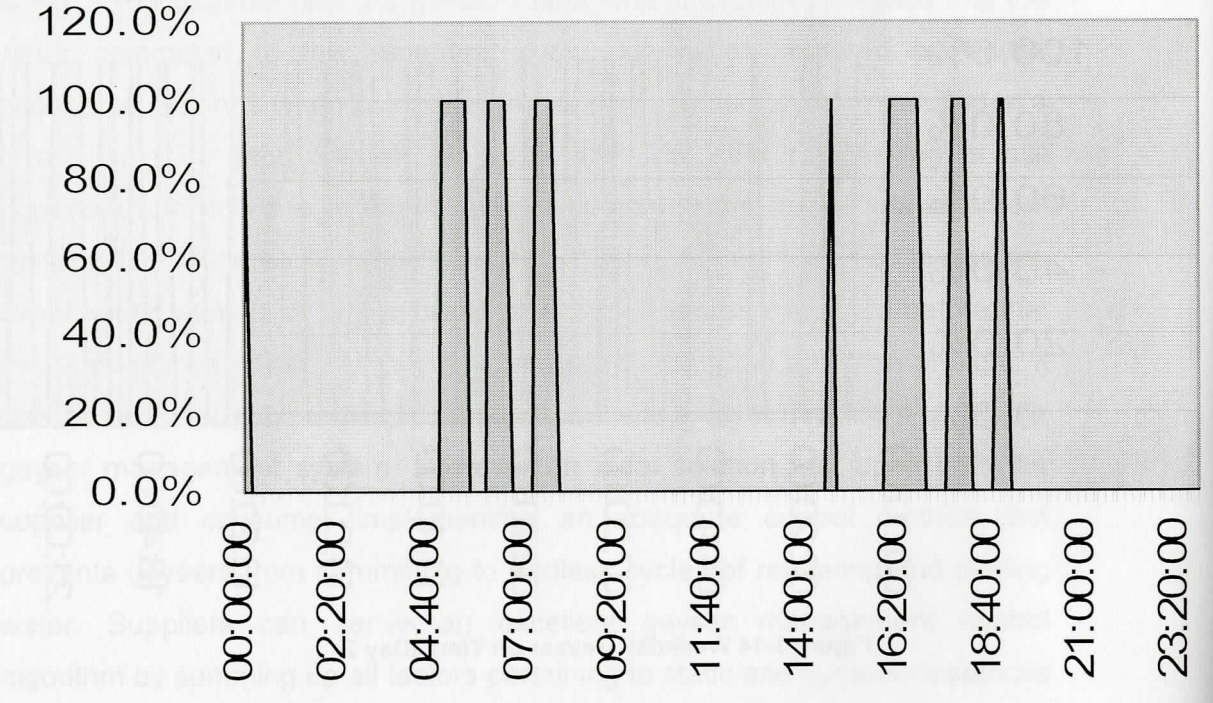


Figure 3-16 Geyser Management System (Day 2)

Chapter 4 Induction Heating

4.1 Introduction to Induction Heating

Induction heating is the process by which metal is heated rapidly. This localised and almost instantaneous form of heating has found many applications. This includes cooking, metal smelting and forging. Induction heating dates back as far as the 1920's (Stansel, 1949, pg 5-20). But because of the high frequency requirement, the concept found modest credit in its earlier years. Induction heating works by cutting a conductor with a magnetic field which continuously forms and collapses. According to Faraday's law, this action would cause a current to be induced in the conductor. This conductor is referred to as the crucible. This extensive heat generated is due to the resistivity of the material which opposes the induced current (Fairchild, 2000, pg 2). Len'z law further explains that this induced current within the crucible would flow in the opposite direction to the current that was used to build the magnetic field.

Many theories surround this principle of induction heating. In order to model the perfect system that enables maximum efficiency, some of these theories will be discussed in this chapter. An induction heating system primarily comprises of an RF power supply (high frequency power supply), coil and a crucible or work piece (Sobotka H, 1963, pg 1-14). The principles surrounding induction heating is best explained through a model of a transformer, since the two principles are fairly similar. A single phase transformer consists of both a primary side and a secondary side. An alternating voltage applied on the primary side would result in a primary current setting up a magnetic field, thus inducing current onto the secondary side. The secondary side would have a load connected to it. A real in depth look at induction heating begins with understanding the fact that there were losses during the process. Within the context of transformers, these losses are listed as follows (H Mileaf, 1999, p 97):

- Copper (I^2R losses) and leakage loss
- Hysteresis loss
- Saturation loss
- **Eddy currents**

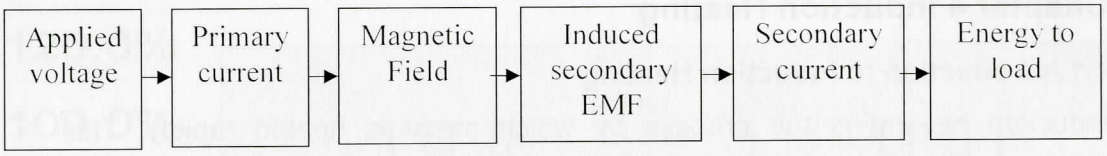


Figure 4-1: Sequence of Transformation (H Mileaf, 1999, P 97)

A block diagram of a transformer is illustrated above (fig4-1).The first loss is copper and leakage loss. Copper losses are commonly referred to as I^2R loss. This is the result of losses within the windings that dissipate power in the form of heat. The next type of loss is due to the magnetizing force and this is referred to as hysteresis loss. Saturation loss occurs when the maximum amount of flux lines is generated and a flux saturation level is reached. Any additional flux results in "lost power". The most important loss as it relates directly to induction heating is termed eddy current loss. This is the result of losses found within the core of the transformer. This is caused by the opposition of current by the core material of the transformer. This relates directly to induction heating because heat inside the crucible is generated in a similar manner. A transformer with a shorted secondary side relates best to an induction heating model. Extensive heat is generated on the secondary side and the heat generated is a direct function of the power dissipated in the secondary winding. This formula is given by:

$$P = \frac{E^2}{R} = i^2 R \qquad (4\text{-}1)$$

As with a resistive element, the power dissipated is a direct result of heat generated, the heat generated within the crucible is formulated as a direct result of the power supplied to the coil (if losses were ignored). This is termed as the Joule effect. The transfer of power from the coil to the crucible is a function of the generated flux given by (J Callebaut, 2007):

$$E = \frac{d\Phi}{dt} \qquad (4\text{-}2)$$

Where

$d\Phi$ = Represent the change in magnetic nature

dt = This change is time dependent

E = voltage

This may also be expressed in terms as it relates to 4.1:

$$i^2R = \frac{d\Phi}{dt} \cdot \frac{1}{R} \qquad (4\text{-}3)$$

$$\therefore R(i^2R) = \frac{d\Phi}{dt} \qquad (4\text{-}4)$$

4.2 Skin Effect

An important factor is the speed at which the build and collapse of this magnetic flux ($\frac{d\Phi}{dt}$) takes place. This is a function of the applied frequency. The applied frequency has to be carefully considered as it relates to skin depth. In South Africa the supply frequency is given at 50Hz. Many times this frequency is not adequate for induction heating purposes and a RF power supply is used to transform this low frequency into a high frequency source. The skin effect describes the tendency for current to flow on the outside of a conductor. The higher the frequency, the less the depth of penetration will be (as illustrated in figure 4-1). Depending on the work to be done, thick materials require a lower frequency to obtain maximum possible penetration depth than thin metals. The equation regarding skin depth is given by the following equation (I Khan, 2000, p15):

$$\delta = \sqrt{\frac{\rho}{\mu \pi f}} \qquad (4\text{-}5)$$

Where:

ρ = resistivity of work piece $(\Omega.m)$

μ = permeability of work piece *(H/m)*

f = frequency *(Hz)*

Another important property about the applied frequency is the type of frequency used. The supplied frequency that Eskom supplies is provided at a low frequency of 50 Hz and the form of this frequency is sinusoidal. For

purposes of induction heating, better results may be achieved if the supply frequency was a square wave.

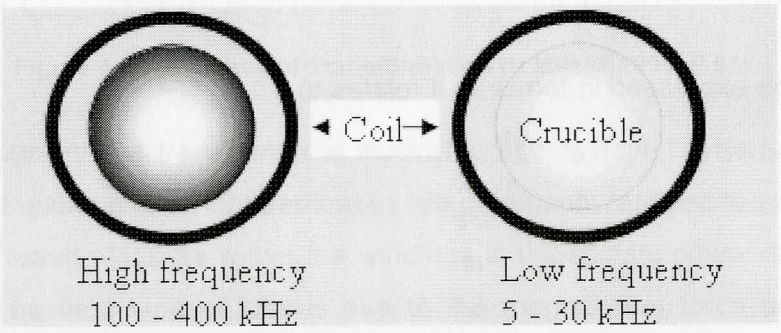


Figure 4-2: Skin Effect

4.3 The Fundamental Frequency

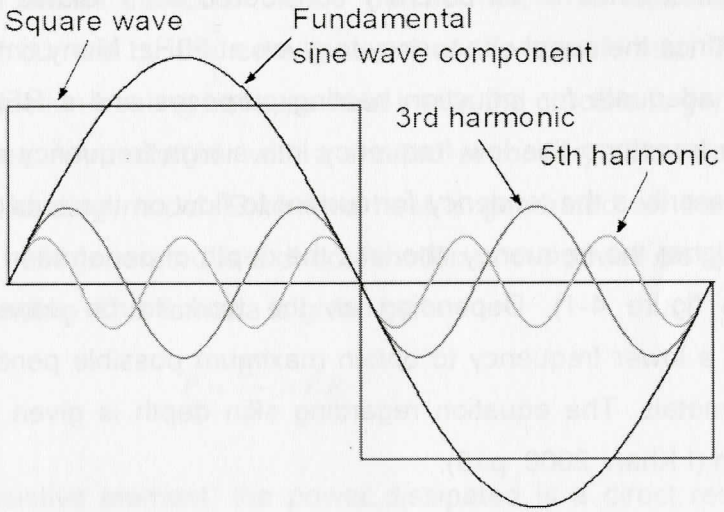


Figure 4-3: Square Wave Consisting Of Multiple Sine Waves

For reasons that would be explained later, induction heating works best at resonance (R Loveless, DC Raymond M Black, 2003, pg 34). A square wave consist of multiple sine waves, and the fundamental frequency would be made to equal the natural frequency of the tank circuit. Maximum power would be generated at this fundamental frequency and additional power would be the result of sub fundamental frequencies. The sub fundamental frequencies are termed harmonics.

The formula for a square wave is given by:

$$x_{square} = \frac{4}{\pi}\sin\omega t + \frac{1}{3}\sin 3\omega t + \frac{1}{5}\sin 5\omega t + ... \qquad (4\text{-}6)$$

Where:

$$\omega = 2 \cdot \pi \cdot freq \qquad (4\text{-}7)$$

The fundamental wave in this equation is given by:

$$\frac{4}{\pi}\sin(\omega t)$$

This would be made to equal the natural frequency of the load (resonance). This expression may be expressed in terms of voltage and power, where the total power would be taken as the sum of powers of the fundamental frequency and sub fundamentals. Given all the requirements that the power supply has to provide, various ways of transforming a low frequency supply to a high frequency supply was investigated.

4.4 Power Supplies

The power supply plays the role of transforming the incoming low frequency sinusoidal supply to a higher frequency square wave supply. There are four forms of power transformation. These are the following:

- Rectifiers (AC-DC)
- Inverters (DC-AC)
- Transformers (AC-AC)
- Converters (DC-DC)

Induction heating furnaces in its earlier years were expensive due to the methods by which the high frequencies were obtained. High frequencies were generally obtained by mechanically coupling generators and motors to drive one another in order to produce the required frequency. Another problem that stems from this sort of configuration was the amount of losses that resulted in this process.

Vast improvements in inverter topologies have brought about power supplies that are cheaper, light weight and more efficient. Many of these inverter topologies consist of a rectifier stage and an inverter stage. The work on the principle of deriving a high frequency by switching a DC source. This stems the need for the rectification stage. Other forms of inverters are illustrated by figure 4-5 as provided by Mr Khan. What must be observed in all of these inverter topologies are the use of high speed switches. Inverters use high speed switches to form the required frequency. These high speed switching devices include:

- FETS
- IGBT'S
- BJT
- SCR
- Thyristors

It is because of these cost effective and efficient devices that RF power supplies are more efficient and cost effective than in the past. For now, the bigger picture regarding an RF power supply is dealt with. A three stage power supply plays the most relevance, since the final design consisted of a transformer (step down), full bridge rectifier and a full bridge inverter. The Figure 4-4 illustrates an RF power supply circuit that was used.T1 represents a variable transformer. C1 and C2 are capacitor banks used to decrease the initial ripple voltage from the bridge rectifier (DC1).The second transformer (T2) and associated rectifier supplied a low voltage (typically +15v & +5v) for the driver and controller circuit.

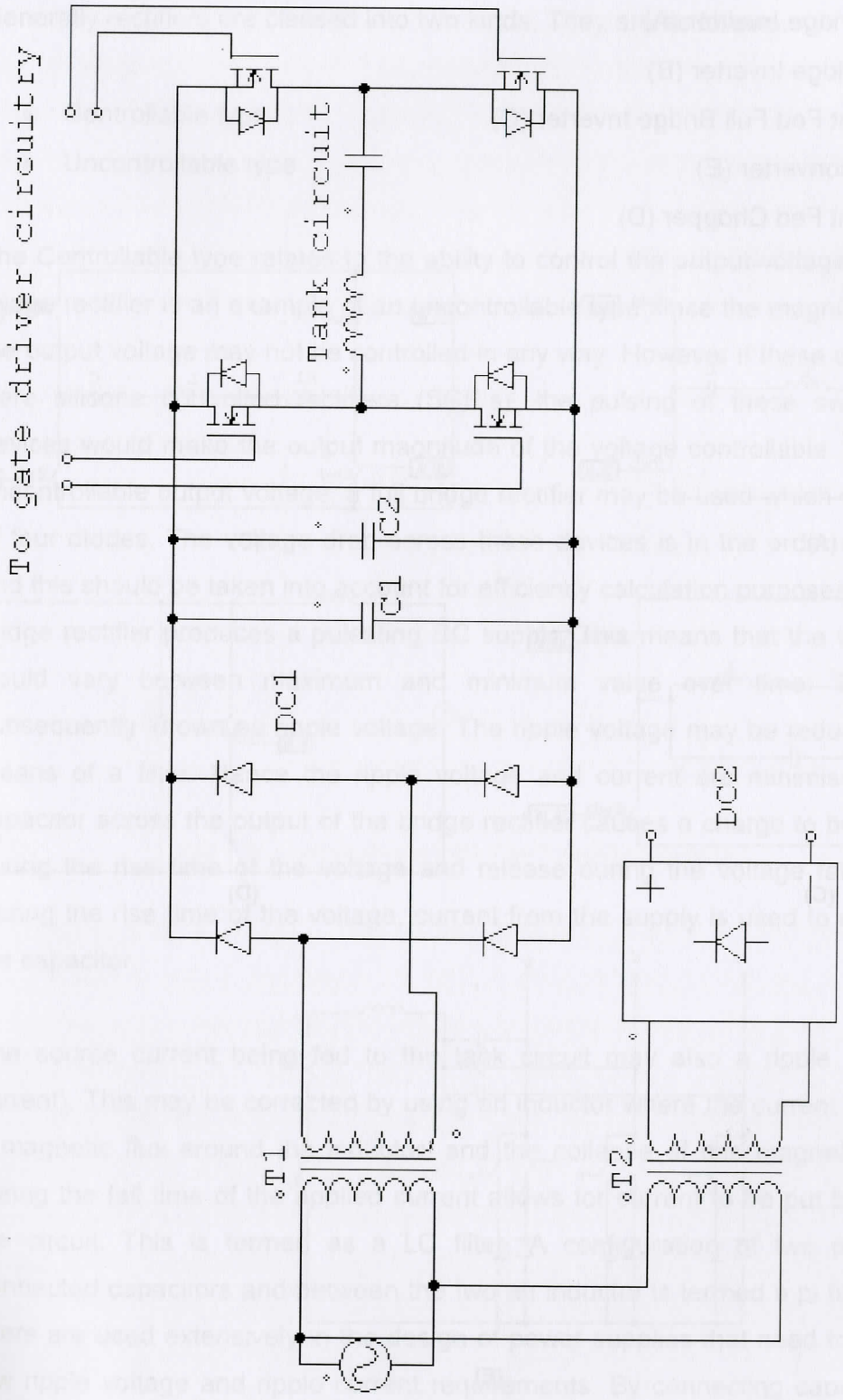
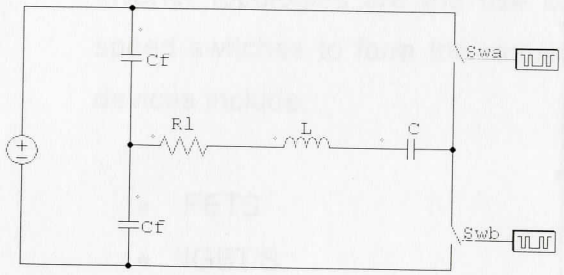


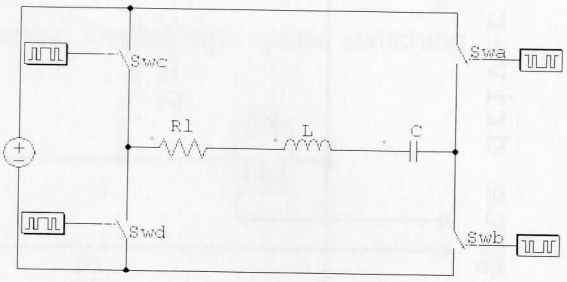
Figure 4-4: RF Power Supply Circuit

Shown are examples of various inverter topologies.

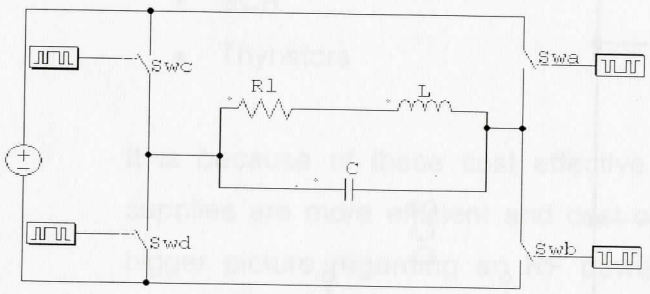
- Half Bridge Inverter (A)
- Full Bridge Inverter (B)
- Current Fed Full Bridge Inverter (C)
- Cycloconverter (E)
- Current Fed Chopper (D)



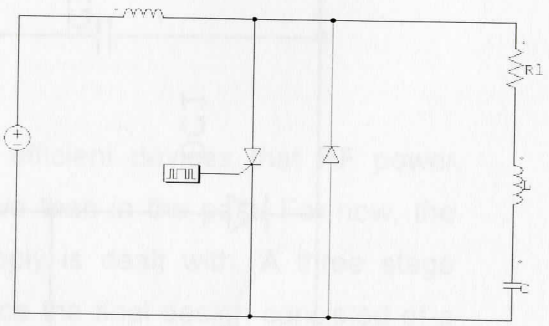
(A)



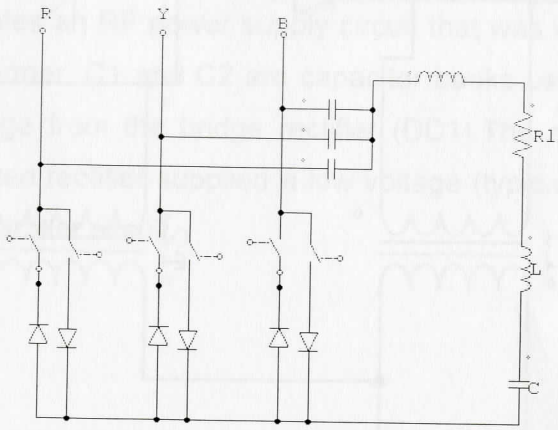
(B)



(C)



(D)



(E)

Figure 4-5: Inverter Topologies (I Khan, 2000, P 19)

4.4.1 The full bridge Rectifier and filter circuit

Generally rectifiers are classed into two kinds. They are as follows:

- Controllable type
- Uncontrollable type

The Controllable type relates to the ability to control the output voltage. A full bridge rectifier is an example of an uncontrollable type since the magnitude of the output voltage may not be controlled in any way. However if these devices were silicone controlled rectifiers (SCR's), the pulsing of these switching devices would make the output magnitude of the voltage controllable. For an uncontrollable output voltage, a full bridge rectifier may be used which consist of four diodes. The voltage drop across these devices is in the order of 0.7v and this should be taken into account for efficiency calculation purposes. A full bridge rectifier produces a pulsating DC supply. This means that the voltage would vary between maximum and minimum value over time. This is subsequently known as ripple voltage. The ripple voltage may be reduced by means of a filter. Hence the ripple voltage and current are minimised. A capacitor across the output of the bridge rectifier causes a charge to build up during the rise time of the voltage and release during the voltage fall time. During the rise time of the voltage, current from the supply is used to charge the capacitor.

The source current being fed to the tank circuit may also a ripple (ripple current). This may be corrected by using an inductor where the current create a magnetic flux around the inductor, and the collapse of this magnetic flux during the fall time of the applied current allows for current to be put back in the circuit. This is termed as a LC filter. A configuration of two parallel connected capacitors and between the two an inductor is termed a pi filter. Pi filters are used extensively in the design of power supplies that need to meet low ripple voltage and ripple current requirements. By connecting capacitors in parallel to form the C-type filter, the total equivalent series resistance is reduced.

This also allow for larger capacitor values to be obtained. Although sometimes unavoidable, as far as possible, the use of passive components in any stage of a power should be avoided. This is because there generally are more losses than semiconductor components. Passive components usually also mean large and heavy power supply designs.

4.4.2 The Full Bridge Inverter

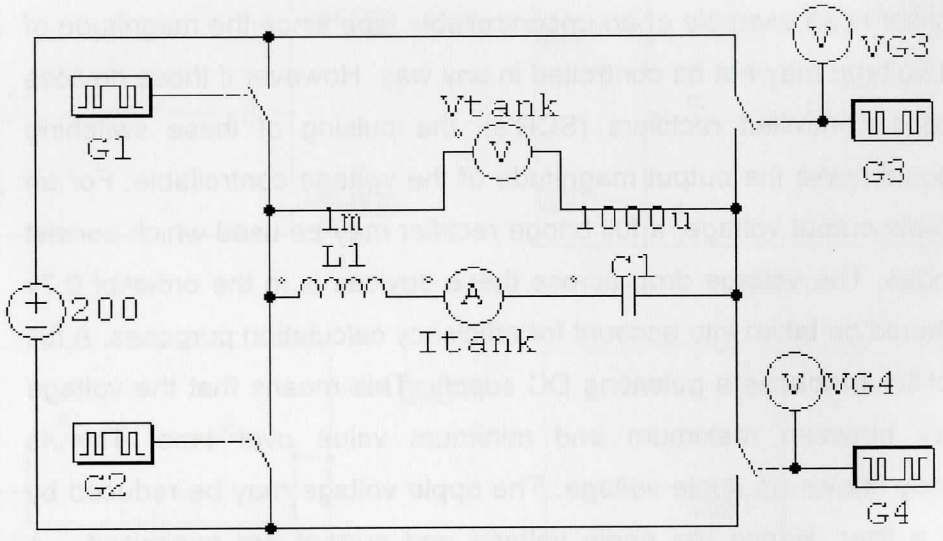


Figure 4-6 Voltage Fed Full Bridge Inverter

Figure 4-6 illustrates a full bridge voltage fed inverter. The DC supply would typically be a full bridge rectifier with a filter as discussed in the previous chapter. The alternating source signal for the resonant tank circuit is produced by alternative switching of switch pairs G2, G3 and G1, G4. In other words, when G1 (high side switch) and G4 (low side switch) are active, current would flow in one direction. When the alternative switches are activated, the current would flow in the opposite direction. Although the logic behind the topology is self explanatory, this topology does present a few challenges. Generally semiconductor switches take longer to switch off than to switch on. If a delay between switching transitions were not put in place, the result would both high and low side switches being on at the same time.

This would cause a short circuit. Many manufactures of full bridge inverter drivers include safety mechanisms that automatically produce a certain amount of dead time between switching transitions. Another challenge is one presented by the high side switching devices. For the low side switch the gate drive signal is referenced to ground and therefore it is easier to drive than the high side switch. The high side switch has its reference voltage floating on top of the voltage across the load. Hence the gate drive signal is referenced to a voltage source that is varying. To solve this, a gate drive signal would have to be shifted to the same reference voltage as the high side switch (Figure 4-7). For this reason a level shifter is used (International Rectifier, 1999) or a gate driver integrated circuit.

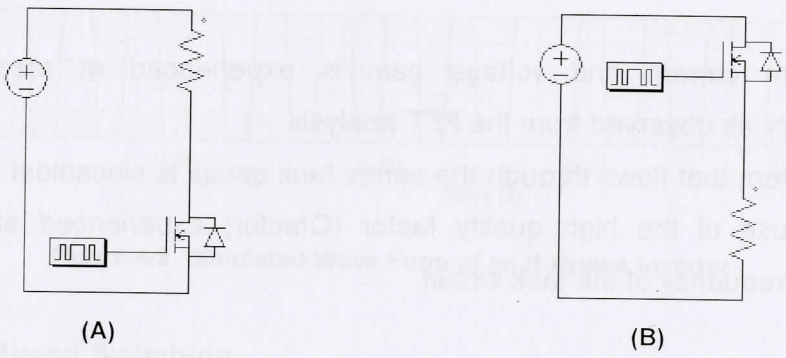


Figure 4-7: Low Side (A) And High Side (B) Switches

In a full bridge or half bridge inverter, the driver uses the mid point voltage to allow the drive signal to be shifted in order to drive the high side switch. FETS or IGBT's usually require a gate voltage to be 10-15V higher than the drain voltage. Gate driver circuits are used in order for devices such as microcontrollers and field programmable gate arrays to meet the gate drive requirements for switching these devices. The power absorbed by the gate drive circuitry should not significantly affect the overall efficiency. Driver circuits are available in integrated packages and these circuits often combine necessary safety features and driving circuits to meet the requirements of high speed switches. These devices are also used in switch mode power supplies. A full bridge inverter may be of the voltage or current fed types. According to Kirchhoff's voltage law, the sum of the voltage drops would be equal to the applied voltage.

Voltages fed inverters are termed this because of the voltage drops across each component of the tank circuit brought on by the resistance or impedance of that device. Hence the voltage is divided across the series tank branch. Kirchhoff's current law explains that the sum of currents found inside parallel branches would equal to the total current or source current. For a converter that supplies a parallel tank circuit, the current would be divided up between the parallel voltages. This is why current fed inverters are termed this. To further explain the concept behind a voltage fed full bridge inverter, a simulation was done where the switching frequency was made to equal the natural frequency of the tank circuit. The following conclusion can be drawn from the simulated wave forms (figure 4-9):

- Maximum current and voltage gain is experienced at resonant frequency as observed from the FFT analysis
- The current that flows through the series tank circuit is sinusoidal. This is because of the high quality factor (Qfactor) experienced at the natural frequency of the tank circuit

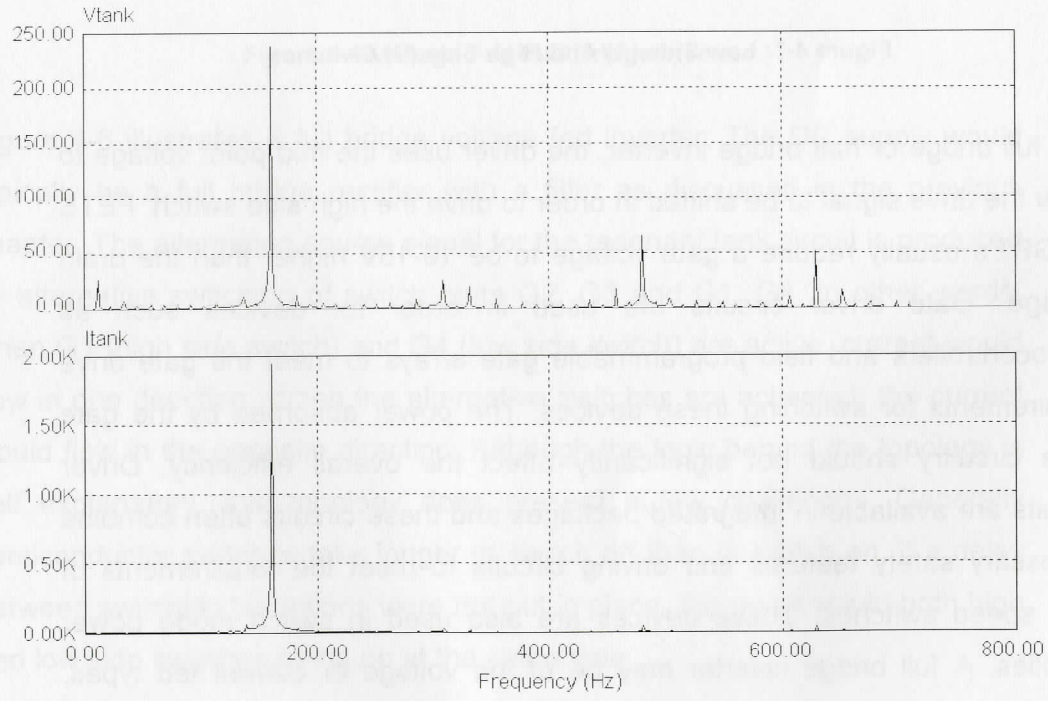


Figure 4-8: Fast Fourier analysis of a Voltage Fed Full Bridge Inverter

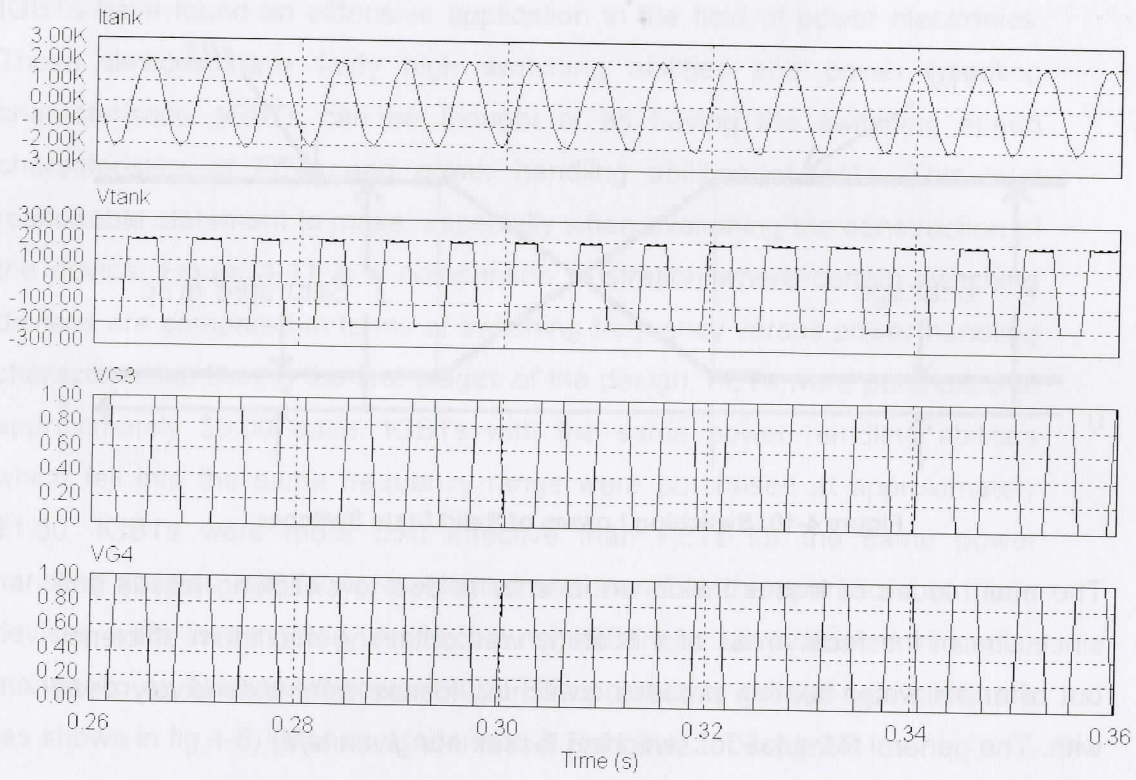


Figure 4-9: Simulated Wave Form of an H-Bridge Inverter

4.5 High Speed Switching

As seen in all inverter topologies, the use of devices that are capable of making and breaking load currents at high speeds is essential. The selection of an appropriate switch serves the utmost importance with regards to achieving high efficiency. Most Semi conductor switches are capable of achieving a high efficiency because of high speed switching with low power dissipation. There are three types of semiconductor switches, namely:

- Diodes
- Thyristors
- controllable switches (Mohan, T M Underland & W P Robbins, 2003)

Inverters require controllable switching. In other words, switches that is capable of making and breaking currents at any given time. Controllable switches include field effect transistors (FET), bipolar junction transistors (BJT) and Insulated gate bipolar transistors (IGBT).

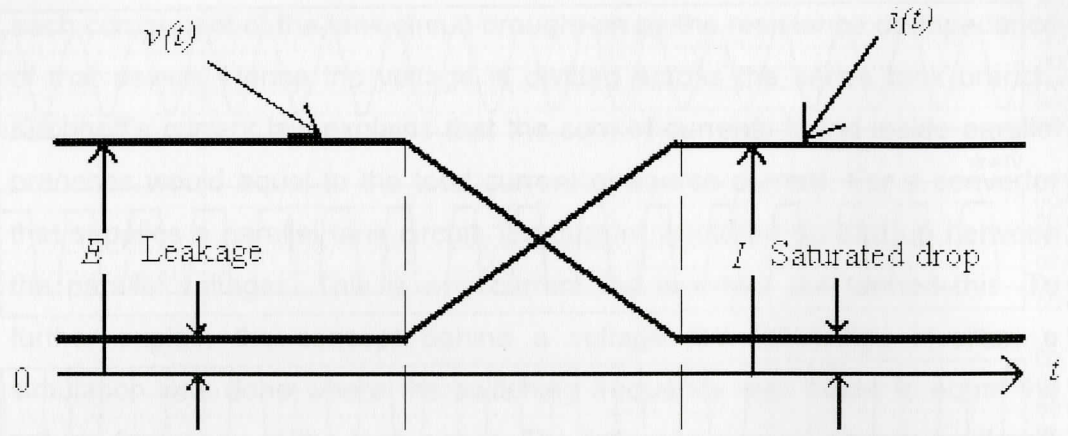


Figure 4-10: Switching Losses of Solid State Switches

The main cause of losses inside an inverter is due to switching losses and since one of the focal areas of this study was obtaining maximum efficiency out of an IH water heating process, switching losses were extensively dealt with. The general formulae for switching losses are given by:

$$P_{SW} = P_{SW(ON)} + P_{ON} + P_{SW(OFF)} + P_{OFF} \qquad (4\text{-}8)$$

As with all semiconductor switching devices, a small leakage current can be expected while the switch is off. During the on stage of the device, there is still a voltage drop across the switching device. The time taken for a device is not instantaneous, and therefore during switch transitions losses occur. Equation 4.8 represents the total losses experienced by the device during one cycle of switching. This dissipated power is transformed into heat and adequate cooling is necessary. Cooling techniques include heat sinks to force air cool that involves cooling fans. Most manufacturers of controllable switches stipulate optimum operation of switching devices around a junction temperature of 25°C. Switching losses may be reduced if the application switching requirements fall within the scope of the switching frequency of the device. FETs are renowned for applications that require very high switching speeds. However these devices do not have high power handling characteristics. BJTs have the opposite characteristics of having high power handling abilities but at generally low switching speeds.

IGBTs have found an extensive application in the field of power electronics. These devices have fairly high switching abilities and power handling characteristics. IGBTs can be thought of as having the switching speed characteristics of FETs and power handling abilities of BJTs. This is a reasonable statement to make, especially when evaluating the construction of the device. Figure 4-11 is a comparison illustration where certain switching devices are compared in terms of switching frequency versus power handling characteristics. During the first stages of the design, FETs were purchased at approximately $9.00 each. IGBTs with the same power handling abilities which fell into the same frequency range were purchased at approximately $1.00. IGBTs were more cost effective than FETs for the same power handling abilities. IGBTs were selected and therefore the operations of these devices were investigated. An N-channel IGBT can be evaluated in similar manner to an N channel power MOSFET constructed on a p-type substrate (as shown in fig 4-8) (Mohan, Underland & Robbins, 2003, pg 27).

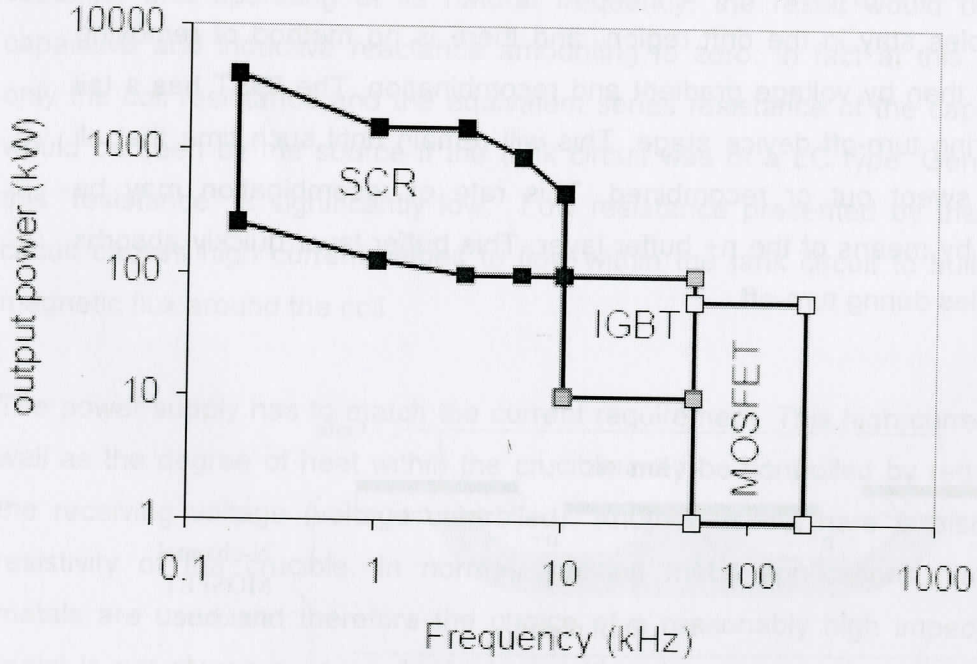


Figure 4-11: Frequency and Output Power Comparisons Of High Speed Devices (Mohan, Underland & Robbins, 2003, P27)

'When a positive voltage is applied from the emitter to the gate terminals of the device, electrons would be drawn in the direction of the gate terminal in the body region. If this positive gate-emitter voltage is above the threshold voltage of the device, then sufficient electrons would be drawn toward the gate to form a conductive channel across the body region. This would allow current to flow from the collector to the emitter. (To be accurate, it allows electrons to flow from the emitter to the collector) (J Dodge, 2002). This flow of electrons causes positive ions to be drawn from the P-type substrate (illustrated in fig 4.12) into the drift region towards the emitter.

The current flow in an IGBT consists of both electrons and holes. To increase conductivity or to reduce the effective resistance to current flow, "holes" are injected (J Dodge, 2002). The resulting decrease in on state voltage is the main advantage of IGBT's over power MOSFETs. However a lower on state voltage results in a slower switching speed, particularly at turn-off. This is due to the fact that the turn-off stage of the device, the electron flow can be stopped immediately by reducing the gate-emitter voltage below the threshold voltage. Holes stay in the drift region, and there is no method of removing them other than by voltage gradient and recombination. The IGBT has a tail current during turn-off device stage. This will remain until such time that all holes are swept out or recombined. This rate of recombination may be controlled, by means of the n+ buffer layer. This buffer layer quickly absorbs trapped holes during turn-off.

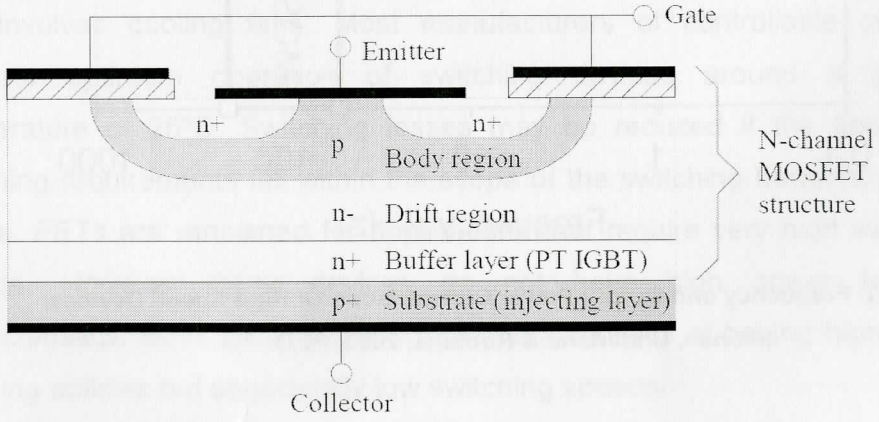


Figure 4-12: Construction of an N Channel IGBT (J Dodge, 2002)

4.6 Efficiency Calculations (Factors affecting the concept design)

4.6.1 Coupling Efficiency

Another criterion was electrical efficiency and coupling. The coupling efficiency deals with the relationship between the working coil and crucible and is calculated by the following equation (I Khan, 2000):

$$\eta = \frac{1}{1+\sqrt{\frac{\rho_c}{\rho_w \cdot \mu_w}}} \qquad (4\text{-}9)$$

Where

ρ_c = resistivity of the coil

ρ_w = resistivity of crucible

μ_w =permeability of crucible

In terms of coupling efficiency, the impedance of the coil and crucible plays a crucial role. The impedance of the crucible has to be infinitely higher, than the impedance of the coil. When a coil is connected in series or parallel with a capacitor and operating at its natural frequency, the result would be the capacitive and inductive reactance amounting to zero. In fact at this point, only the coil resistance and the equivalent series resistance of the capacitor would be seen by the source if the tank circuit was of a LC type. Generally this "resistance" is significantly low. Low resistance presented by the tank circuit causes high current values to flow within the tank circuit to build the magnetic flux around the coil.

The power supply has to match the current requirement. This high current as well as the degree of heat within the crucible may be controlled by reducing the receiving voltage (voltage controlled). Another aspect here is also the resistivity of the crucible. In normal smelting metal applications, various metals are used and therefore the choice of a reasonably high impedance metal is not always presented. However within the context of this design, a suitable crucible material has to be selected with the emphasis on having high impedance. High permeability materials such as iron will result in having a high coupling efficiency. As it has been proven by the equation (equation 4.9), this increases coupling efficiency.

4.6.2 Electrical efficiency

Another criterion with regards to efficiency is the electrical efficiency. Electrical efficiency is measured in terms of power induced and power dissipation in the working coil. This calculated by (I Khan, 2000):

$$\eta_e = \frac{P}{P + P_i} \qquad (4\text{-}10)$$

Where:

P = power induced in the load

P_i = power dissipated in the inductor

The power induced in the load is calculated taking into account various properties of the metal. If the crucible was a cylinder, the following formulae holds true (J Callebaut, 2007, p6):

$$P = \pi \cdot d \cdot h \cdot H^2 \cdot \sqrt{\pi \cdot \rho \cdot \mu_0 \cdot \mu_r \cdot f} \cdot C \cdot F \qquad (4\text{-}11)$$

Alternatively:

$$P = A \cdot H^2 \cdot \sqrt{\pi \cdot \rho \cdot \mu \cdot f} \cdot C \cdot F \qquad (4\text{-}12)$$

Where:

$$\mu = \mu_0 \cdot \mu_r \qquad (4\text{-}13)$$

A = area of a cylinder ($\pi \cdot d \cdot h$) or ($2 \cdot \pi \cdot r$)

d = diameter of cylinder

h = height of cylinder

H = magnetic field intensity

ρ = resistivity of working coil

μ_o = permeability of a vacuum

μ_r = relative permeability

f = applied frequency to coil

C =coupling factor

F = power transmission factor

From this equation it is evident that high permeability or "magnetic" materials lead to increased power induced in the load or crucible.

4.7 Tank Circuits

It was proven previously that coupling efficiency is ideal when the coil has a much less impedance than the crucible. This is achieved when the working coil is connected with a capacitor and supplied at its natural frequency. Another advantage of having a resonant tank circuit is that zero voltage and zero current switching are achieved within the inverter, hence increasing the efficiency of the inverter. At the natural frequency of the tank circuit, the inductive reactance would equal the capacitive reactance. The phase angle of the capacitor and inductor reactance would be equal in magnitude but opposite in direction resulting to the total reactance amounting to zero. The coil has a natural resistance and a capacitor has an equivalent series resistance. The source from the inverter or rather the *fundamental resonant frequency* would see the capacitor ESR and coil resistance as a pure resistance. The total resistance found in the tank circuit must be lower than the impedance of the crucible *(maximum power transfer).*

To understand the principle of maximum power transfer, take a microphone connected in series to an amplifier. The microphone has a resistance with a voltage across it. By means of ohms law it can be deduced that most of the applied voltage would rest upon the device with the highest impedance. Therefore more power will rest upon this device. It is ideal to have an amplifier with high input impedance so that more of the signal rest upon the input of the amplifier. The more signal available to amplify, the larger the output signal. This also explains the frequent use of FET's in amplifiers. These devices are synonymous with high input impedance values. This concept is no different when applied to induction heating. **Maximum power transfer** will be the result of having a tank circuit at far lower impedance than the crucible. The result of this would be more power resting on the crucible and therefore more of the electrical energy is available to produce heat. Low impedance in the tank circuit also leads to high current values (the lower the resistance, the higher the current). The power supply must match the load (capable of supplying this current). Another aspect of having a resonant load is the quality factor. This determines the ratio between the reactive power and real power present in the circuit (I Khan, 2000).

The quality factor is calculated by:

$$Q_L = \frac{X_{lp}}{R_L} \tag{4-14}$$

Where:

Q_L = Quality factor of the coil

X_{lp} = inductive reactance of coil

R_L = resistance of the coil

A high Q-factor results in a sharper Fast Fourier Transform (FFT) wave. Resonant frequency, overall impedance and reactance are calculated using basic formulas. This first starts by calculating the impedances of a coil and a capacitor. For an inductive branch the following equation is used:

$$Z = R_{coil} + jX_l \tag{4-15}$$

$$X_l = 2 \cdot \pi \cdot f \cdot l \tag{4-16}$$

In a similar method, the impedance is derived for a capacitive branch.

$$X_c = \frac{1}{2 \cdot \pi \cdot f \cdot C} \tag{4-17}$$

$$Z = R_{ESR} - jX_c \tag{4-18}$$

The total impedance in a tank circuit is calculated by:

$$Z = \sqrt{R^2 + (X_l - X_c)} \tag{4-19}$$

Using the above formulae's (4.15 - 4.19), the resonant frequency is derived.

$$2 \cdot \pi \cdot f \cdot L = \frac{1}{2 \cdot \pi \cdot f \cdot C} \tag{4-20}$$

$$1 = (2\pi fL) \cdot (2\pi fC)$$

$$1 = 2^2 \cdot \pi^2 \cdot f^2 L \cdot C$$

$$\frac{1}{f^2} = 2^2 \cdot \pi^2 \cdot L \cdot C$$

$$f_{res} = \frac{1}{2\pi \cdot \sqrt{LC}} \tag{4-21}$$

A practical method of designing a tank circuit would be to wind the coil first and then measure its inductance value, then an appropriate resonance frequency is calculated and a practical capacitor value is selected. Unfortunately, this resonant frequency tends to shift as the crucible begins to heat up. This is due to the loading effect of the crucible on the working coil. The process of induction heating works best at resonance and a shift in the resonant frequency leads to a minor drop in operating efficiency. Mr Khan solved this by means of a phase lock loop which commits the tank circuit to operate at its natural frequency even when this shift occurs. Phase lock loop works by altering the switching frequency of the inverter to compensate for the shift in natural frequency. Hence resonance is always maintained.

4.8 Coil Design

4.8.1 Helical spring type

The importance of the working coil has been emphasised a great deal thus far. A coil is made from insulated copper and the inductance for a helical spring type is formulated by the following equation (Simpson PG, 1960, pg 4-20)

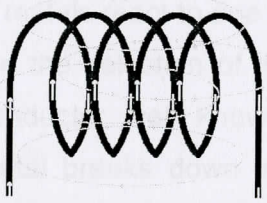
$$\mu H = \frac{R^2 N^2}{9R + 10L} \qquad (4\text{-}22)$$

Where:

R = radius of the coil

N = number of turns

L = length



$$\frac{d\Phi}{dt}$$

Figure 4-13: Helical Spring Type Coil

From the above formulae (equation 4.22), it is obvious that the inductance of a coil is directly proportional to the number of turns and the radius of the coil used.

4.8.2 Flat type

Another type of coil used in induction heating is the flat type. The application of this type includes induction cooking. The inductance of such a coil is calculated by the following equation:

$$L = \frac{(NR)^2}{8R + 11W} \qquad (4\text{-}23)$$

Where:

R = radius of the coil

N = number of turns

L = length

W = width

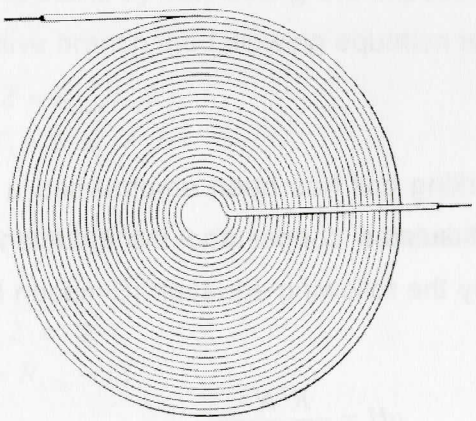


Figure 4-14: Flat Type Coil

Chapter 5 Crucible Properties and Water Heating Principles

5.1 Comparing Metals

There are means by which an induction heating system may be optimised. The tank circuit being supplied at its natural frequency and the supply frequency being a square wave are optimum attributes with regard to the power supply. However there are optimum attributes that the crucible may have in order to convert induced current into heat. The purpose of the crucible would be to generate heat and transfer this generated heat to the water into which it has been immersed. A crucible moulded for the purposes of water heating (the new "element"), would ideally have the following properties:

- A good thermal conductor or thermal conductivity
- A high resistivity
- A high relative permeability
- Break resistance in water

A metal with a high permeability may not necessarily be a good thermal conductor. This problem may be addressed in two ways. The first is to have a single metal that satisfy all requirements fairly or to have two metals mechanically coupled offering the best of all requirements. The latter solution may present a problem. Some metals react to one another when mechanically coupled together and therefore the selection of these two metals has to be made carefully. Iron is a conductor well known for having a very high permeability. However this metal breaks down in water. An Alloy such as stainless steel does not break down as easily but the compromise is that this metal does not have such a high permeability as iron. A high purity iron may prove costly and not as easily obtainable as other metals with fairly good properties. Another criterion is that the chosen metal has to also be able to be machined and welded together easily. A general comparison between metals was done in terms of thermal, permeability and heat conduction properties. These are shown in the following tables (tables 5-1 to 5-3):

Table 5-1 Specific Heat Capacities of Materials (Engineeringtoolbox, 2008)

Metal	Specific Heat Capacity - cp (kcal/kg°C)	Metal	Specific Heat Capacity - cp (kcal/kg°C)	Metal	Specific Heat Capacity - cp (kcal/kg°C)
Aluminium	0.22	Manganese	0.114	Thorium	0.03
Antimony	0.05	Mercury	0.033	Tin	0.054
Beryllium	0.436	Molybdenum	0.06	Titanium	0.125
Bismuth	0.03	Nickel	0.106	Tungsten	0.032
Cadmium	0.055	Niobium (Columbium)	0.064	Uranium	0.028
Carbon Steel	0.12	Osmium	0.031	Vanadium	0.116
Cast Iron	0.11	Platinum	0.032	Zinc	0.093
Chromium	0.11	Plutonium	0.032	Wrought Iron	0.12
Cobalt	0.1	Potassium	0.18	Sodium	0.29
Copper	0.092	Rhodium	0.058	Tantalum	0.034
Gold	0.031	Selenium	0.077	Lead	0.031
Iridium	0.031	Silicon	0.17	Magnesium	0.243
Iron	0.108	Silver	0.057		

Table 5-2 Permeability of Materials (engineeringtoolbox, 2008)

Material	Maximum relative Permeability
Iron, 99.8% pure	5000
Iron, 99.95% pure	200,000
78 Permalloy	100,000
Superpermalloy	1,000,000
Cobalt, 99% pure	250
Nickel, 99% pure	600
Steel, 0.9% C	100

Table 5-3: Material Resistivity (engineeringtoolbox, 2008)

Material	Resistivity (ohm m)
Silver	1.59x10^-8
Copper	1.68x10^-8
Aluminium	2.65x10^-8
Tungsten	5.6x10^-8
Iron	9.71x10^-8
Platinum	10.6x10^-8
Manganin	48.2x10^-8
Lead	22x10^-8
Mercury	98x10^-8
Nichrome	100x10^-8
Constantan	49x10^-8

5.2 Permeability and Resistivity of Metals

An in depth look at each of the afore mentioned criteria is necessary, with the first being permeability. Relative permeability is defined as the ability for a material to attract and conduct magnetic lines of flux. Many materials such as copper and gold have a relative permeability value of less or equal to one. Iron and alloys of this metal are well known for their high permeability values. Usually these values given in tables refer to maximum permeability. High permeability metals are best for induction heating due to the tendency to resist magnetic flux causing additional heat to be generated. Permeability is formulated by the following equation:

$$\mu_0 \times \mu_R \qquad (5\text{-}1)$$

Where

μ_0: Physical constant: $4 \cdot \pi \cdot 10^{-7}$ Henries/meter

μ_R: Relative permeability: $\mu_R = \frac{\Delta_B}{\Delta H}$ (Gauss/Oersted)

Permeability of ferromagnetic materials is a nonlinear factor. Heat being one of the contributing factors which affect materials permeability. As the crucible begins to heat up, the permeability of that material changes and hence the load factor on the working coil also changes. Permeability is not a linear function and is often understood by means of HB curves which illustrate the relationship of force to flux (field intensity H to flux density B). When graphed, this is referred to as the B-H curve. A few examples of |B-H curves are illustrated in figure 5-1.

The resistivity of metals is considered because heat is generated due to the induced current being opposed by the resistivity of the material. The power present in the crucible (i^2R) is proportional to the heat generated. High resistant values found in the crucible would lead to good coupling efficiency and good heat generation. Iron has a fair amount of resistance (9.71x10^-8 Ω/m) and high permeability.

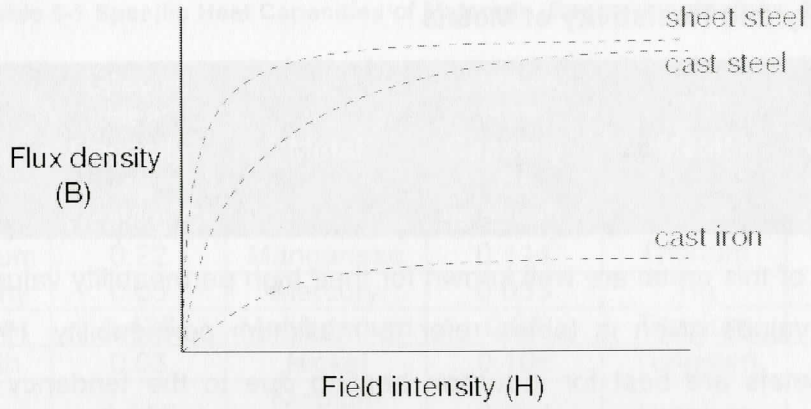


Figure 5-1 B-H Curve for Iron and Steel

5.3 Thermal Conductivity

In induction heating, heat is generated within the crucible. A most important factor is the transfer of this generated heat to the water. The crucible was directly immersed inside the liquid; therefore there would be no heat loss due to the distribution of heat. Good examples of heat conductors include brass. Thermal conductivity defines a metals ability to conduct heat. When metals are heated, they expand and when cooled contract. This property that describes a materials ability to conduct heat is referred to as the **k value**. This is defined by the following (engineeringtoolbox, 2008):

$$\text{Thermal}_{\text{conductivity}} = \frac{\text{heat flow rate} \cdot \text{distance}}{Area \cdot Temperature} \qquad (5\text{-}2)$$

This is formulated by the following:

$$k = \frac{\Delta Q}{\Delta t} \times \frac{L}{A \cdot \Delta T} \qquad (5\text{-}3)$$

(or) $$k = \frac{\Delta Q}{A \times \Delta t} \times \frac{L}{\Delta T}$$

Where

ΔQ: Quantity of heat

ΔT: Temperature

Δt: Time

L: Distance

A: Area

Table 5-1 provides the specific heat capacities of metals in calorie. Calorie is defined as the amount of heat needed to raise one gram of water by 1°C (engineeringtoolbox, 2008).

5.4 Principles of Water Heating

There are many misconceptions and realities surrounding the heating of water. Presented are facts concluded by Mr Delport (Eskom energy consultant) with regards to principles and concepts surrounding heating water and geysers.

- *It takes 4180J to raise the temperature of water by one degree*

It takes 4180 Joules of energy per litre to raise the temperature of water by one degree. Efficiency of any water heating process is measured by how much electrical energy is effectively converted to raise the water temperature. The following equation is used to calculate the total amount of energy needed to raise the temperature of water inside a tank from any initial temperature to the temperature that is required:

$$Q = m \times c \times \Delta T \qquad (5\text{-}4)$$

Where:

c = specific heat of water which is 4,180 joules per ℓ (kg) per °C

ΔT = change in temperature in °C

m = mass in ℓ of water

Q = energy in Joules

The temperature inside a cylinder is not expected to reach boiling point. Many geysers thermostats are set to reach a maximum of 65°C. The average ambient temperature inside a roof is around 25°C. Using equation 5.4, the energy needed is calculated:

$$Q = 3000 \times 4.180 \times (65°C - 25°C) \qquad (5\text{-}5)$$
$$= 501{,}600{,}000J$$

This high figure is made simple through the use of British thermal units (BTU). It takes one BTU to raise one pound of water by one degree. Therefore it would require 40 BTU's to raise one pound of water from 25°C to 65°C.

- *A 3kw element uses the same amount of energy as a 5kw element (the 5kw will heat the water faster)*

The capacity of commonly used geysers found in South Africa is 3000 litres with a 3kw element. If a 5kw element was used, the water would have just been heated faster. A 3kW resistive element will contribute 3,000 Joules per second (J Delport, 2004). The time taken for the above is calculated by:

$$T_{\sec} = \frac{energy_{needed}}{energy_{applied}} = \frac{501{,}600{,}000}{3{,}000\,j/\sec} \qquad (5\text{-}6)$$

= 167,200 s (for a 3kw element)

$$T_{\sec} = \frac{energy_{needed}}{energy_{applied}} = \frac{501{,}600{,}000}{5{,}000\,j/\sec} \qquad (5\text{-}7)$$

= 100,320 s (for a 5kw element)

- *The same amount of energy is needed to raise the temperature of water from 1 °C to 2 °C degrees is needed to raise the temperature from 64 °C to 65 °C.*

The initial temperature is irrelevant when raising the temperature of water. The same amount of energy to raise the temperature of the water by one degree is needed at high temperatures as well as low temperatures. When water inside the storage tank is used, this water is replenished. This would mean that the cold water will now be mixed with the hot water. Using the following equation, the total energy as a result of having two different temperatures can be calculated (J Delport, 2004):

$$Q_c = m_c \cdot c \cdot T_c \qquad \textit{(Energy of cold water) (5-8)}$$

$$Q_h = m_h \cdot c \cdot T_h \qquad \textit{(Energy of hot water) (5-9)}$$

$$Q_t = Q_c + Q_h \qquad \textit{(Total energy) (5-10)}$$

The amount of hot water within the storage tank can be calculated by substituting equation 5.4, (5.7) & 5.8 into equation 5.9.

$$m_t \cdot c \cdot T_t = (m_c \cdot c \cdot T_c) + (m_h \cdot c \cdot T_h) \qquad (5\text{-}11)$$

$$m_t \cdot c \cdot T_t = c\{(m_c \cdot T_c) + (m_h \cdot T_h)\}$$

$$m_t \cdot T_t = m_c \cdot T_c + m_h \cdot T_h$$

$$m_h = \frac{m_t \cdot T_t - m_c \cdot T_c}{T_h}$$

Chapter 6 System Design

6.1 Introduction

The complete system design for the induction water heater consists of the following:

- Step down transformer
- Rectifier (DC stage)
- Inverter (DC-AC stage)
- Element design
- Control circuit
- Temperature and data logger

The idea was to design, build and test the possibility of using the concept of induction heating for water heating inside the home. It was first perceived that an existing water storage tank commonly found in households be modified to cater for a new type of element design. This proved to be impractical because all proposed element design were simply too large to be able to be retrofitted into existing tanks. Another problem was that existing elements were not very lengthy to allow for uniform heating throughout the storage tank and any proposed element design had to allow for a more uniform method of heating.

6.2 Step down Transformer

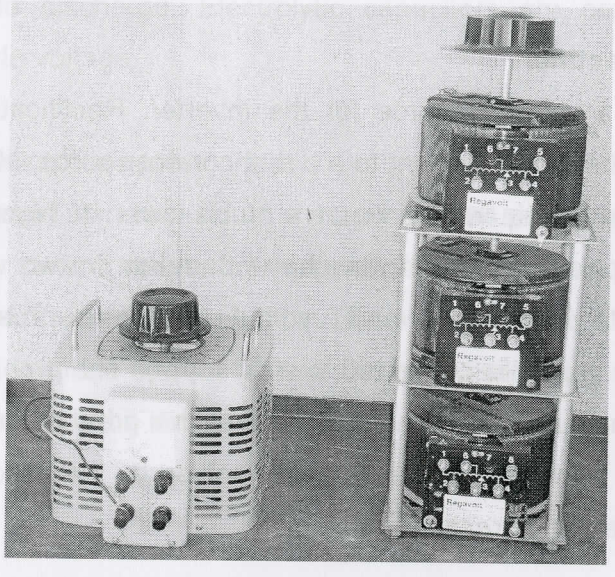


Figure 6-1: Single and Three Phase Variable Transformers

To vary the source voltage (up/down), a variable transformer was used. This was a method of controlling the output voltage to the rectifier. Transformers present a bulky and expensive solution to stepping down the source voltage. The transformers in Figure 6-1 were used since they were freely available at the lab where the original system was built. This illustration shows a single phase transformer on the left and a three phase transformer on the right. The advantage of using three phase topologies was that after the rectifier stage there would be much less of a ripple voltage as in the case of a single phase AC-DC power supply. This eliminated the need for high value capacitors to reduce the initial ripple voltage. The single phase variable transformer was used in many cases because it was easy to transport. This transformer had the following specifications:

Input voltage: 240V
Output voltage: variable between 0-240V

The transformer was supplied from a source of 220V AC. The maximum voltage on the secondary side of the transformer was expected to be 220V at a ratio of 1:1. This voltage was made into a DC source by means of a single phase rectifier and C-type filter (capacitive) to reduce the ripple voltage.

6.3 Rectification

6.3.1 Single Phase Rectifier

The rectifier acts as a voltage source for the inverter. Rectification is the transformation of an alternating current to a direct current source. Many times the derived DC source is required to be at a much lower or higher voltage than the rectified supply. Solving this may be undertaken in two ways. The simplest method is to step down and up the voltage by means of a transformer before the supply is converted to a dc supply. The problem with a large power supply that uses a transformer is that the greater the required current, the larger the transformer. This is easily solved by the second option that entails controllable bridge rectifier topologies.

An example of one type would be a full bridge rectifier that uses silicon controlled rectifiers to control the output voltage instead of uncontrollable diode. SCRs require sometimes complicated gate driver circuitry and many designers choose rather to go with stepping down the supply voltage and using a full bridge rectifier that consist of uncontrollable switches. A variable transformer connected to a bridge rectifier was the chosen design for this project. It was simple and involved a bulky transformer. The full bridge rectifier used, namely the skd30 had a maximum forward current of 30A (Id) (Semikron, 2007, pg 2).

Besides the power rating of components used, a general concern of DC supplies is that of the ripple voltage and current. This ripple voltage would be imposed onto the square wave produced by the inverter and hence the resulting high frequency would appear distorted if this ripple is not significantly reduced. A pi filter was used to reduce both dc ripple voltage and current. Topology is illustrated in Figure. 6-2 and the operation is as follows:

- For reducing the voltage ripple

The capacitors presented in the circuit are primarily responsible for the reduction of ripple voltage. When there is a rise in the supply voltage, the capacitor would start to charge and when the supply voltage drops the capacitor would discharge. Electrolytic capacitors are commonly used to reduce the ripple voltage.

- For reducing the ripple current

The inductor would start to build up a magnetic filed while the current starts to rise. When this current drops, the magnetic filed collapses forcing current to be induced back inside the conductor. This induced current would flow in the opposite direction to the current that was used to build the magnetic field. The result of this would be the reduction in ripple current.

The general formulae for ripple voltage reduction are given by:

$$V_{r(p-p)} = \frac{Vm}{2fR_lC} \quad \textit{(Ripple voltage)} \qquad \textit{(6-1)}$$

$$C = \frac{V_m}{2fRV_{r(p-p)}} \quad \textit{(In terms of the capacitor value)} \qquad \textit{(6-2)}$$

Where

Vm : Maximum voltage

$V_{r(p-p)}$: Peak to peak ripple voltage

C: capacitor value

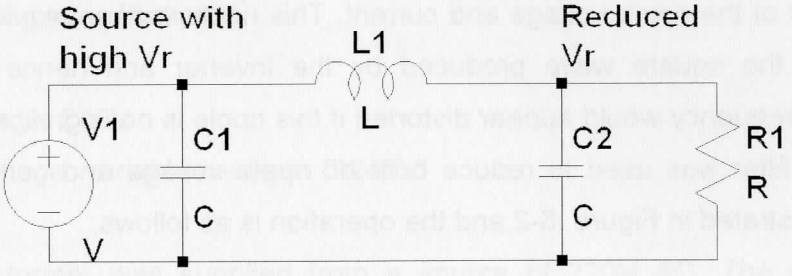


Figure 6-2 Pi Type Filter

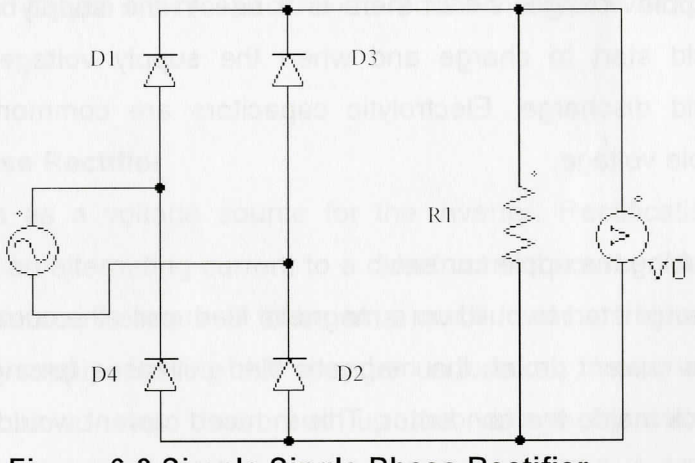


Figure 6-3 Simple Single Phase Rectifier

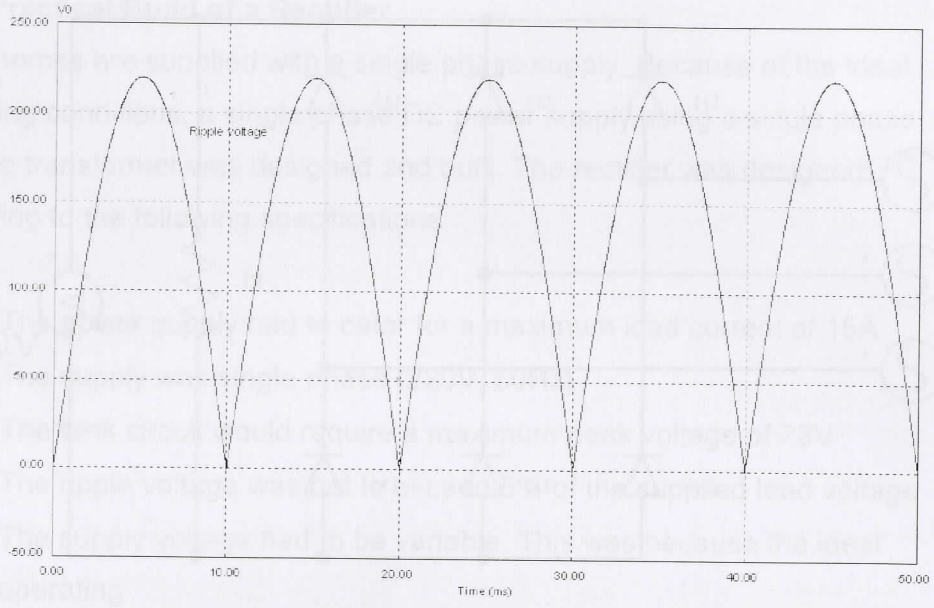


Figure 6-4 Output Wave Form (Voltage) Of A Single Phase Rectifier

6.3.2 Three Phase Rectifier

A transformer was used to control the total output power to the load according to the equation:

$$P = \sqrt{3} \cdot V \cdot I \cdot \cos\phi \qquad (6\text{-}3)$$

This equation is for a three phase supply (6.4). Fig 6.4 shows a much lower ripple than the equivalent single phase supply. With a single phase supply, all the current would be drawn from one phase; therefore a single transformer has to match the requirements of the load. However with a three phase variable transformer, current is drawn from all three phases. The solution incorporating the three phase topology was preferred, since this eliminated the need for a fairly large capacitor bank to minimise the DC ripple voltage.

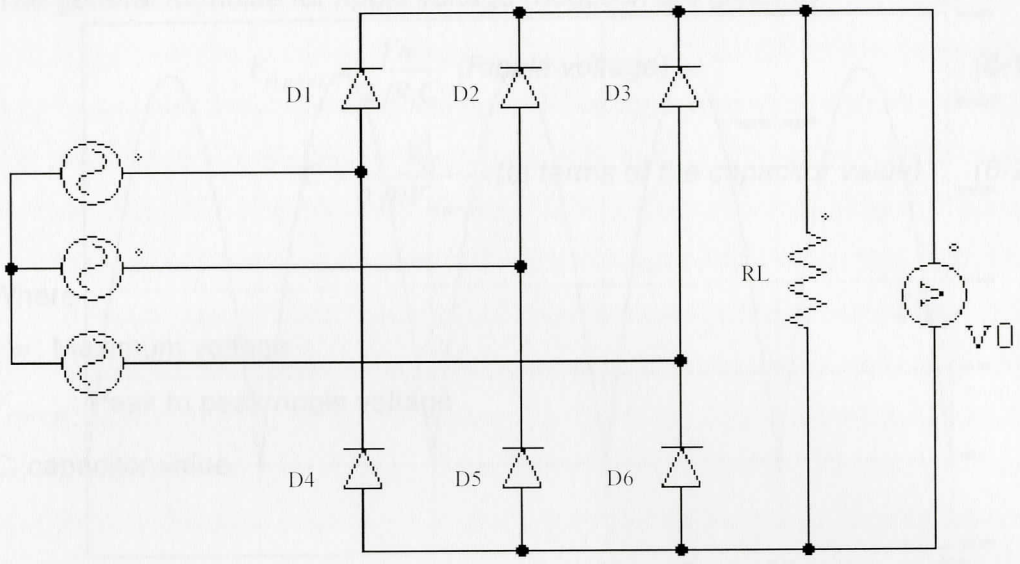


Figure 6-5 Three Phase Bridge Rectifier

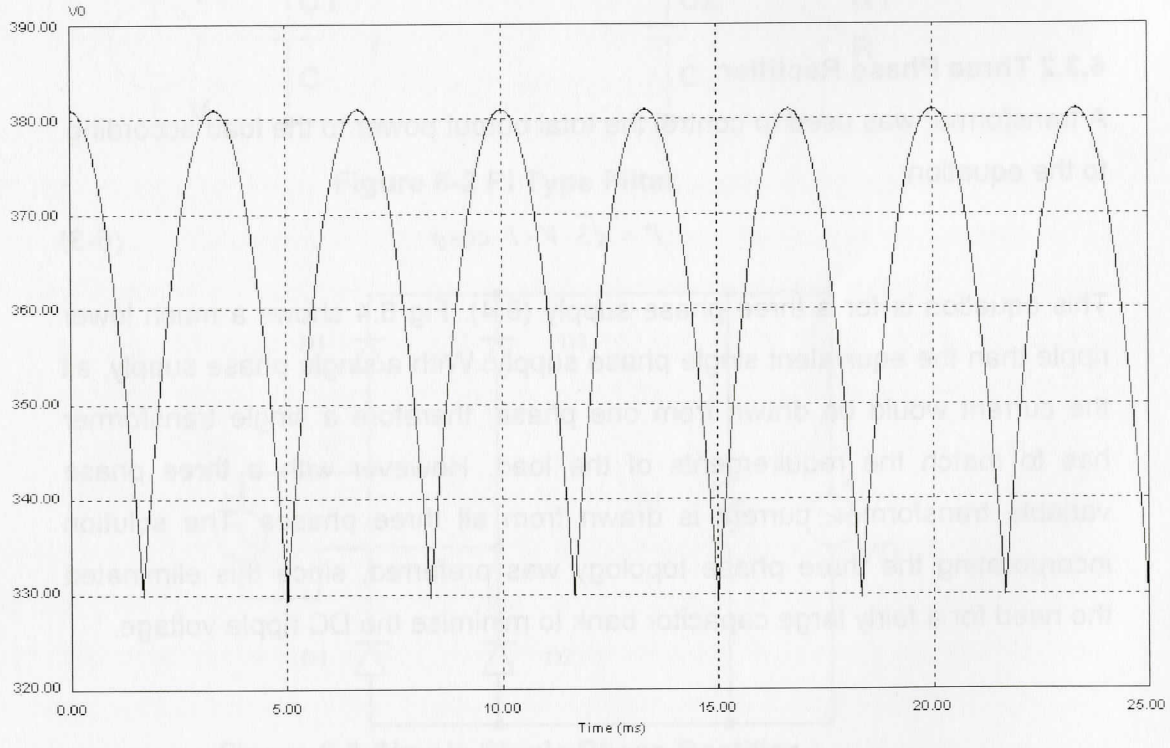


Figure 6-6 Output Wave Form (Voltage) Of A Three Phase Rectifier

6.3.3 Practical Build of a Rectifier

Many homes are supplied with a single phase supply. Because of the ideal operating conditions, a single phase DC power supply using a single phase variable transformer was designed and built. The rectifier was designed according to the following specifications:

- The power supply had to cater for a maximum load current of 15A
- The supply was single phase (220V, 50Hz)
- The tank circuit would require a maximum peak voltage of 73V
- The ripple voltage was not to exceed 5% of the supplied load voltage
- The supply voltage had to be variable. This was because the ideal operating
- Specifications had to be found.

A transformer was the most convenient way of stepping down the incoming supply. As mentioned prior, this would present a bulky and expensive solution. However this was preferential for experimental purposes. The transformer requirements were calculated by taking into account the needs of the load (apparent power). These values were matched up against the selected transformer.

$$P_{apparent} = V_p I_p = V_s I_s$$

= 73 x 15

= 1.1 KVA (turns ratio: 3:1)

The selected transformer was rated at 5KVA. Far greater than what was required and therefore this single phase transformer was used. This supplied a full bridge rectifier which resulted in a high ripple voltage of between 0v and the peak voltage of 103.237v (if the volt drops across the diodes were ignored). The resulting supply is commonly referred to as a pulsating DC supply. The peak inverse voltage and load current were calculated for the selection of the diodes.

These were calculated as follows:

- Peak inverse voltage (PIV)

$$PIV \geq V_m = \sqrt{2}V_{rms} = 103.7V \quad \text{(6-4)}$$

- Average output voltage

$$Vo_{avg} = \frac{2 \cdot V_m}{\pi} = 66.028V \quad \text{(6-5)}$$

- Peak load current (15A)

$$I_{peak} = \sqrt{2}I_{out} = 21.2A \quad \text{(6-6)}$$

- RMS diode current in the rectifier

$$Id_{rms} = \frac{I_o(avg)}{\sqrt{2}} = \frac{0.636 \times I_{peak}}{\sqrt{2}} = 9.524A \quad \text{(6-7)}$$

A full bridge rectifier topology was chosen. These were available as a single package or could be done using four bridge connected diodes. The SKB26/08 was chosen from the manufacturer Semikron. This was a package type single phase bridge rectifier with a maximum forward current of 22A and a reverse mode operating voltage of 800v. A simulation was done using a load resister of 4.86Ω with a supply peak Voltage 103.237V. This resulted in a load current of 21.213A (measured with the simulator).

The required capacitance was calculated using the following equations:

$$Vr_{(p-p)} = \frac{V_m}{2 \cdot f \cdot R_1 \cdot C_1} \quad \text{(6-8)}$$

Make C_1 (equation 6-8) the subject of the formulae:

$$C = \frac{V_m}{2 \cdot f \cdot R_1 \cdot Vr_{p-p}} \quad \text{(6-9)}$$

$$C = \frac{103.237V}{2 \cdot 50 \cdot 4.56 \cdot 5}$$

= 42 484uF

The ripple current within steady state conditions reached a maximum current of 21.3A and minimum current of 20.41A. A ripple current of less than 1A was achieved and eliminated the need for an inductor. The simulation showed a ripple voltage of between 103.6v and 99.23v. The ripple voltage was less than 5v. The average voltage and current is 97.19v and 20A respectively. Practical implementation of such a circuit was difficult due to the high value of the capacitor at the required voltage.

A capacitor bank was used that consisted of an array of parallel connected capacitors. This was ideal since this configuration reduced the overall impedance of the C type filter and increased the capacitance as seen by the source. Each capacitor bank consisted of eighteen 980uF capacitors with a total capacitance of 17,640uf. Two banks of capacitors were used with a total capacitance of 35,280uf. Using the equation (6.8):

$$Vr_{(p-p)} = \frac{103.237}{2 \cdot 50 \cdot 4.86 \cdot 35280uf}$$

$$= 6.021\text{v ripple}$$

This was still found to be acceptable.

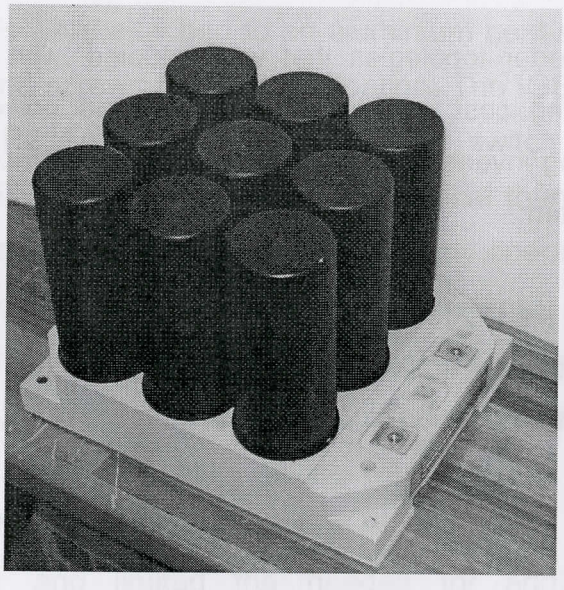


Figure 6-7 Capacitor Bank Used To Decrease the Ripple Voltage

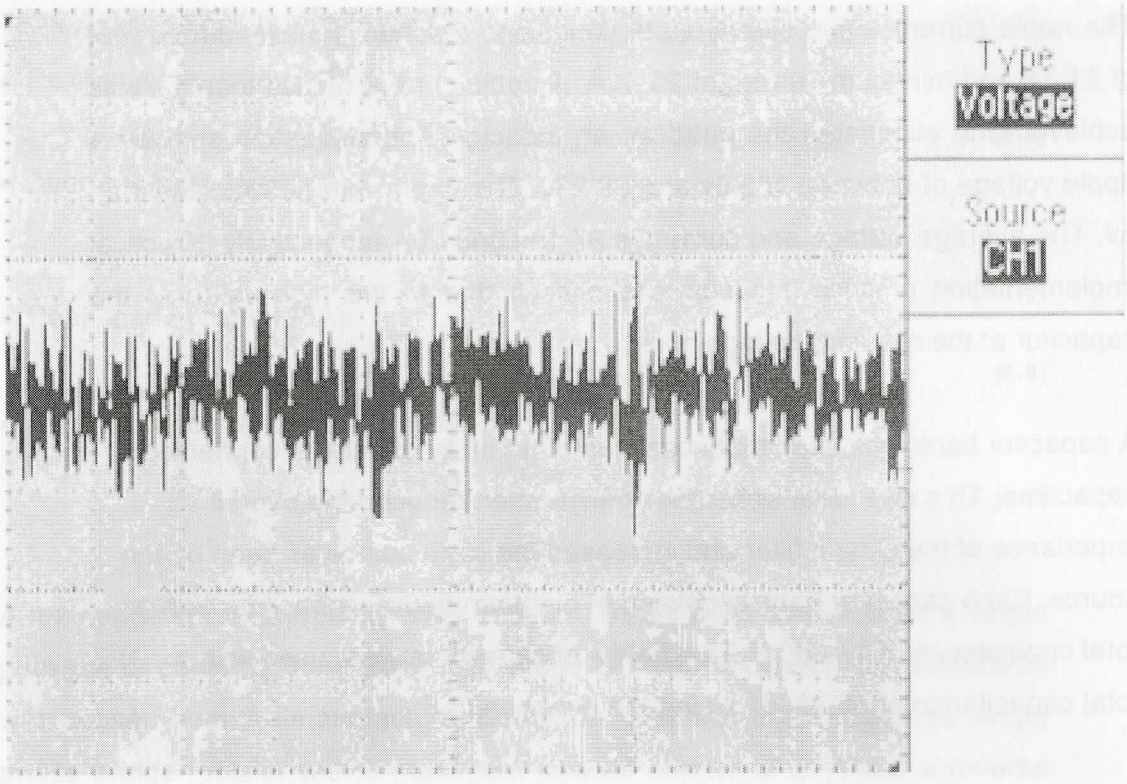


Figure 6-8 Rectifier Stage Testing: Ripple Voltage

The output of the rectifier was measured using a digital oscilloscope. The above figure shows the results of the measured voltage where the ripple voltage was less than 1v at an output voltage of 100v.

6.4 Inverter Overview

There were various inverter topologies that were studied, with differences between topologies being cost, operating frequency and power handling capabilities. The following inverter designs will be discussed since each one of the following were tested:

- H-bridge based upon the IR2110 driver
- Semikron stack inverter (SKHI 22A)
- Semikron stack inverter (SKHI 61)

6.4.1 The H Bridge Inverter Based Upon the IR2110 Driver

The first inverter design was one similar to the one built by Mr Khan for an induction heater smelter (I Khan, 2000). This used an IR2110 driver which consisted of a single end, high and low side driver. Therefore two drivers were used to drive both pairs of high and low side switches that made up the full bridge inverter. The driver circuit is illustrated in figure 6-9. This design did not include a current sensor. This device had a propagation delay of 120ns (turn on) and 95ns (turn off) (International rectifier, 1999). This is fairly reasonable when considering the required operating speed range of the H-bridge. Another attribute was that this MGD (Mosfet gate driver) could be driven by logic level signals as low as 2v. Hence a low power microprocessor that operates typically between logic levels of 0-3v may be used. Both devices may be turned off by providing a logic high signal on the shut down input (pin 11). This was not used, since the H-bridge was simply turned off by means of providing both the high and low inputs to the driver with logic low level.

The IR2110 driver could sink or source gate currents between 0.12-2A. The maximum load current that the inverter may provide was ultimately determined by the switching devices used. In this design, four IGBT (part number: IRG4PC40F) were used. This device had a maximum forward conduction current of 27A (Ic) and a reverse blocking voltage of up to 600V (Vces). The IGBTs were attached to an aluminium heat sink bar by means of heat sink paste and screws for heat dissipation. The IGBT gates were driven directly by the IR211A driver which received switch on signals from a microprocessor. This design was more economical than the second design; however the selected switching devices could only operate at resonant mode below a frequency of 20 kHz. This was considered sufficient for testing purposes but not for the final design. When the switching frequency was increased above 20 kHz, significant heat conduction was found at the high side switches. A faster switching device was needed. The microprocessor used to supply the logic signals was a PIC16F628. This device had an internal oscillator and limited the needed for additional hardware or components.

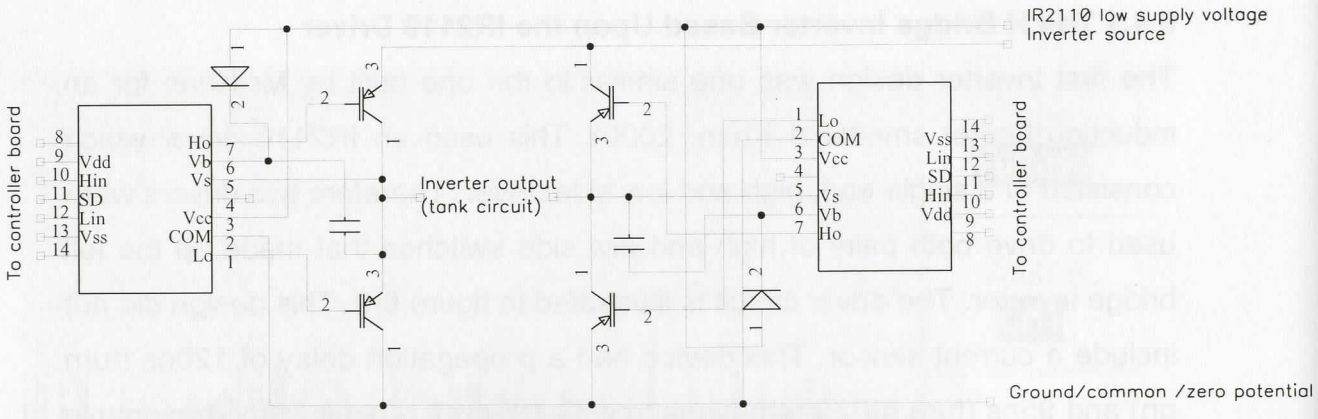


Figure 6-9: H Bridge Circuit Using Two IR2110 Drivers

6.4.2 The H Bridge Inverter Based Upon the SKHI 22A Driver

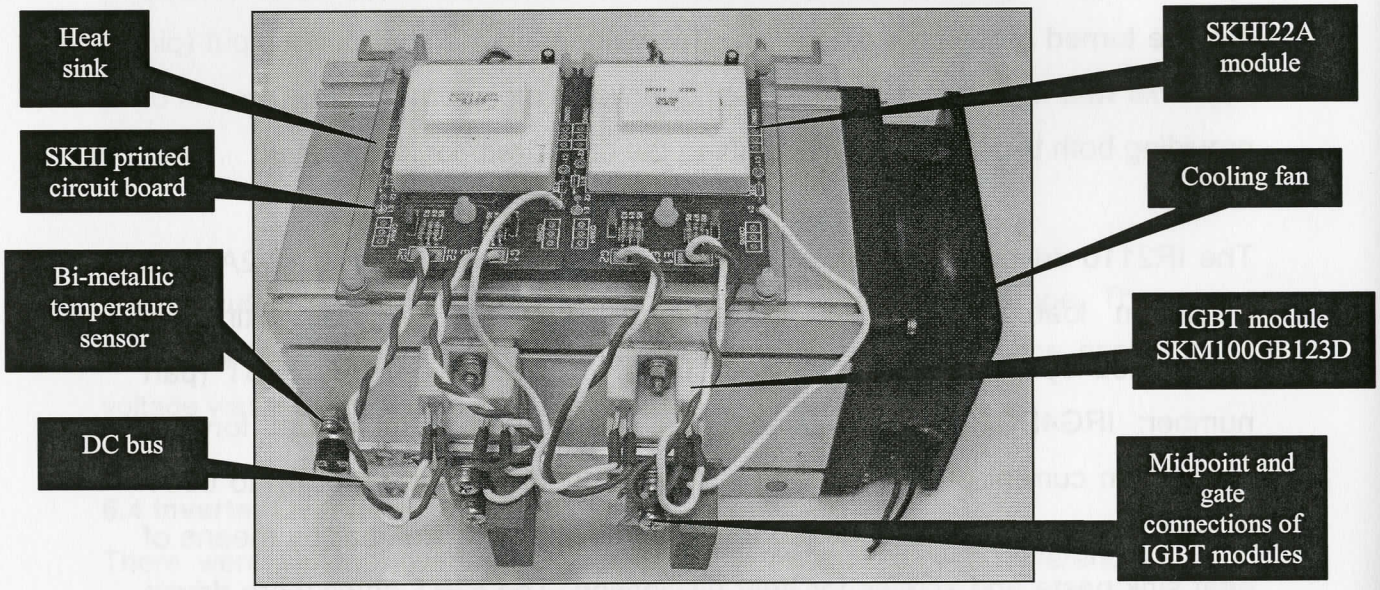


Figure 6-10: The Semikron Stack Inverter

The second inverter design was the Semikron stack inverter (illustrated in figure 6-10). This more robust solution than the previous design and consisted of a self contained unit that housed all the drivers and switching devices necessary for a full bridge circuit. This design was more expensive than the first inverter topology. The manufacturer of the stack, Semikron has provided a full inverter solution and all that was needed externally was a DC source and controller unit to provide the pulse train signals and for error monitoring.

The stack inverter consisted of the following parts:

I. Cooling System (Heat Sink, Cooling Fan And Bi-Metallic Temperature Sensor)

The IGBT units were mounted onto an aluminium heat sink block with internal aluminium chambers. This block dissipated any excess heat from the IGBT modules. A bi-metallic temperature sensor was attached to the heat sink block. When the temperature of the block started to rise, the two metal strips found inside the temperature sensor would expand and close a set of internal contacts. This was used to operate a cooling fan that forced air down the internal chambers of the block.

II. SKM100GB123D (IGBT Modules)

The main advantage of using the IGBT modules (SKM100GB123D) from Semikron was that the unit consisted of an interconnected high and low side IGBT's with the following available output connections (Semikron, 2005):

- A midpoint output: This essentially was used as a reference point for the high side signal to float on top of this reference voltage.
- High and low side gate outputs: For switching the high and low side switches
- High side collector output: To connect to the positive DC bus rail
- Low side emitter output: To connect to the negative bus rail

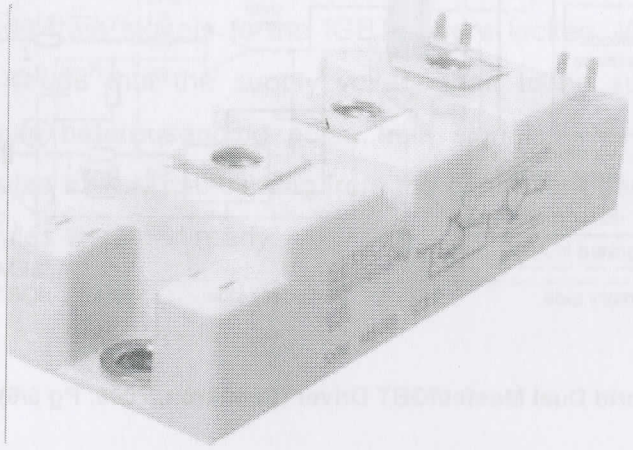


Figure 6-11 SKM100GB123D IGBT Modules (Semikron, 2005)

III. SKPC Board & SKHI22A (IGBT Driver Module)

Semikron has provided an IGBT driver board together with a driver module that was used for controlling the IGBT modules. The driver board required 15V supply voltage, ±15V logic input for the high and low side gate triggers. In addition an error output was also present for the monitoring of any errors. Fundamentally, everything revolved around the SKHI21A driver module. The internal structure is illustrated in figure 6-12. The explanation of this device begins with the two pulse transformers that divide the module into a primary and secondary side. The first pulse transformer was used to isolate the incoming and outgoing logic signals between the controller board and secondary side of the pulse transformer. Therefore this bidirectional pulse transformer delivered signals with relevance to turn-on and turn off gate signals for the IGBT's. Lastly the pulse transformer also provided the error feedback between the primary and secondary side. The second pulse transformer provided an isolated supply voltage for the IGBT driver circuits (Semikron, 2006).

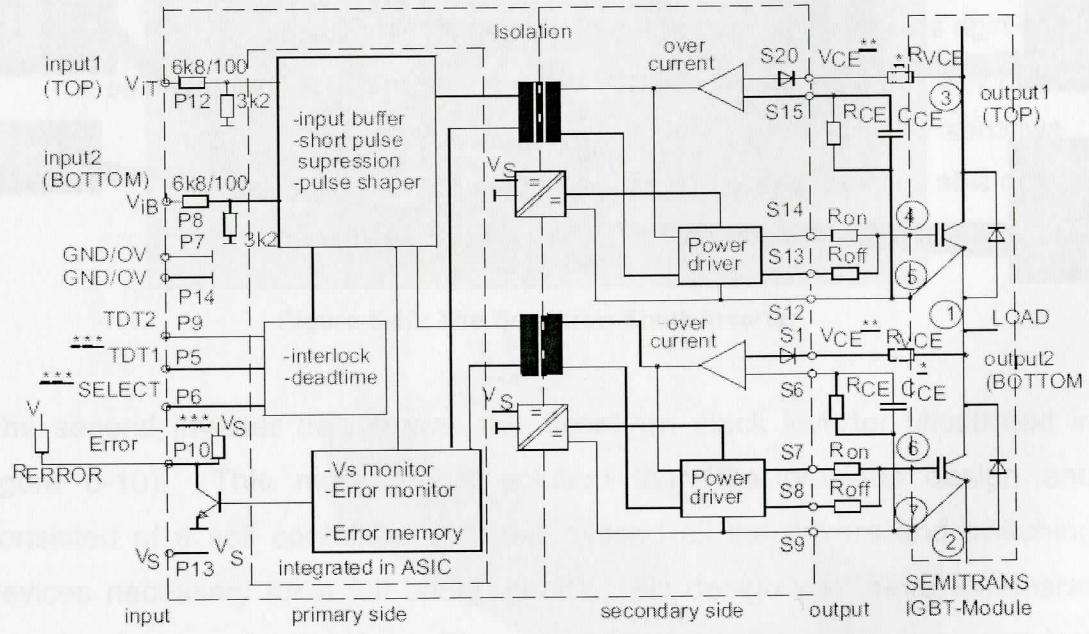


Figure 6-12: Hybrid Dual Mosfet/IGBT Driver (Semikron, 2006, Pg 5/6)

The SKHI22A module consists of an interlock and dead time generator which prevents both low and high side IGBT's being simultaneously on. This meant that the pulse train signals supplied to the driver module did not have to incorporate any dead time since this was already catered for by the driver modules. This adjustable dead time (through a series of resistors found on the board) had to be longer than the turn off time of the IGBT. The secondary side consisted of two symmetrical driver switches. These switches consisted of a gate driver and a Vce monitoring circuit. For the secondary side of the driver, the power outputs were provided by MOSFETs. Through the source of these MOSFETs by means of external resistors, the turn on (through R_{on}) and turn off (through R_{off}), switching speed was set (Semikron, 2006, pg1). The IGBT was switched on by the driver at +15V (through R_{on}) and turned off at - 7 V (through R_{off}). Safety features of the hybrid module included short pulse suppression which prevented pulses having a time span of less than 500ns from turning any of the IGBT's on. An under voltage protection feature generated an error signal when the supply voltage dropped below the required 15V supply. Another safety feature was Vce monitoring which essentially controlled the collector emitter voltage of the IGBT during the on state. Vce was limited to 10V by the driver module. An error signal was generated when the steady state collector emitter voltage of the IGBT exceeded the reference voltage (Vce_{ref}). All errors signals were monitored by the controller board by means of the error signal output. When an error did occur, all pulses train signals to the IGBT's were locked. When testing the device it was found that the supply voltage had to be supplied to these controller signals before sending pulse train signals. This was solved by delaying the pulse train signal coming from the controller board to ensure that the driver modules were first ready.

6.4.3 The H Bridge Inverter Based Upon the SKHI 61 Drivers

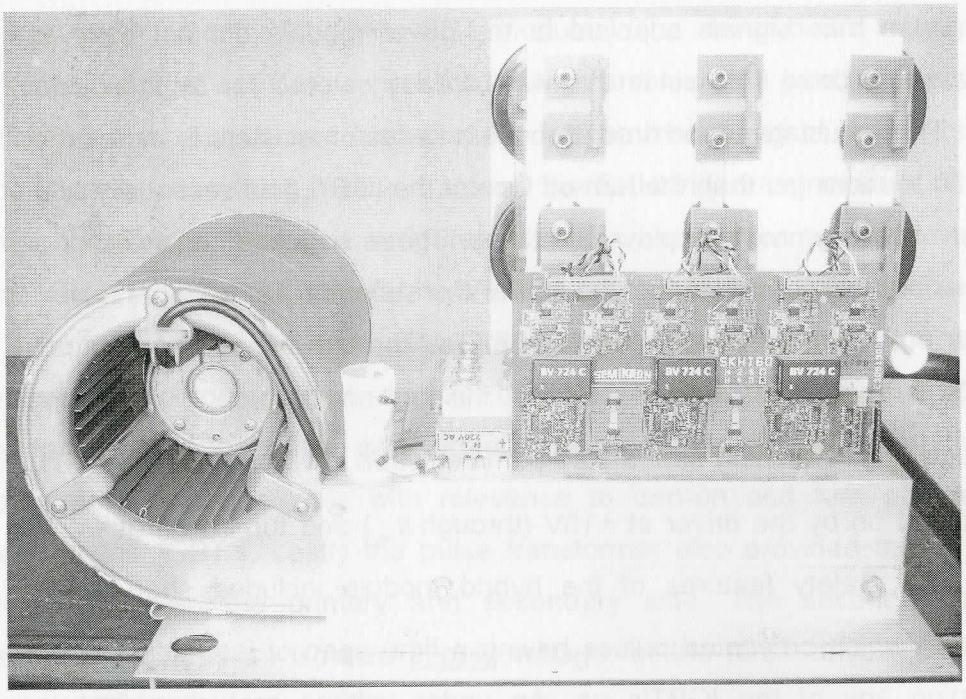


Figure 6-13: Illustration of A SKHI 61 Semikron Stack

The SKHI 61 driver operation is similar to that of the SKHI22A module. This stack also consists of a three phase rectifier and capacitor filter circuit built into the full stack. This inverter also consists of three pairs of high and low side IGBT modules, similar to the SKM100GB123D. All units were mounted on an aluminium base. This aluminium base was mechanically coupled to the cooling fan which was much larger than the stack based upon the SKHI 22A design. The advantage of this design was that it made using a three phase supply much easier. Also an additional rectifier circuit was not needed to be built as in the case with the other two modules. The three phase rectifier meant that current would be drawn from three phases and not just one. Also the advantage of using a three phase power supply was a much less ripple after rectification than what may be found after rectifying a single phase supply.

6.5 The Element Design

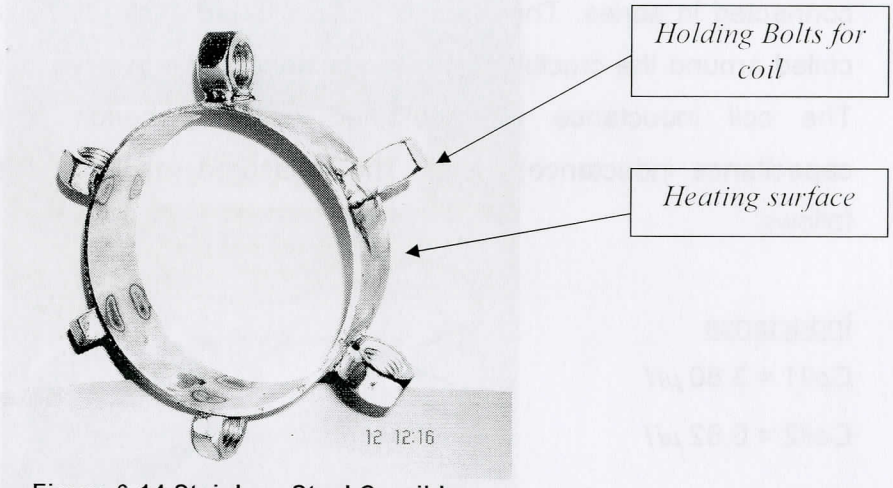


Figure 6-14 Stainless Steel Crucible

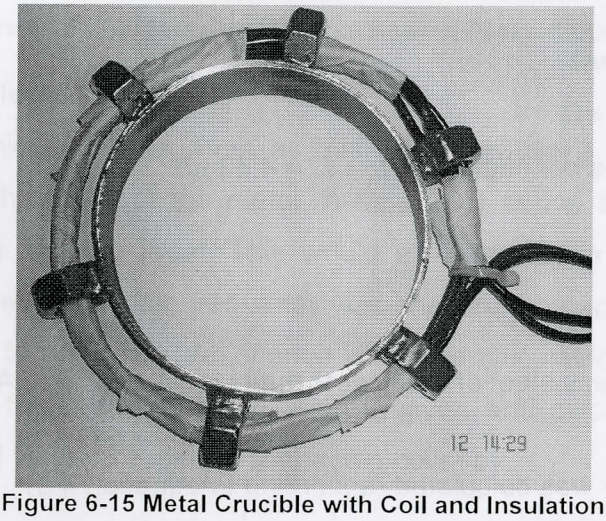


Figure 6-15 Metal Crucible with Coil and Insulation

Above is an illustration of the crucible (figure 6-14 & 6-15). The crucible was made out of stainless steel because it had many desirable properties. This metal would not easily oxidise in water, it had a fair amount of permeability and thermal conductivity. The crucible design was a 100mm in internal diameter and 40mm in width stainless steel cylinder with six 40mm stainless bolts attached all around it. These bolts were used to support the 5mm laminated copper conductor which made up the working coil. This coil was then moulded into fibre glass to insulate the expected high current carrying copper core from water. There were two coils used. The first coil only had one turn and the second coil had two turns. Two sets of coils were used because it was difficult to insert many turns around the crucible using the same wire due to the thickness of the cable used.

However the total inductance would be the sum of the two coil values when connected in series. The inductor used a 5mm thick copper rod which was coiled around the crucible using the guidance bolts welded onto the cylinder. The coil inductance was obtained using a bench RCL (resistance, capacitance inductance) meter. The measured results of the coil were as follows:

Inductance

Coil1 = 3.80 μH

Coil2 = 0.82 μH

Coil resistance

Coil1 resistance =9.3 $m\Omega$

Coil2 resistance = 4.5 $m\Omega$

Total inductance (series connected) = $L_1 + L_2$ = 4.62 μH

Crucible

Resistance =36 $m\Omega$

Permeability (for stainless steel of the lowest purity level) = 1 (*BSSA, 2008*)

The coupling efficiency was calculated (according to equation 4.9)

$$\eta = \frac{1}{1+\sqrt{\frac{13.8m}{36m \cdot 1}}}$$

=61.761%

The permeability of the metal was expected to be much higher than one.

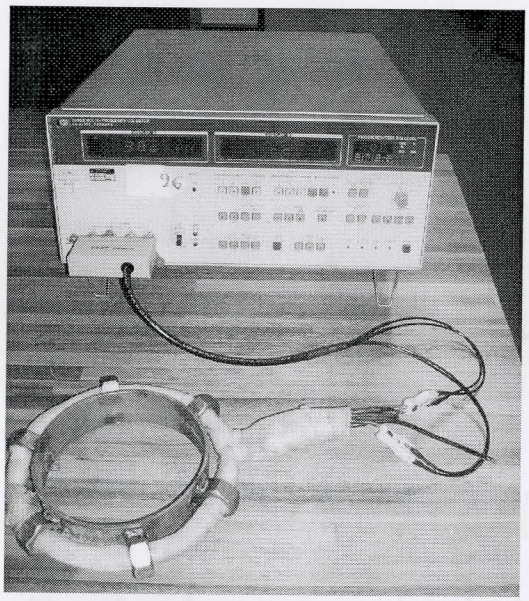


Figure 6-16: Coil Measured Using a Hewlett Packard LCR Mater

6.6 Tank Topology

The crucible thickness was 4mm as this would require a low frequency to penetrate the thickness of the metal. A frequency above the audible range (about 20 kHz) is more ideal. This would eliminate minimal losses due to sound. If the lowest possible frequency was chosen, the capacitor needed for the tank circuit to operate at resonance would be calculated by manipulating the resonance frequency formulae. This is given and calculated (using the sum of both coil values i.e. series connected coils) by:

$$C = \frac{1}{4\pi^2 \cdot f_{res}^{\ 2}} \cdot \frac{1}{L} \qquad (6\text{-}10)$$

$$= \frac{1}{4 \cdot \pi^2 \cdot 20000^2} \cdot \frac{1}{4.62\mu}$$

$$= 13.7 \text{ uF}$$

The practical value of the capacitor that was used was 10uF. A FFT analysis was done using the simulator.

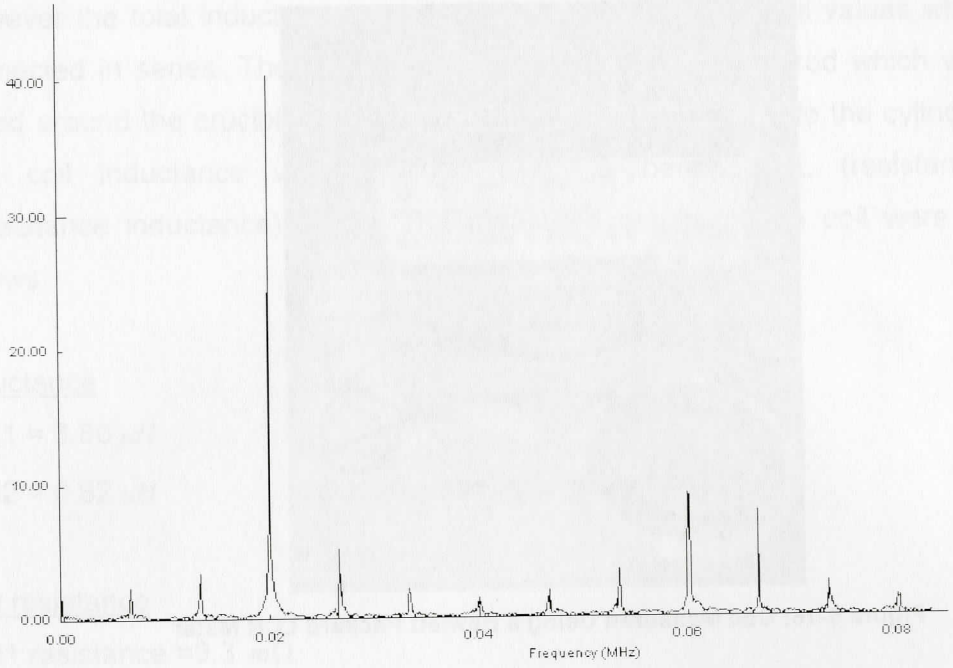


Figure 6-17 FFT Simulation Results of Series Tank Circuit

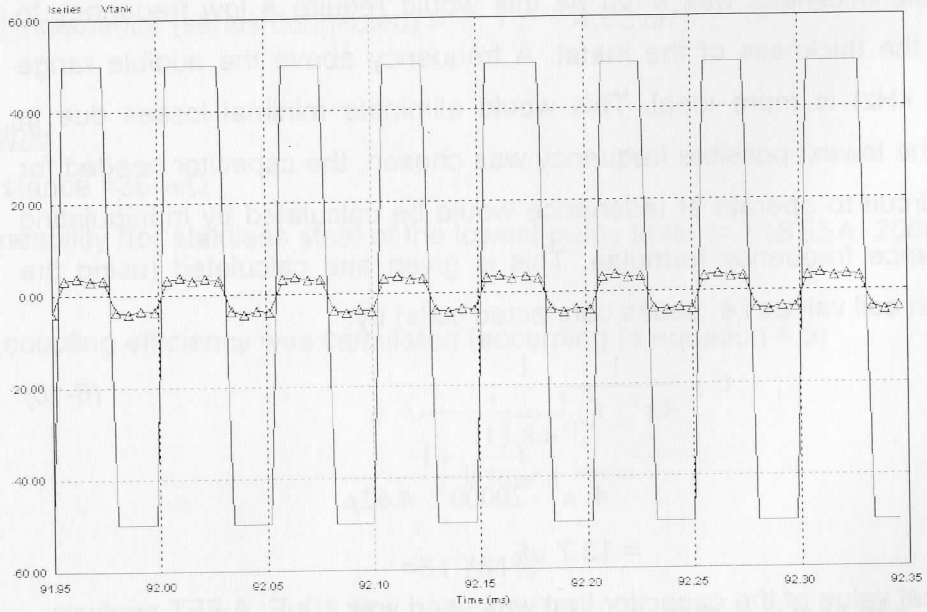


Figure 6-18 Power Simulation Waveforms of Tank Circuit

The Pspice simulation shows a high gain at the expected resonant frequency. The tank circuit being supplied by a square wave supply would produce high gain spurs at lower frequencies to the fundamental. The simulation fails however to illustrate this. The simulation was done using a 50V supply. From the simulation, it was concluded that the current (Iseries: triangle wave) was expected to alternate between ±3.86A. The power supply of course matched this.

6.7 Control Board Design

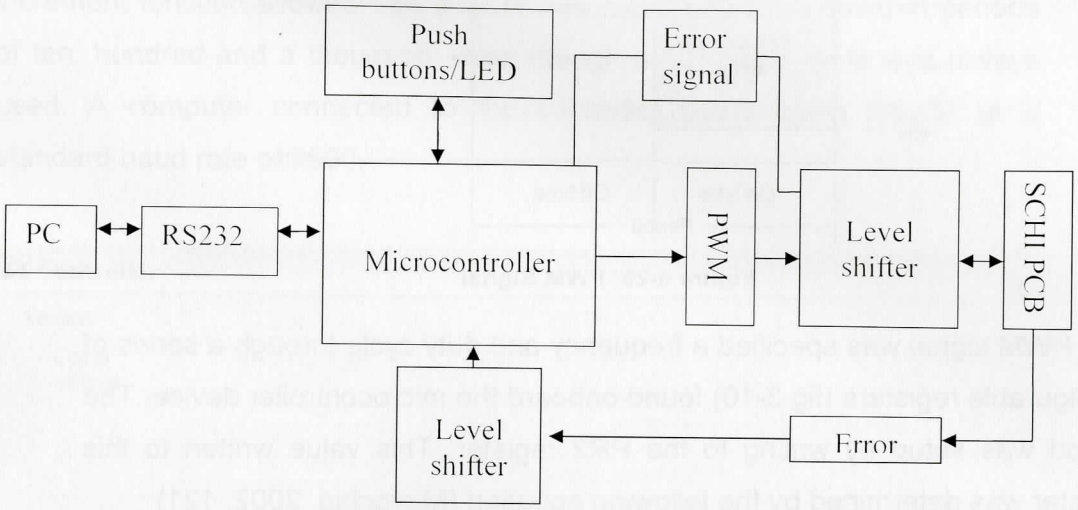


Figure 6-19: Outlay of Controller Board

The controller board consists of a Microchip PIC18F452. This device was programmed using Sourceboost C compiler. This device was chosen because of its many peripheral features that eliminate the need for additional hardware. This includes PWM generator and an analogue to digital converter. This device also implemented communication protocols that were used to communicate to peripheral devices such as a computer. The PWM signal was generated by the microprocessor. The problem with this was that the microprocessor generated a pulse train at a logic high level of +5v and not at +15V as required by the driver board. This was easily solved by use a logic level shifter, namely the CD4504B (Texas instruments, 2004) (fig 7.16). A pulse train consist of a series of high and low pulses. The two IGBT drivers needed two pulse train signals at 180° out of phase with one another. In other words when one signal was at a high logic level, the other would be a low logic level. Generating a PWM signal with a microprocessor (peripheral driven) works best for the application because the signal can easily be altered and the microprocessor could be used to perform other control functions as well.

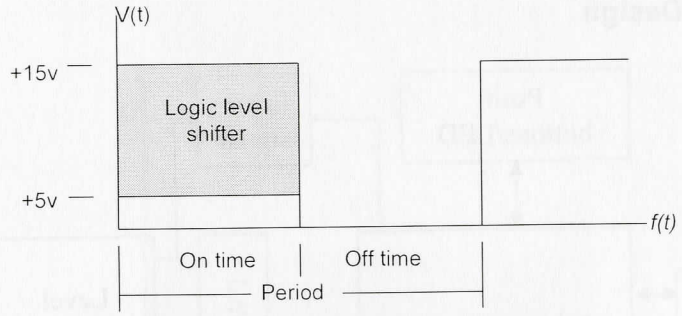


Figure 6-20: PWM Signal

The PWM signal was specified a frequency and duty cycle through a series of configurable registers (fig 3-10) found onboard the microcontroller device. The period was setup by writing to the PR2 register. This value written to this register was determined by the following equation (Microchip, 2002, 121)

$$PWM_{period} = \{PR2 + 1\} \cdot 4 \cdot Tosc \cdot TMR2_{prescale} \qquad (6\text{-}11)$$

Where

PR2: value to be written to this register for a specified period

$Tosc$: Oscillator time that is determined by the crystal oscillator

$TMR2_{prescale}$: rescale value of the associated timer

The frequency was determined by:

$$f = \frac{1}{PWM_{period}} \qquad (6\text{-}12)$$

For the inverter duty cycle (50%) the register that had to be configured was the CCPR1L and to the CCP1CON register. These were used to setup the ten bit resolution duty cycle of the PWM generator. The value to be written to is specified by use of the following equation:

$$\text{PWM duty cycle} = (\text{CCP REG}) \bullet T_{osc} \bullet (\text{TMR2 pre-scale value}) \qquad (6\text{-}13)$$

A second pulse was configured to provide the second pulse train (inverse of the other). This was set up in a similar way. It was necessary to be able to seamlessly change the frequency without needing to reprogram the processor. A program was written using visual basic in order to communicate to the controller (Fig 6.21). The GUI was used to set and store a specified frequency in the controller. Four frequencies could be stored with variable

duty cycles. All frequencies could also be read back using the GUI. An increment function allowed that frequencies could be incremented in periods of ten, hundred and a thousand, even though a 50% duty cycle was always used. A computer connected to the controller board using RS232 at a standard baud rate of 9600.

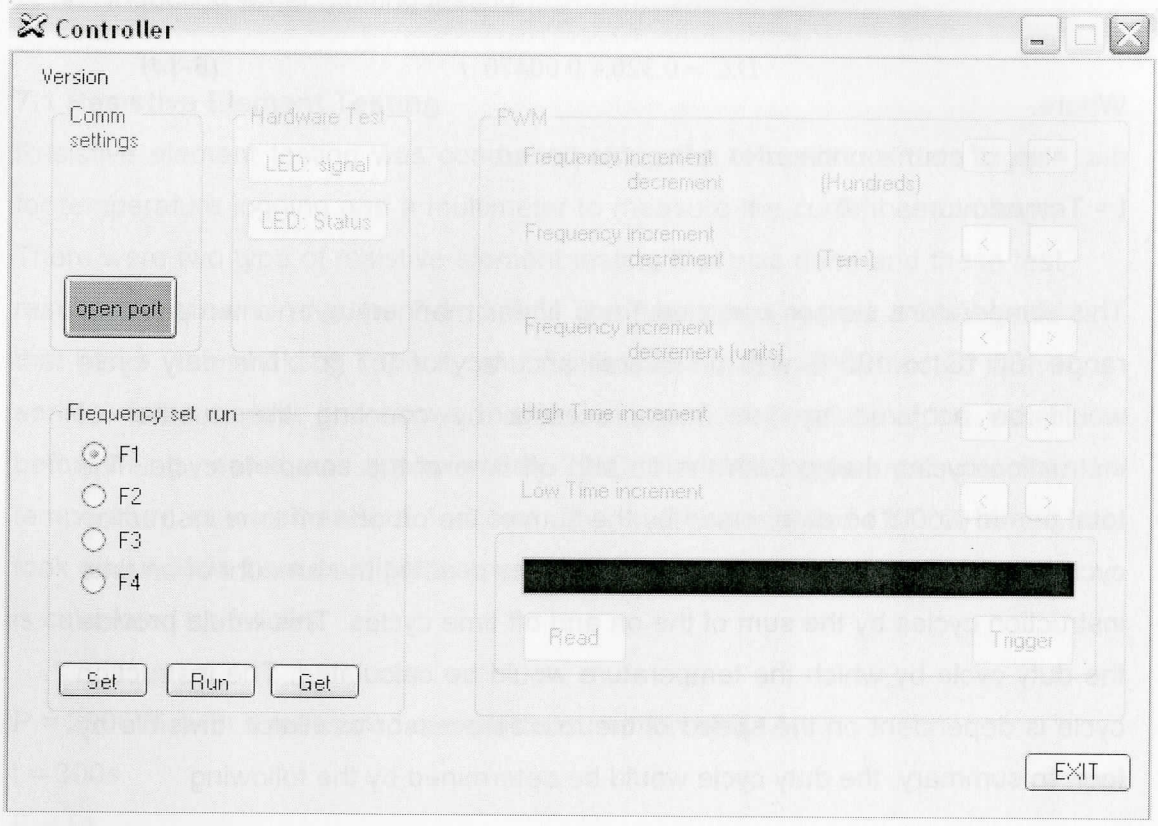


Figure 6-21 GUI of Controller

6.8 Temperature Sensing and Data Logging

A data logger was built in order to conduct the comparative study. The main interest was the response with regards to temperature versus time. A digital sensor was connected to a Microchip PIC16F628. Data was relayed from the microcontroller via RS232 to a computer where all data was time stamped using the computer time. A developed software program was used to create a text file consisting of all logged data. This "engine" had to run in order for any logging to be done. All data was written to a text file and this was done in a format that enabled the text file to be easily imported into an excel spread sheet where a graph was drawn using this data. The temperature sensor that

was used was a Smartec SMT16030 digital temperature sensor. This device worked by providing an output square wave signal. The frequency of the square wave bared no relevance on the temperature but the duty cycle of this frequency was used to calculate the temperature according to the following equation (Smartec, 2005):

$$D.C = 0.320 + 0.00470 \cdot t \qquad \textbf{(6-14)}$$

Where:

d.c. =No. of counts ontime/No. of counts period

t = Temperature in °C

This temperature sensor operated (in a linear manner) over a temperature range -30 °C to 130°C with an overall accuracy of 0.7 °C. The duty cycle would be acquired by the microprocessor by counting the number of instruction cycles during both the on and off time of the complete cycle. The total period would be determined by the sum of the on and off time instruction cycle counts. The duty cycle was calculated by dividing the amount of on time instruction cycles by the sum of the on and off time cycles. This would provide the duty cycle by which the temperature would be calculated. The instruction cycle is dependent on the speed of the microprocessor oscillator, divisible by four. In summary, the duty cycle would be determined by the following:

$$D.C = \frac{no.of.counts_{on-time}}{no.of.counts._{period}}$$

The output frequency of the temperature sensor was 4 kHz. The period would therefore be 250us. To reduce the margin for error, the time of the instruction cycle had to be much less than the period of the temperature sensor. The microprocessor had an onboard 4MHz RC oscillator. This would allow for a maximum error of 62.5ns. With the use of an external high speed crystal oscillator (20 MHz), the margin for error would be reduced to 12.5ns. Therefore the high speed crystal was used.

Chapter 7 Testing and Conclusion

There were a number of tests that were conducted. They may be summed up as follows:

- Resistive element testing
- Inverter and crucible testing
- Induction water heating testing

7.1 Resistive Element Testing

Resistive element testing was conducted using the temperature data logger for temperature logging and a multimeter to measure the current and voltage. There were two type of resistive element testing that was done and these test results are shown in figures 7-1 to 7-5. The first type involved a 2kW kettle that had a water holding capacity of 1.7 litres. The test was conducted in the earlier winter months and shows that the ambient temperature of the water before being heated was approximately 23°C. The data logger measured the temperature in increments of 1second. The water was boiled (100°C) and it took about 300s from its initial temperature of 25°C. The energy consumption is calculated as follows:

P = 2000W (with a measured current consumption of 9.1A)

t = 300s

E = Pt

= 600kJ

Comparing this to the theoretical value using formulae 5.4:

c = 4,180

ΔT = 100-23 = 77

m = 1.7l

$Q = 1.7 \times 4.180 \times 77 =$ 547.162kj

The difference between the theoretical value of 547.162kJ and practical value 600kJ may be due to excessive heat loss during the heating process. Steam escapes from the kettle while heating the water and the vessel that contains the water also absorbs some of the heat. I a similar manner test was also conducted using a geyser with a 3kW element. The data logging was done in increments of 10 seconds and figures 7-4 to 7.5 shows test results. The storage tank was a plastic drum which allowed both the resistive element and IWH element to be inserted. Unfortunately the storage tank did not have a cover and therefore the test was more prone to heat loss. Figure 7.4 illustrates the rate at which this heat loss occurred. The capacity of the storage tank was 45l. Once again it can be seen that the ambient temperature of the water was around 23°C. Many of these tests were conducted around 20h00- 01h00 (night time). As in the case with most domestic geysers, the water inside the tank is not expected to reach boiling point. The element was switched off at about 70°C. The energy consumption is calculated as follows:

Measured current consumption = 13.8A

Measured supply voltage = 221.2v

t = 302 * 10 = 3020s

E = 3020 x 221.2 x 13.8

= 9218.731kJ

Comparing this to the theoretical value using formulae 5.4:

c = 4,180

ΔT = 70-23 = 47

m = 45l

Q = 45 x 4.180 × 47 = 8847.8kJ

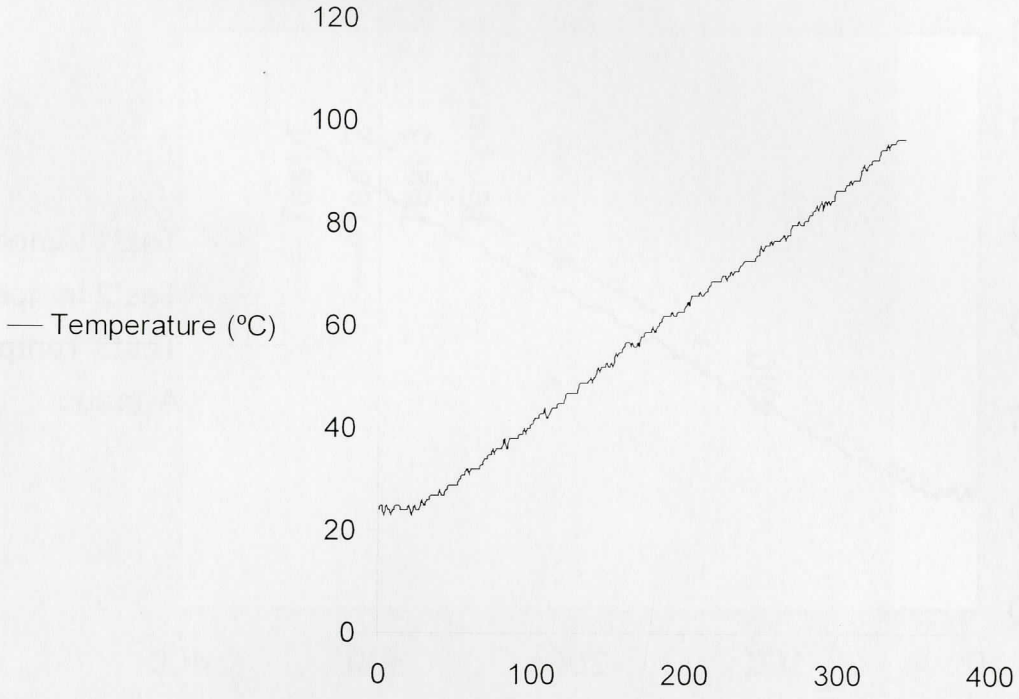


Figure 7-1 Boiling Kettle Test 1(2kW)

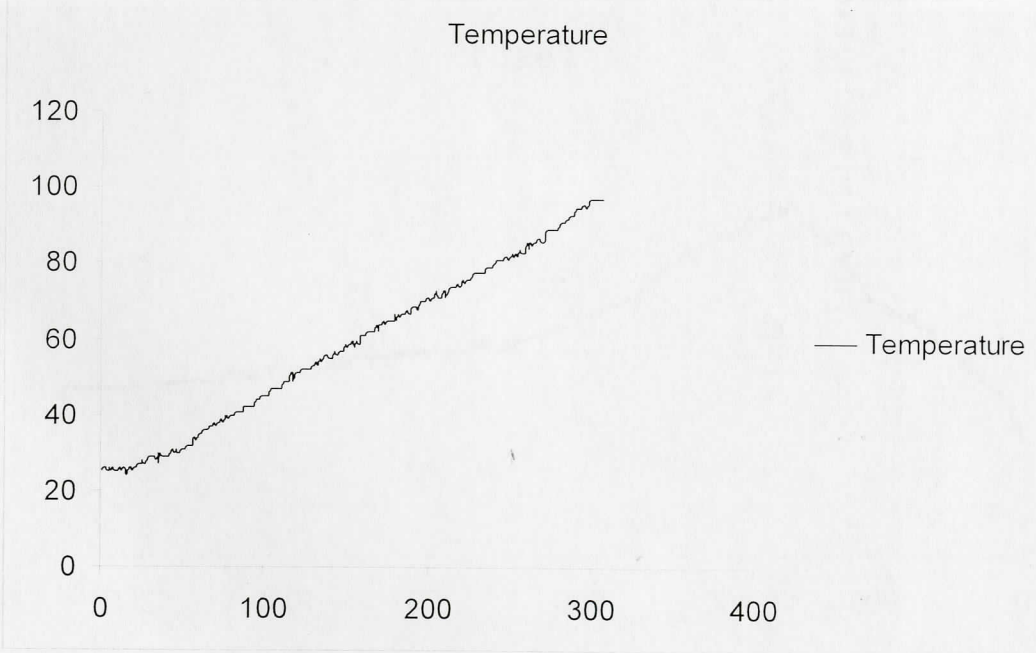


Figure 7-2 Boiling Kettle Test 2 (2kW)

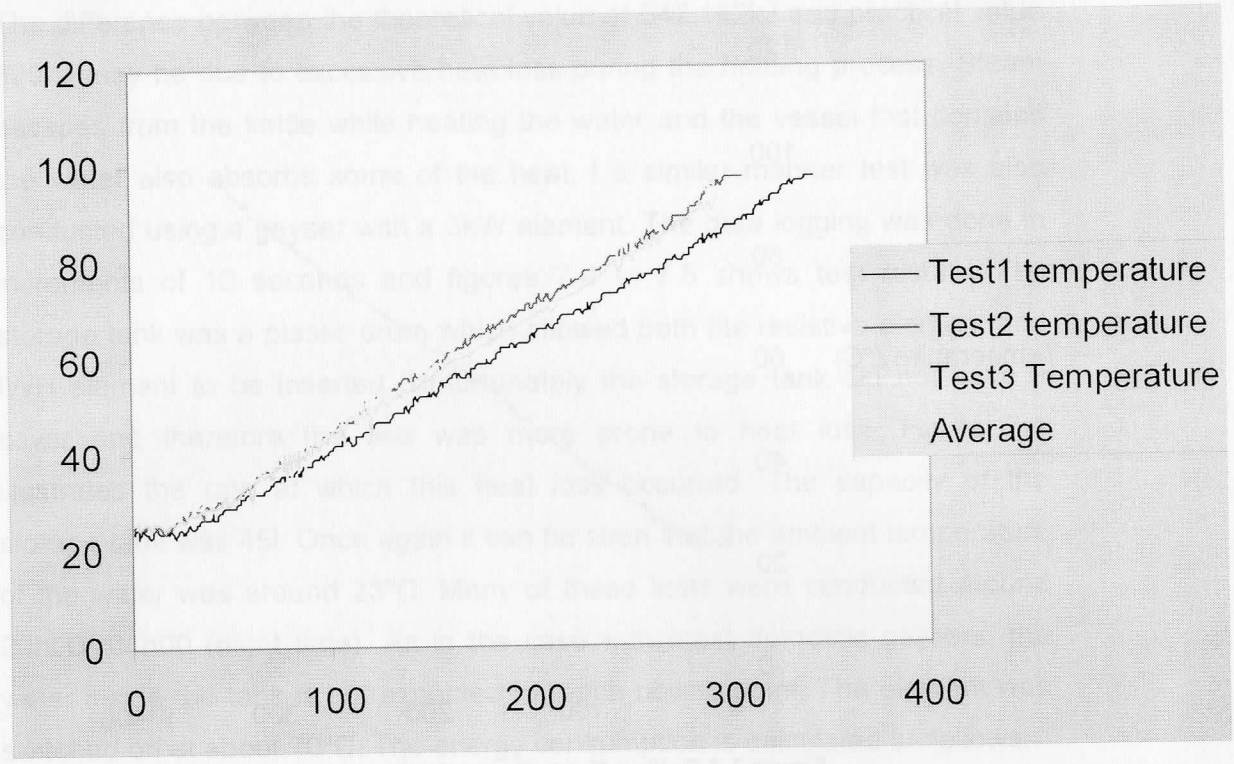


Figure 7-3 Boiling Kettle Test 1/2/3/Avg (2kW)

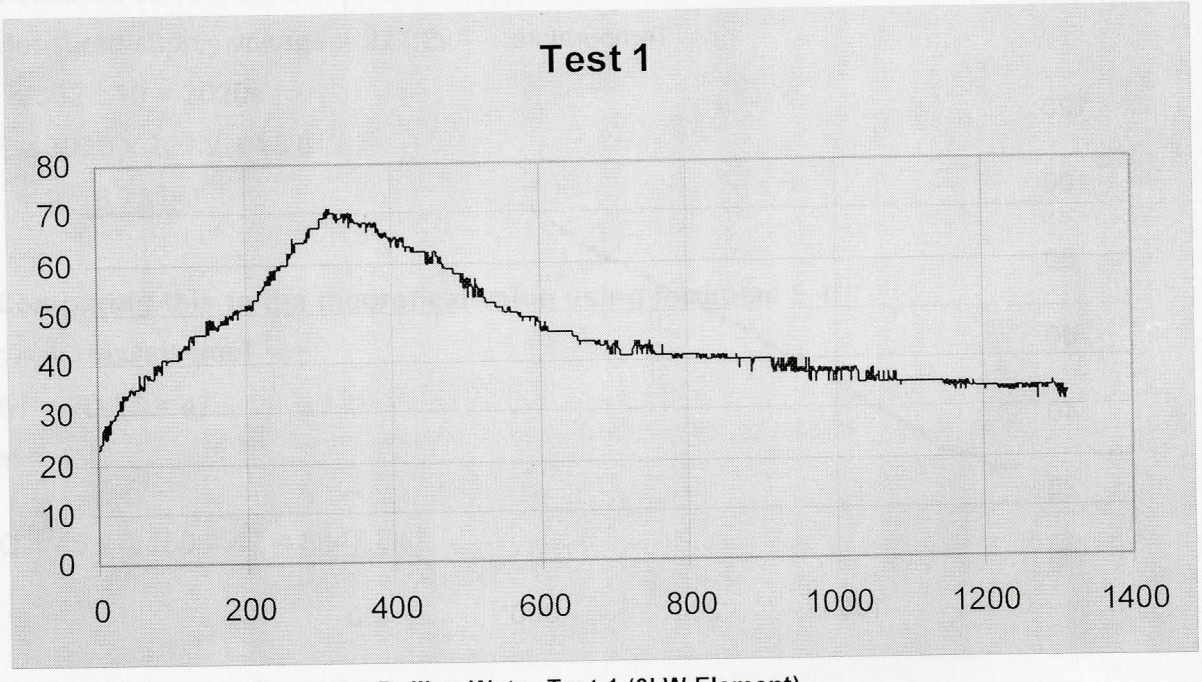


Figure 7-4 Boiling Water Test 1 (3kW Element)

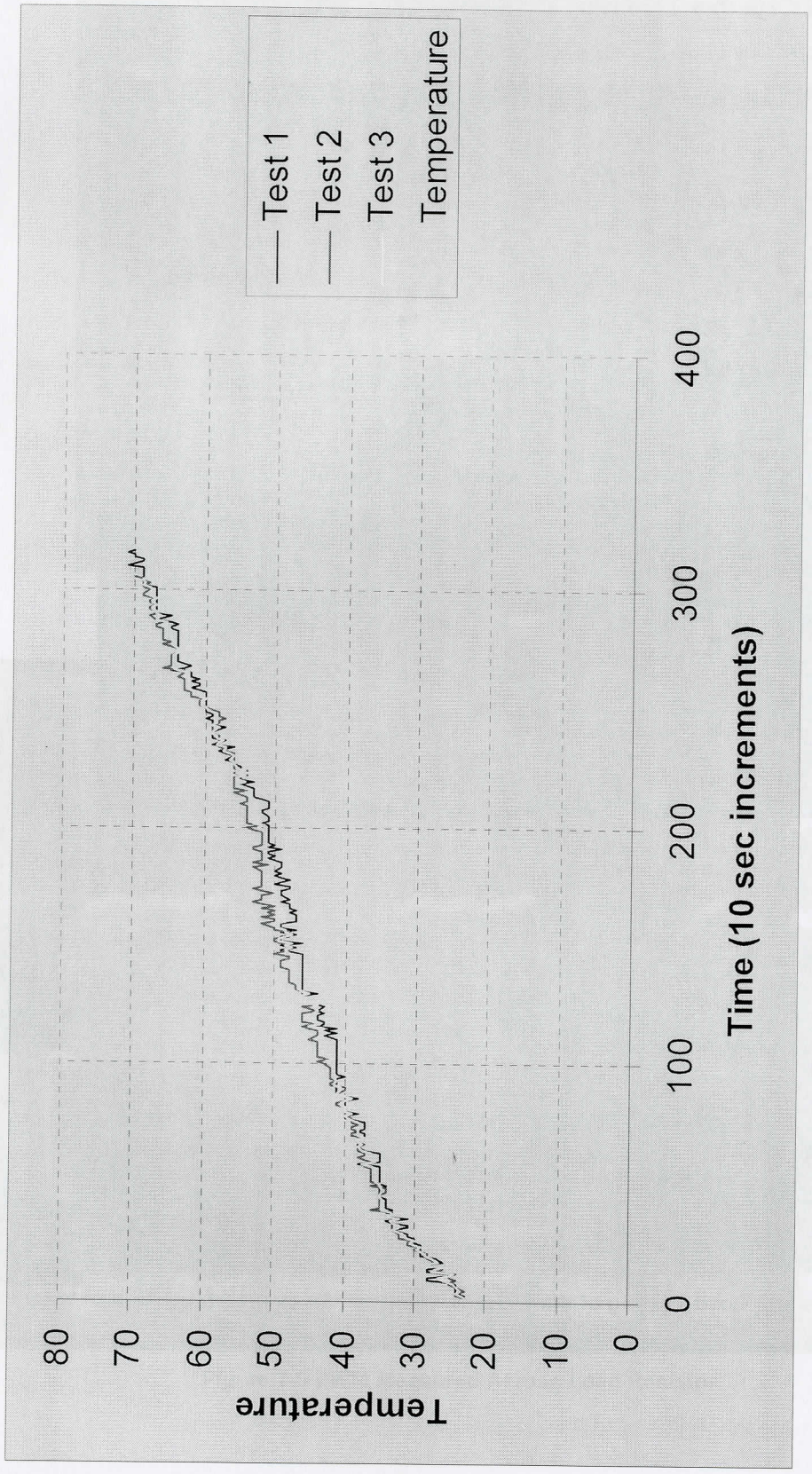


Figure 7-5 Boiling Water Test 1/2/3/Avg (3kW Element)

7.2 Inverter and Crucible Testing

7.2.1 Inverter Testing Using a Resistive Load

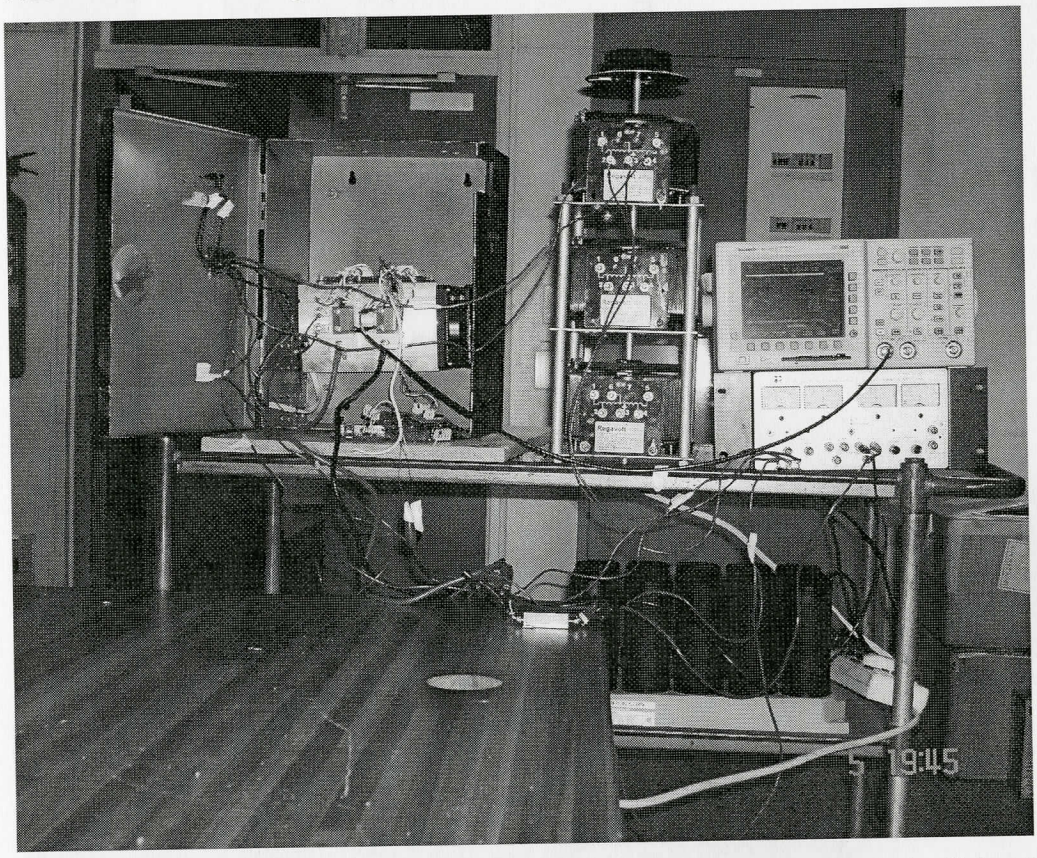


Figure 7-6: Resistor Load Testing of the SKHI 22A Semikron Stack Inverter Using A Single Phase Supply

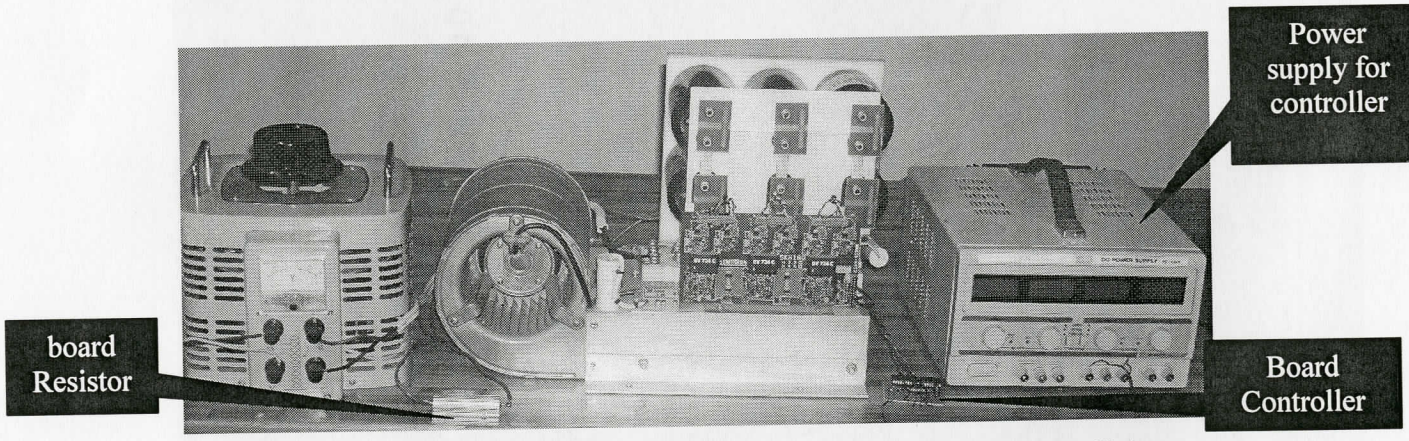


Figure 7-7: Resistor Load Testing of the SKHI 61 Semikron Stack Inverter Using a Single Phase Supply

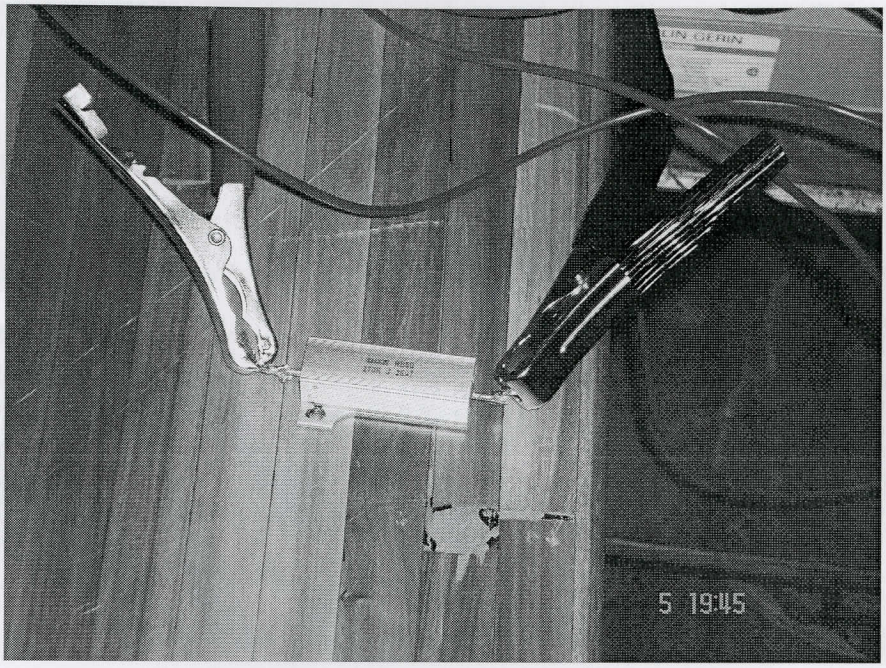


Figure 7-8 Resistor under Test

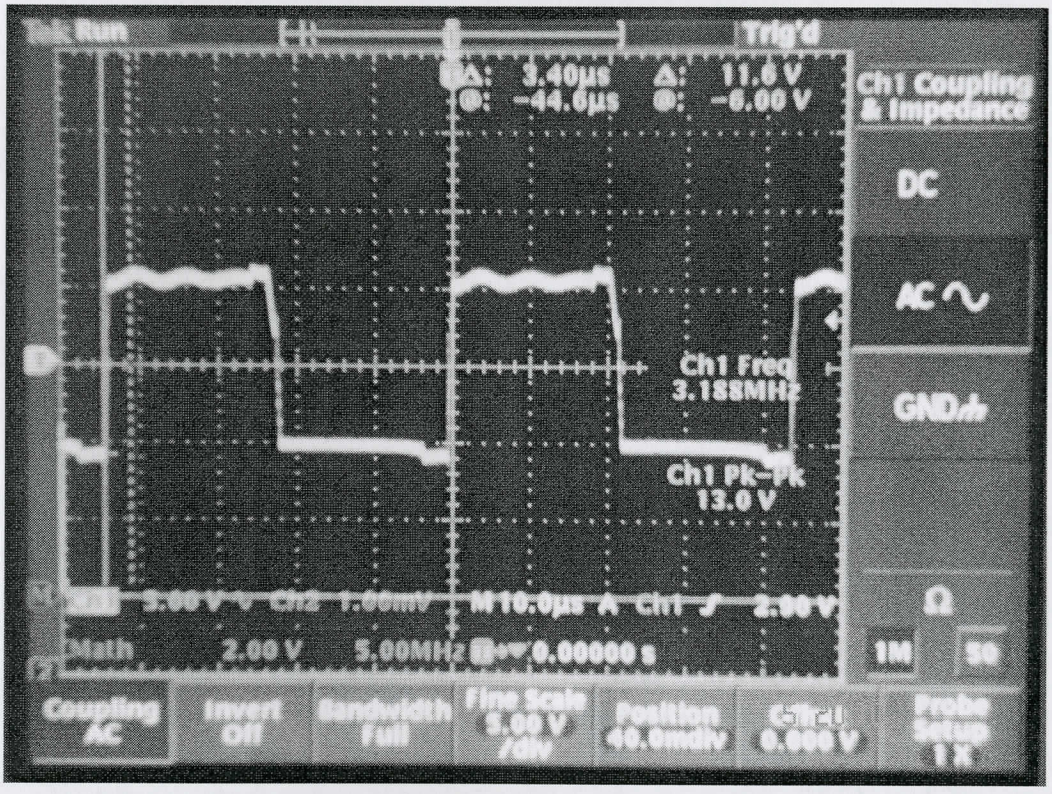


Figure 7-9 PWM Measured Across Load Resistor

Figure7-6 to 7-9 illustrates a series of test done using the various inverters. The inverters were connected to a load resistor of 60Ω. Fig 7.9 illustrates the output waveform across the resistor. This is a square wave that swings between a negative and positive value (alternating square wave). Note that all inverters gave the similar results. When the input AC voltage to the rectifier was varied, the output voltage across the resistive load would also vary. Therefore the output voltage across the load resistor could be controlled by the variable transformer. When the input voltage was adjusted to be below 15V, their would be no output voltage (dropout voltage). Forced air cooling (switching on the heat sink fan) was not necessarily since the temperature of the IGBT modules stayed at a nominal 23°C.

7.2.2 Inverter Testing Using an LC Tank Circuit

A coil was connected in series with a capacitor and supplied at a natural frequency (20 kHz) derived from the output of the inverter. Various metal items were placed in close proximity to the coil and inside the coil. These items included the following:

- A drill bit (made from tungsten to minimise heat, 15mm)
- A coke can (illustrated in fig 7-10, thin sheet metal, about 60mm in diameter)
- A screw driver (chrome vanadium, approximately 4mm in diameter)

When the coil in close proximity to the can, heat was immediately generated and the coke can began to bend and screech. The temperature of the can reached about 200°C in fewer than 50s. The result were far different to when a metal piece such as the screw driver was inserted inside the coil as oppose to being in close proximity to the coil. The screw driver began to glow red hot at a measured temperature reading of 700°C. It took 110s to reach this temperature of 700°C. At this point the natural frequency was 20 kHz. Fig 7-11 shows the fundamental frequency as well as a few sub fundamental or harmonic frequencies. Fig 7.12 illustrates the FFT. The output wave across the load was a sinusoidal one at the fundamental frequency of 20 kHz.

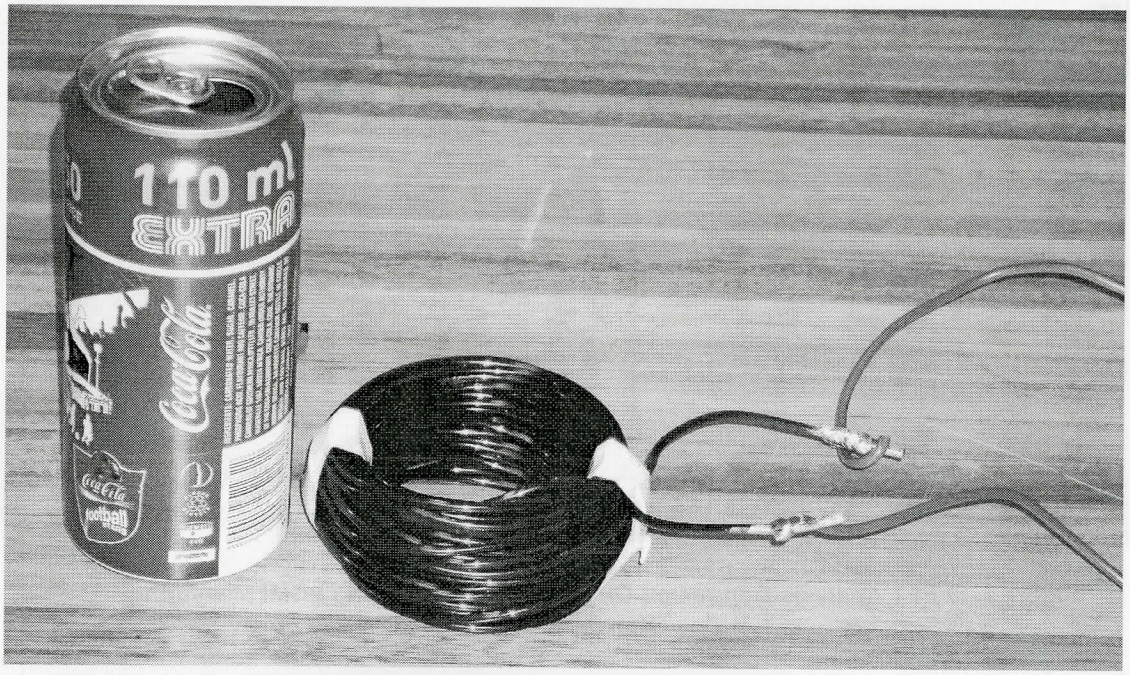


Figure 7-10 Coil Used To Heat A Coke Can

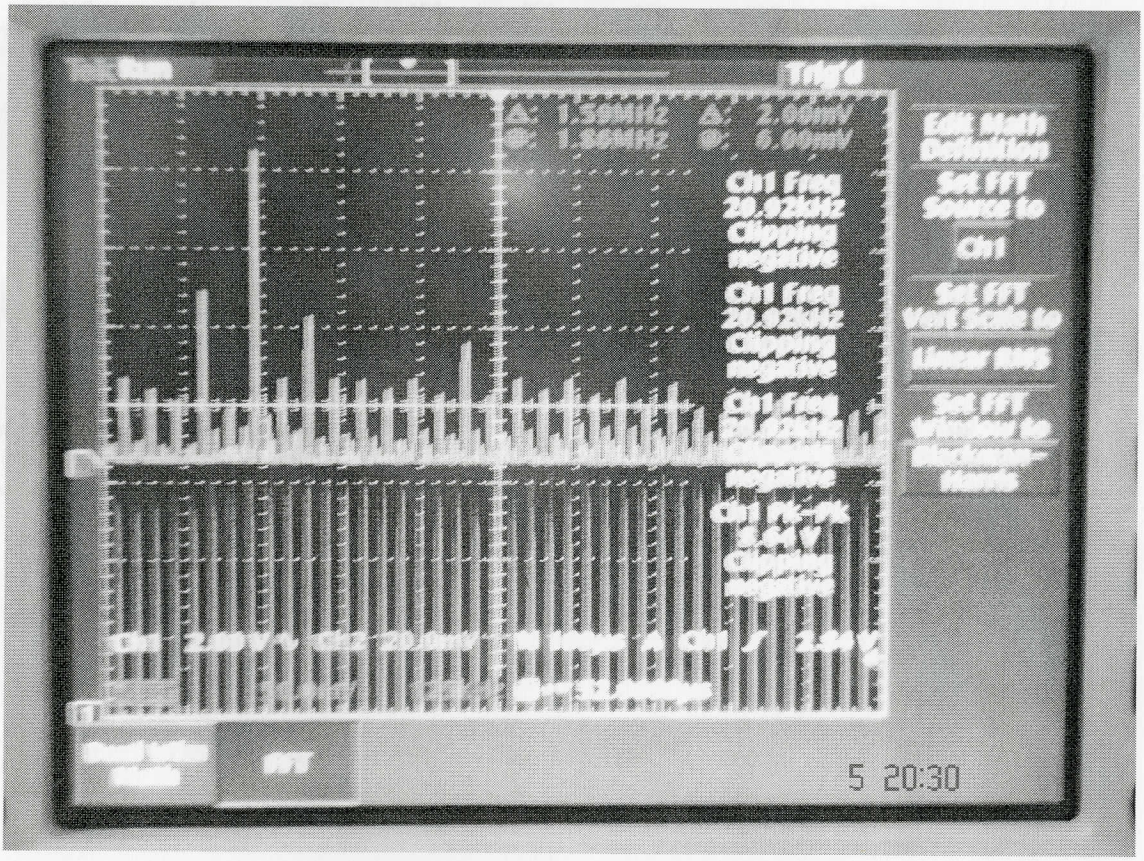


Figure 7-11 FFT Analysis Conducted On New "Element"

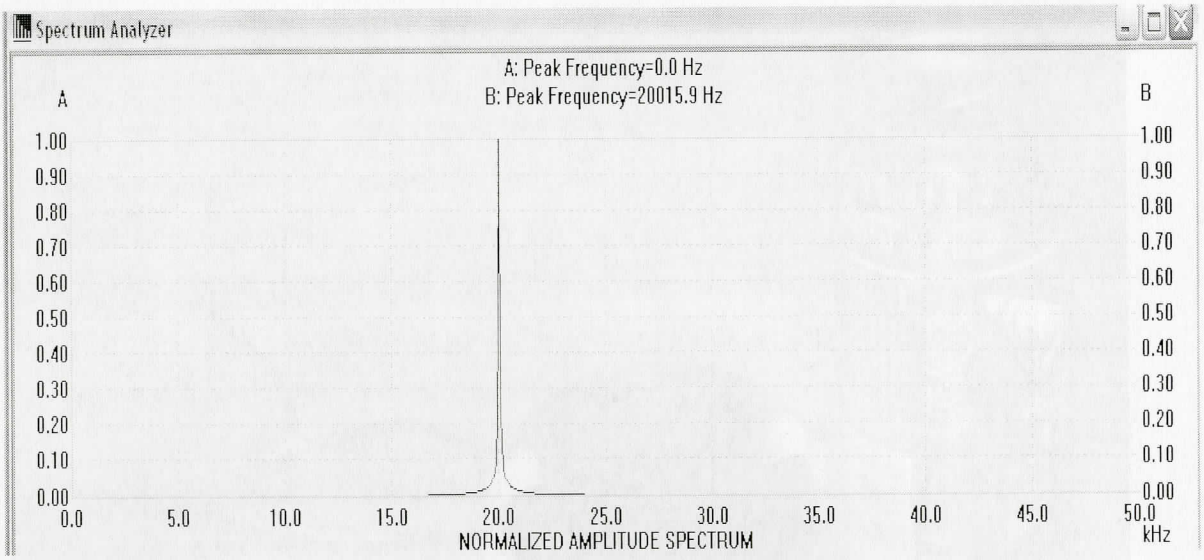


Figure 7-12 FFT Analysis Conducted On New "Element" Using SCMI Measuring Software

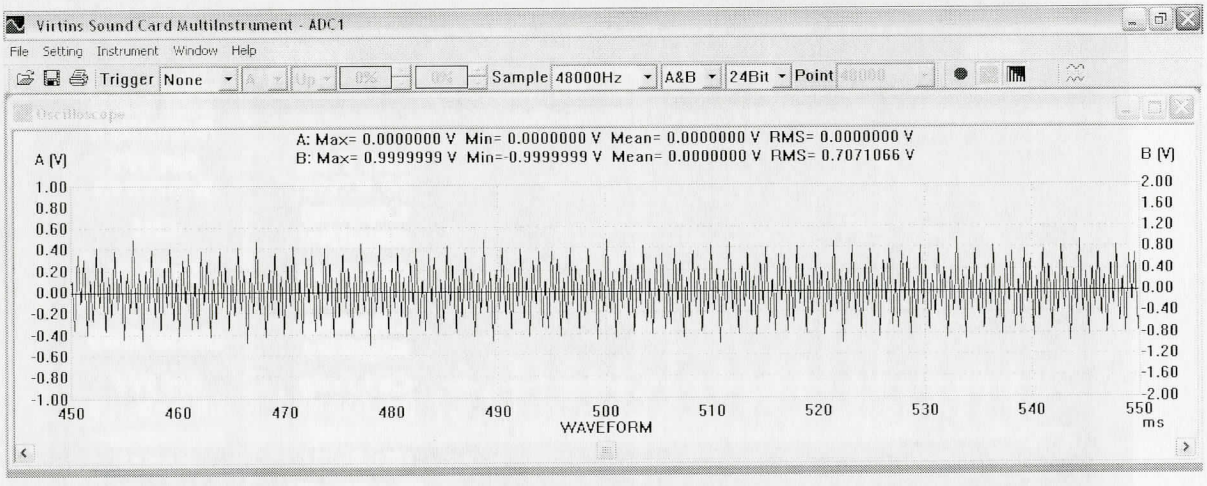


Figure 7-13 Output Wave Form across the Load When Not At Resonance

7.3 Induction Water Heater Testing

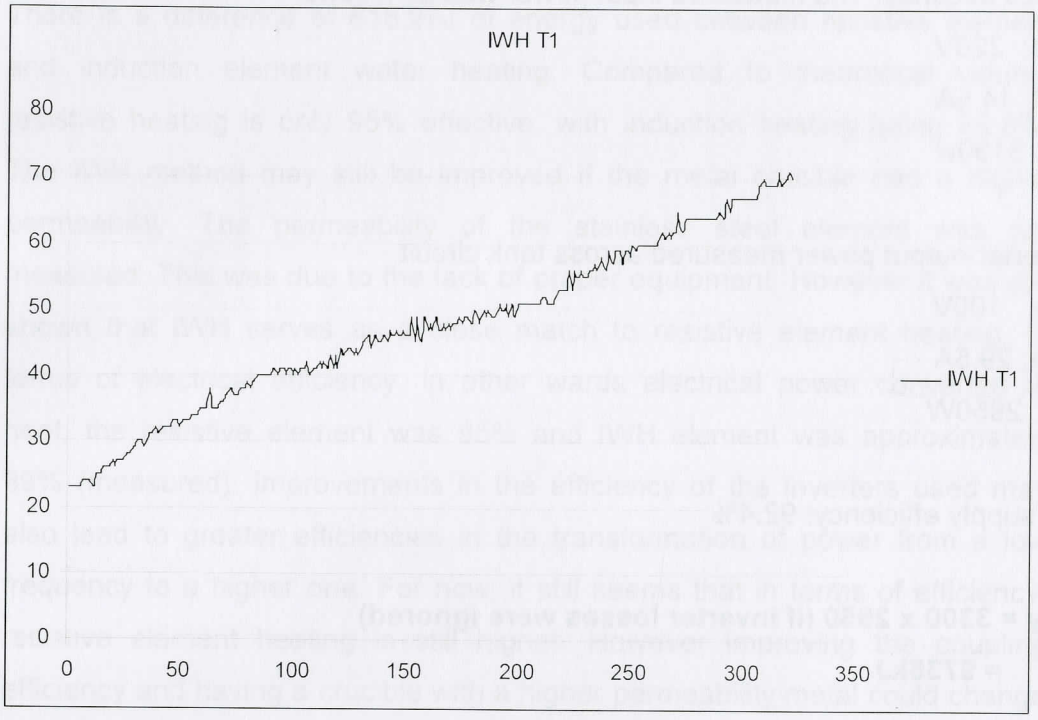


Figure 7-14 IWH Test 1

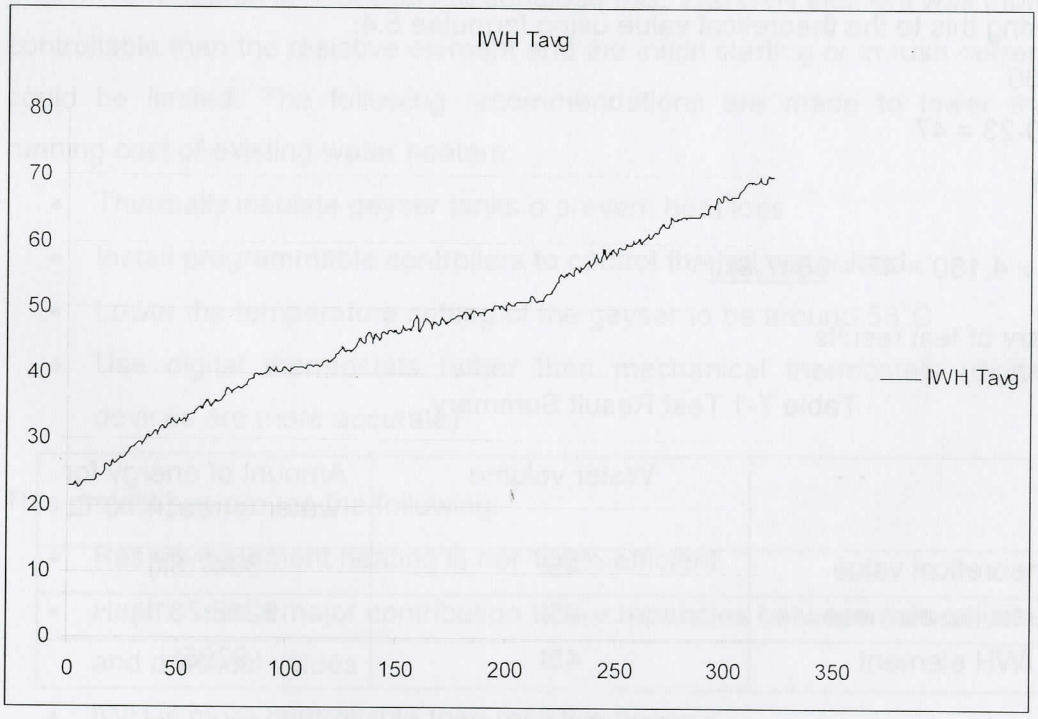


Figure 7-15 IWH Average Test Results Of Four Test Conducted

It took an average of 3300 seconds to reach 70°C. For resistive element it was 3020 seconds. The measured input power was as follows:

Voltage: 220V

Current: 14.5A

Output: 3190w

For inverter output power measured across tank circuit:

Voltage: 100V

Current: 29.5A

Output: 2950W

Power supply efficiency: 92.4%

Energy = 3300 x 2950 (if inverter losses were ignored)

= 9735kJ

Comparing this to the theoretical value using formulae 5.4:

c = 4,180

ΔT = 70-23 = 47

m = 45l

$Q = 45 \times 4.180 \times 47 =$ 8847.8kJ

Summary of test results

Table 7-1 Test Result Summary

	Water volume	Amount of energy for water to reach 70°C
Theoretical value	45l	8847.8kj
Resistive element	45l	9218.731kj
IWH element	45l	9735kj

7.4 Conclusion/Recommendation

There is a difference of 616.27J of energy used between resistive element and induction element water heating. Compared to theoretical values, resistive heating is only 95% effective, with induction heating being 90.8%. The IWH method may still be improved if the metal crucible had a higher permeability. The permeability of the stainless steel element was not measured. This was due to the lack of proper equipment. However it was still shown that IWH serves as a close match to resistive element heating. In terms of electrical efficiency, in other wards electrical power converted to heat, the resistive element was 95% and IWH element was approximately 89% (measured). Improvements in the efficiency of the inverters used may also lead to greater efficiencies in the transformation of power from a low frequency to a higher one. For now, it still seems that in terms of efficiency, resistive element heating is still higher. However improving the coupling efficiency and having a crucible with a higher permeability metal could change this. More research is necessary to conclude this. The IWH element was more controllable than the resistive element and the initial starting or in rush current could be limited. The following recommendations are made to lower the running cost of existing water heaters:

- Thermally insulate geyser tanks o prevent heat loss
- Install programmable controllers to control the hot water load
- Lower the temperature setting of the geyser to be around 58°C
- Use digital thermostats rather than mechanical thermostats (digital devices are more accurate)

This project has proven the following:

- Resistive element heating is not 100% efficient
- Heat loss is a major contribution to discrepancies between theoretical and practical values
- IWH is more controllable than resistive heating
- IWH matches fairly close to resistive element heating

Referances

A Harris, M Kilfoil and E-A Uken, 2008, " *Options for residential water heating*", Paper presented at the international DUE conferance, South Africa,18-19 March 2008, pg 141-148 ..... 5, 11

B F Grobbelaar & J Wheeler, 2006, " *Geyser management system*" , Paper presented at the 2nd BTech conferance in electrical engineering, South Africa, 4 December,p 99- 102 3

BSSA, 2008,"British Stainless Steel Association: Technical information"[online] Available from: http://www.bssa.org.uk/technical_information.php [01 April 2008] 77

Calmeyer JE and Britz EA, 2005,"*A case study on the effect of cylinder cycling in centralized hot water control systems*" Paper presented to the international conference on Domestic use of energy,29-31 March 2005,pp.5-10 16

Engineeringtoolbox, 2008, "Units of heat" [online] Available from: http://www.engineeringtoolbox.com/heat-units-d_664.html [4/14/2008] 57, 58

Fairchild, 2000, " Induction Heating System Topology Review ", Fairchild Semiconductor,USA..... 33

H Mileaf, 1999, *Electricity one-seven*, Prentice Hall Columbus, Ohio..... 33

Horowitch & Hill, 1989, "*The art of electronics second edition*", Cambridge University Press, Cambridge 19

I khan, 2000, Automatic frequency control of an induction furnace, Cape Technikon, Cape Town .....

International Rectifier, 1999, "*HV floating MOS-gate driver ic application note AN978* ", International Rectifier,USA 43

J Delport, 2005, "*The geyser gadgets that work and do not*", Paper presented to the international conference on Domestic use of energy, South Africa, 29-31 March 2005, pg 139-144..... 4

J Dodge, 2002, IGBT tutorial Application note APT0201 Rev B, Advanced power technology, USA..... 1.5, 48

J.Jantzen, 2006, *Tutorial on fuzzy logic*, Technical University of Denmark, Denmark 27

LJ Grobler & C.A. van der Merwe,2004, *Measurement and Verification Methodology of a Residential Load Management*, North-West University, South Africa..... 6

Microchip, 2002, " *Data sheet: PIC18FXX*", Microchip Corperation, USA..... 81

N Mohan, T M Underland & W P Robbins,2003, Power electronics,John Wiley,Minnesota 1.5, 47

Proxim wireless, 2007, "*Tsunami MP.11 Referance manual*",Proxim, England 22

RV Loveless, DC Raymond and M Black, Handbook of induction Heating , 2003, Marcel Dekker inc, Michigan 36

Semikron, 2005, "*SKM1000GB123D data sheet*", Semikron, Germany 72

Semikron, 2006, Hybrid dual IGBT driver Prelimanary data, Semikron,|Germany 73

Semikron, 2007, "*SKD30 Product datasheet*" ,Semikron, Germany 62

Simpson PG, 1960, Induction heating coil and system design, McGraw Hill book company, London 53

Smartec, 2005,"*SMT16030 Datasheet*", Smartec, Netherlands 82

Sobotka H, 1963, Industrial HF heat generators, Philips Technical library, Netherlands 33

Stansel, 1949, *Induction heating*, The maple trees company, New York 33

Texas instruments, 2004, "*Data sheet: Cmos hex voltage level shifter for TTL to CMOS or CMOS to CMOS operation*", Texas Instruments Incorporated, USA 80

TL Floyd, 1997, "Digital fundamentals 6th addition", Prentice Hall, New Jersey 1.5, 19, 20

Appendices A: *IR211A application note*

International
IOR Rectifier

Data Sheet No. PD60147 rev.U

IR2110(-1-2)(S)PbF/IR2113(-1-2)(S)PbF

HIGH AND LOW SIDE DRIVER

Features

- Floating channel designed for bootstrap operation
  Fully operational to +500V or +600V
  Tolerant to negative transient voltage
  dV/dt immune
- Gate drive supply range from 10 to 20V
- Undervoltage lockout for both channels
- 3.3V logic compatible
  Separate logic supply range from 3.3V to 20V
  Logic and power ground ±5V offset
- CMOS Schmitt-triggered inputs with pull-down
- Cycle by cycle edge-triggered shutdown logic
- Matched propagation delay for both channels
- Outputs in phase with inputs

Product Summary

V_{OFFSET}	(IR2110)	500V max.
	(IR2113)	600V max.
I_O+/-		2A / 2A
V_{OUT}		10 - 20V
$t_{on/off}$ (typ.)		120 & 94 ns
Delay Matching	(IR2110)	10 ns max.
	(IR2113)	20ns max.

Packages



14-Lead PDIP
IR2110/IR2113

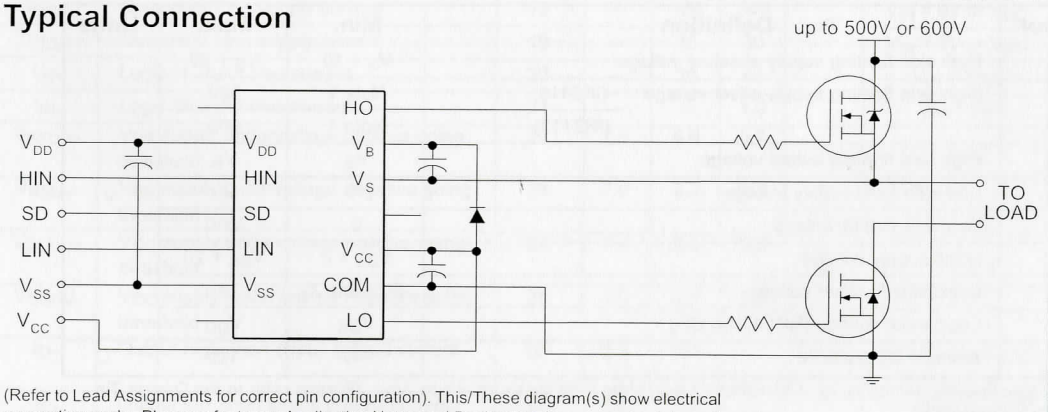


16-Lead SOIC
IR2110S/IR2113S

Description

The IR2110/IR2113 are high voltage, high speed power MOSFET and IGBT drivers with independent high and low side referenced output channels. Proprietary HVIC and latch immune CMOS technologies enable ruggedized monolithic construction. Logic inputs are compatible with standard CMOS or LSTTL output, down to 3.3V logic. The output drivers feature a high pulse current buffer stage designed for minimum driver cross-conduction. Propagation delays are matched to simplify use in high frequency applications. The floating channel can be used to drive an N-channel power MOSFET or IGBT in the high side configuration which operates up to 500 or 600 volts.

Typical Connection



(Refer to Lead Assignments for correct pin configuration). This/These diagram(s) show electrical connections only. Please refer to our Application Notes and DesignTips for proper circuit board layout.

Absolute Maximum Ratings

Absolute maximum ratings indicate sustained limits beyond which damage to the device may occur. All voltage parameters are absolute voltages referenced to COM. The thermal resistance and power dissipation ratings are measured under board mounted and still air conditions. Additional information is shown in Figures 28 through 35.

Symbol	Definition		Min.	Max.	Units
V_B	High side floating supply voltage	(IR2110)	-0.3	525	V
		(IR2113)	-0.3	625	
V_S	High side floating supply offset voltage		V_B - 25	V_B + 0.3	
V_{HO}	High side floating output voltage		V_S - 0.3	V_B + 0.3	
V_{CC}	Low side fixed supply voltage		-0.3	25	
V_{LO}	Low side output voltage		-0.3	V_{CC} + 0.3	
V_{DD}	Logic supply voltage		-0.3	V_{SS} + 25	
V_{SS}	Logic supply offset voltage		V_{CC} - 25	V_{CC} + 0.3	
V_{IN}	Logic input voltage (HIN, LIN & SD)		V_{SS} - 0.3	V_{DD} + 0.3	
dV_S/dt	Allowable offset supply voltage transient (figure 2)		—	50	V/ns
P_D	Package power dissipation @ $T_A \leq +25°C$	(14 lead DIP)	—	1.6	W
		(16 lead SOIC)	—	1.25	
R_{THJA}	Thermal resistance, junction to ambient	(14 lead DIP)	—	75	°C/W
		(16 lead SOIC)	—	100	
T_J	Junction temperature		—	150	°C
T_S	Storage temperature		-55	150	
T_L	Lead temperature (soldering, 10 seconds)		—	300	

Recommended Operating Conditions

The input/output logic timing diagram is shown in figure 1. For proper operation the device should be used within the recommended conditions. The V_S and V_{SS} offset ratings are tested with all supplies biased at 15V differential. Typical ratings at other bias conditions are shown in figures 36 and 37.

Symbol	Definition		Min.	Max.	Units
V_B	High side floating supply absolute voltage		V_S + 10	V_S + 20	V
V_S	High side floating supply offset voltage	(IR2110)	Note 1	500	
		(IR2113)	Note 1	600	
V_{HO}	High side floating output voltage		V_S	V_B	
V_{CC}	Low side fixed supply voltage		10	20	
V_{LO}	Low side output voltage		0	Vcc	
V_{DD}	Logic supply voltage		V_{SS} + 3	V_{SS} + 20	
V_{SS}	Logic supply offset voltage		-5 (Note 2)	5	
V_{IN}	Logic input voltage (HIN, LIN & SD)		V_{SS}	V_{DD}	
T_A	Ambient temperature		-40	125	°C

Note 1: Logic operational for V_S of -4 to +500V. Logic state held for V_S of -4V to -V_{BS}. (Please refer to the Design Tip DT97-3 for more details).
Note 2: When V_{DD} < 5V, the minimum V_{SS} offset is limited to -V_{DD}.

Dynamic Electrical Characteristics

V_{BIAS} (V_{CC}, V_{BS}, V_{DD}) = 15V, C_L = 1000 pF, T_A = 25°C and V_{SS} = COM unless otherwise specified. The dynamic electrical characteristics are measured using the test circuit shown in Figure 3.

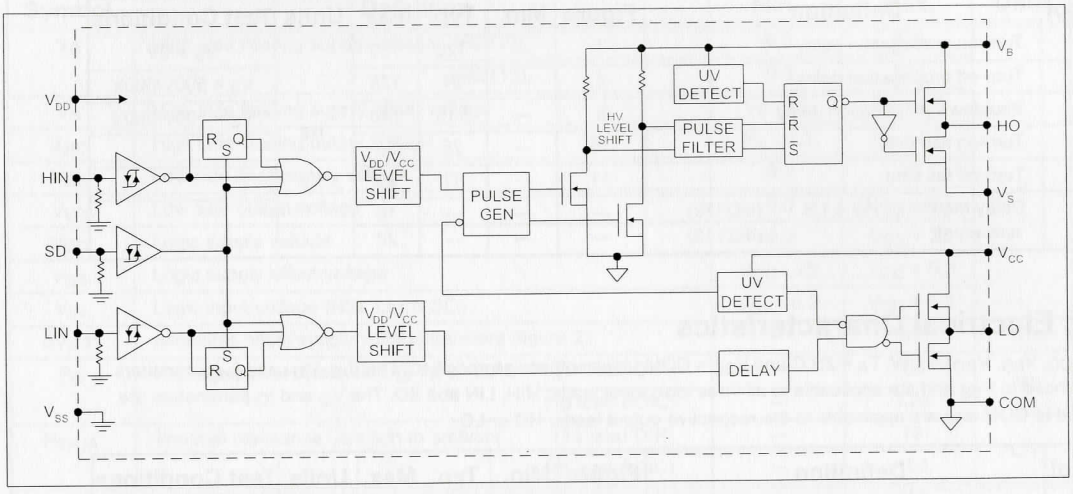
Symbol	Definition	Figure	Min.	Typ.	Max.	Units	Test Conditions
t_{on}	Turn-on propagation delay	7	—	120	150	ns	V_S = 0V
t_{off}	Turn-off propagation delay	8	—	94	125		V_S = 500V/600V
t_{sd}	Shutdown propagation delay	9	—	110	140		V_S = 500V/600V
t_r	Turn-on rise time	10	—	25	35		
t_f	Turn-off fall time	11	—	17	25		
MT	Delay matching, HS & LS turn-on/off (IR2110)	—	—	—	10		
	(IR2113)	—	—	—	20		

Static Electrical Characteristics

V_{BIAS} (V_{CC}, V_{BS}, V_{DD}) = 15V, T_A = 25°C and V_{SS} = COM unless otherwise specified. The V_{IN}, V_{TH} and I_{IN} parameters are referenced to V_{SS} and are applicable to all three logic input leads: HIN, LIN and SD. The V_O and I_O parameters are referenced to COM and are applicable to the respective output leads: HO or LO.

Symbol	Definition	Figure	Min.	Typ.	Max.	Units	Test Conditions
V_{IH}	Logic "1" input voltage	12	9.5	—	—	V	
V_{IL}	Logic "0" input voltage	13	—	—	6.0		
V_{OH}	High level output voltage, V_{BIAS} - V_O	14	—	—	1.2		I_O = 0A
V_{OL}	Low level output voltage, V_O	15	—	—	0.1		I_O = 0A
I_{LK}	Offset supply leakage current	16	—	—	50	µA	V_B=V_S = 500V/600V
I_{QBS}	Quiescent V_{BS} supply current	17	—	125	230		V_{IN} = 0V or V_{DD}
I_{QCC}	Quiescent V_{CC} supply current	18	—	180	340		V_{IN} = 0V or V_{DD}
I_{QDD}	Quiescent V_{DD} supply current	19	—	15	30		V_{IN} = 0V or V_{DD}
I_{IN+}	Logic "1" input bias current	20	—	20	40		V_{IN} = V_{DD}
I_{IN-}	Logic "0" input bias current	21	—	—	1.0		V_{IN} = 0V
V_{BSUV+}	V_{BS} supply undervoltage positive going threshold	22	7.5	8.6	9.7	V	
V_{BSUV-}	V_{BS} supply undervoltage negative going threshold	23	7.0	8.2	9.4		
V_{CCUV+}	V_{CC} supply undervoltage positive going threshold	24	7.4	8.5	9.6		
V_{CCUV-}	V_{CC} supply undervoltage negative going threshold	25	7.0	8.2	9.4		
I_{O+}	Output high short circuit pulsed current	26	2.0	2.5	—	A	V_O = 0V, V_{IN} = V_{DD} PW ≤ 10 µs
I_{O-}	Output low short circuit pulsed current	27	2.0	2.5	—		V_O = 15V, V_{IN} = 0V PW ≤ 10 µs

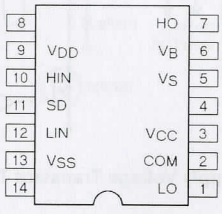
Functional Block Diagram



Lead Definitions

Symbol	Description
V_{DD}	Logic supply
HIN	Logic input for high side gate driver output (HO), in phase
SD	Logic input for shutdown
LIN	Logic input for low side gate driver output (LO), in phase
V_{SS}	Logic ground
V_B	High side floating supply
HO	High side gate drive output
V_S	High side floating supply return
V_{CC}	Low side supply
LO	Low side gate drive output
COM	Low side return

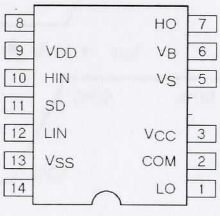
Lead Assignments



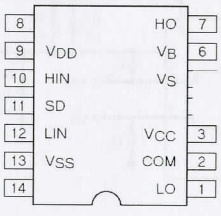
14 Lead PDIP
IR2110/IR2113



16 Lead SOIC (Wide Body)
IR2110S/IR2113S



14 Lead PDIP w/o lead 4
IR2110-1/IR2113-1



14 Lead PDIP w/o leads 4 & 5
IR2110-2/IR2113-2

Part Number

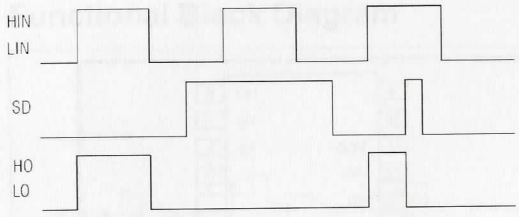


Figure 1. Input/Output Timing Diagram

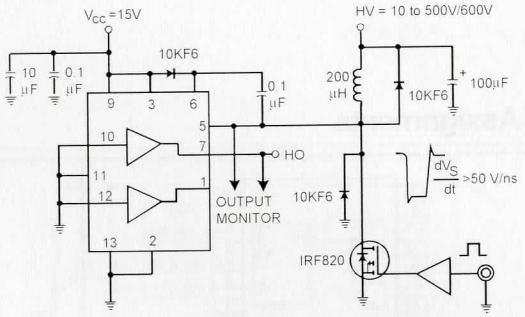


Figure 2. Floating Supply Voltage Transient Test Circuit

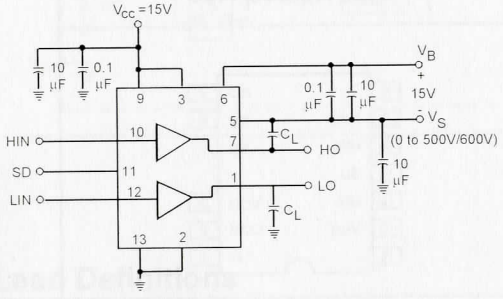


Figure 3. Switching Time Test Circuit

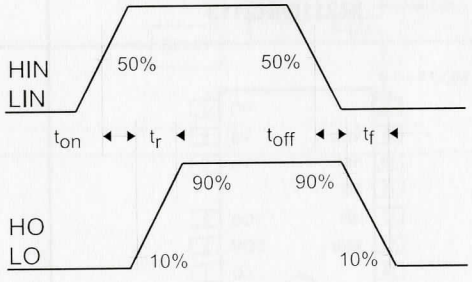


Figure 4. Switching Time Waveform Definition

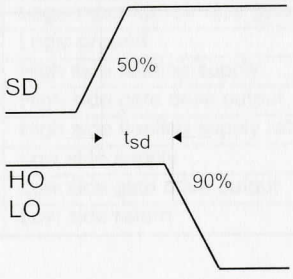


Figure 5. Shutdown Waveform Definitions

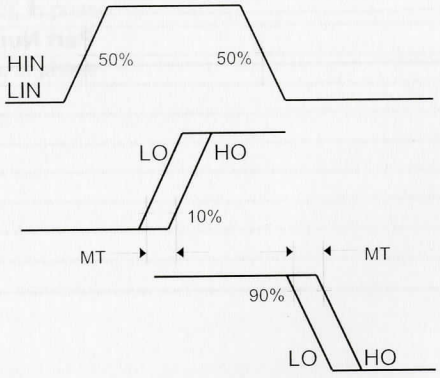


Figure 6. Delay Matching Waveform Definitions

Appendices B: Controller Board schematic

CONN3
CONN
U12
REG
{Value}
C17 C18 C19
C25 C24 C23 C22
R30
R31
R29 R27
R28 R26
R25
D3
D4
ICD
16F877A QFP
U11
CONN
CONN5
CONN
CONN4
C21 C20
HS1
U1
C1 C2 C3 C4
C5 C6 C7 C8
R4
R12
R3
R11
R19
R6
R2
R24
R13
R23
R20
R7
R5
R1
R14
R8
D1
U2
U3
U4
U5
U10
C13 C14 C15 C16
C9 C10 C11 C12
R18
R22
R15
R17
R21
R16
D2
U8
U6
U9
U7
CONN1
CONN
CONN2
CONN

Appendices C: SKPC PCB by Semikron

14.1 SEMIDRIVER®-Accessories (for SEMIDRIVER® SKHI 21 and SKHI 22)

Recommended piece parts list

Part No. [1]	Function [2]	Designation	Recommended Values [2]
C1	V_S [4]	Radial Electrol. cap.	10...47 µF / 35 V
C2	C_{CE}BOT	Polystyrene cap.	0,33 nF > 25 V
C3	C_{CE}TOP	Polystyrene cap.	0,33 nF > 25 V
R1	$R_{TD}1$	Resistor [2]	0 - 100 kΩ / 0,25 W
R2	$R_{TD}2$	Resistor [2]	0 - 100 kΩ / 0,25 W
R3	R_{CE2}BOT	Resistor [2]	typ. 24 kΩ / 0,6 W
R4	R_{Gon2}BOT	Resistor [3]	3,3 ... 100 Ω
R5	R_{Goff2}BOT	Resistor [3]	3,3 ... 100 Ω
R6	R_{Goff1}TOP	Resistor [3]	3,3 ... 100 Ω
R7	R_{Gon1}TOP	Resistor [3]	3,3 ... 100 Ω
R8	R_{CE1}TOP	Resistor [2]	typ. 24 kΩ / 0,6 W
Conn 1	input	1 x MOLEX 7395 [6]-(5 way - 2,54 pitch)	
Conn 2...5	out par.	for cables joining to slave boards	
Conn 6 - 4	out	4 x MOLEX 90030 - 1001 [7] (for 2,8 x 0,5)	
TP1	V_{CE} Top +	Wire connection to + V_ERAIL	
TP2	V_{CE} mon E1	1 jumper [5] to connect BOTT.C2 to TOP emitter (E1)	
TP3	V_{CE} mon C2		

[7] MOLEX Mini T Terminal with solder post, loose-form (Chain form: 90030-0001)

Printed Circuit Board (PCB) SKPC 2006 [1]

Features

- blank PCB
- glass fibre epoxy
- without piece parts
- ready to fit parts for wave soldering
- output connectors positioned for direct push-on to SEMITRANS-3
- 3 hole fixing

[1] SKPC 2006 normally should be completed by the customer, but it can be made available with parts fitted, on mutual agreement on request.
[2] See datasheet SKHI 21, SKHI 22 page B14 – 21
[3] Values to be chosen as per datasheet of SKHI 22 and of the device to be driven.
[4] For decoupling the power supply at input
[5] Must be connected (C2 - E1) for VCE monitoring
[6] Right Angle Friction LOCK mates with MOLEX 6471, 7720S, 2695

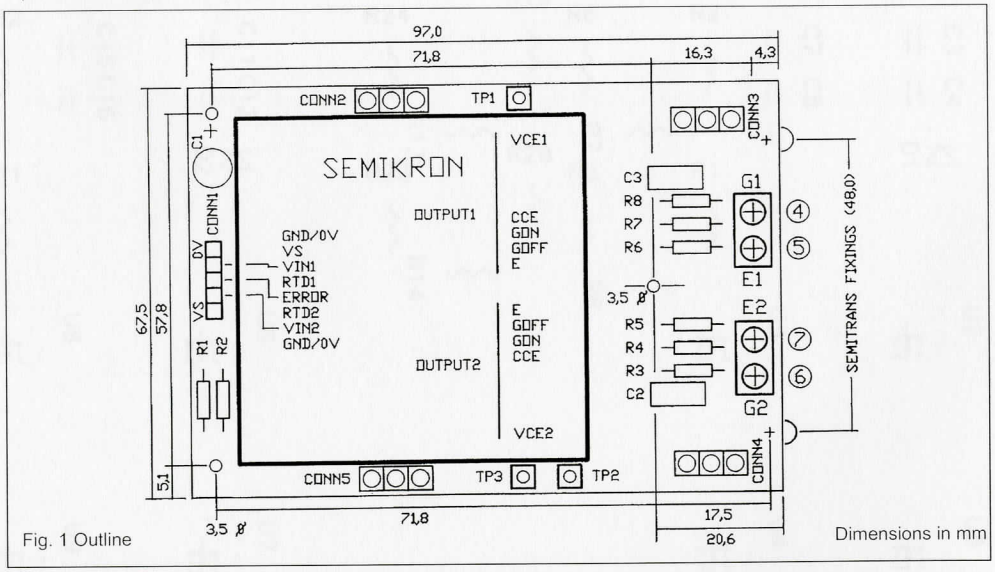


Fig. 1 Outline

Dimensions in mm

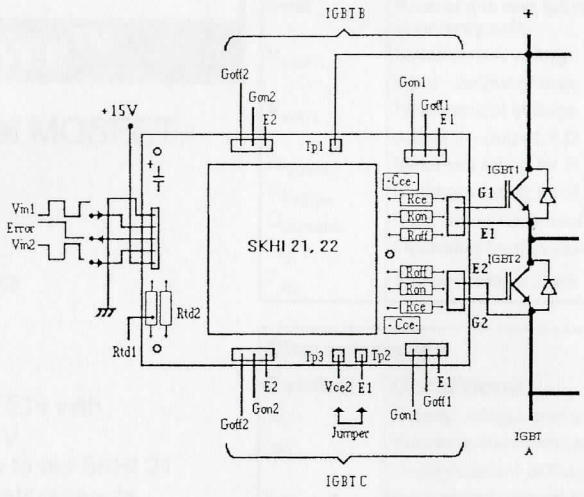


Fig. 2 Layout and connection to drive 1 IGBT DUAL module

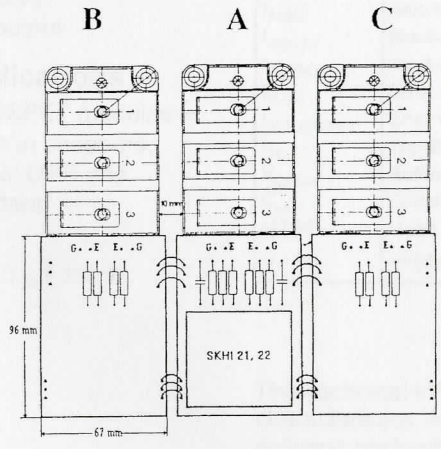


Fig. 3 One SKPC 2006 driving 3 DUAL modules SKM 200 GB 123 D via 2 slave boards

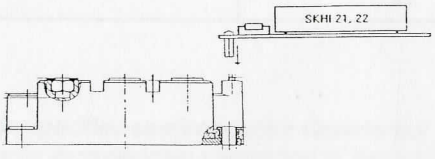


Fig. 4 SKPC 2006 fitting directly to the gate pins of SEMITRANS 3 (For SEMITRANS 2 use soft wiring to the gate connectors)

 © by SEMIKRON

Appendices D: SKHI21A module data sheet

SKHI 21A (R) ...



SEMIDRIVER™

Hybrid Dual MOSFET Driver

SKHI 21A (R)

Preliminary Data

Features

- drives MOSFETs with $V_{DS(on)}$ < 10 V
- is compatible to old SKHI 21
- CMOS compatible inputs
- Short circuit potection by V_{CE} monitoring and switch off
- Drive interlock top / bottom
- Isolation by transformers
- Supply undervotage protection (13 V)
- Error latch / output

Typical Applications

- Driver for MOSFET modules in bridge circuits in choppers, inverter drives, UPS and welding inverters

1) see fig. 6

2) At R_{CE} = 18 kΩ, C_{CE} = 330 pF

Absolute Maximum Ratings

Symbol	Conditions	Values	Units
V_S	Supply voltage prim.	18	V
V_{iH}	Input signal volt. (High)	V_S + 0,3	V
$Iout_{PEAK}$	Output peak current	8	A
$Iout_{AVmax}$	Output average current	40	mA
f_{max}	max. switching frequency	50	kHz
V_{CE}	Collector emitter voltage sense across the IGBT	1200	V
dv/dt	Rate of rise and fall of voltage secondary to primary side	50	kV/µs
V_{isolIO}	Isolation test voltage input - output (2 sec. AC)	2500	Vac
V_{isol12}	Isolation test voltage output 1 - output 2 (2 sec. AC)	1500	V
R_{Gonmin}	Minimum rating for R_{Gon}	3	Ω
$R_{Goffmin}$	Minimum rating for R_{Goff}	3	Ω
$Q_{out/pulse}$	Max. rating for output charge per pulse	4[1)]	µC
T_{op}	Operating temperature	- 40 ... + 85	°C
T_{stg}	Storage temperature	- 40 ... + 85	°C

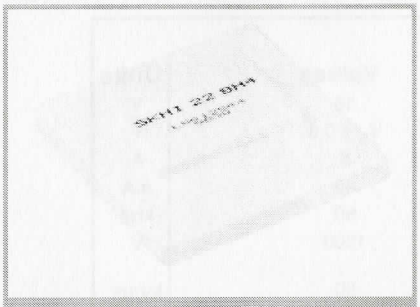
Characteristics T_a = 25 °C, unless otherwise specified

Symbol	Conditions	min.	typ.	max.	Units
V_S	Supply voltage primary side	14,4	15	15,6	V
I_{SO}	Supply current primary side (no load)		80		mA
	Supply current primary side (max.)			290	mA
V_i	Input signal voltage on/off		15 / 0		V
V_{iT+}	Input threshold voltage (High)	10,9	11,7	12,5	V
V_{iT-}	Input threshold voltage (Low)	4,7	5,5	6,5	V
R_{in}	Input resistance		10		kΩ
$V_{G(on)}$	Turn on gate voltage output		+ 15		V
$V_{G(off)}$	Turn off gate voltage output		0		V
R_{GE}	Internal gate-emitter resistance		22		kΩ
f_{ASIC}	Asic system switching frequency		8		MHz
$t_{d(on)IO}$	Input-output turn-on propagation time	0,85	1	1,15	µs
$t_{d(off)IO}$	Input-output turn-off propagation time	0,85	1	1,15	µs
$t_{d(err)}$	Error input-output propagation time		0,6		µs
$t_{pERRRESET}$	Error reset time		9		µs
t_{TD}	Top-Bot Interlock Dead Time	3,3		4,3	µs
V_{CEsat}	Reference voltage for V_{CE}-monitoring		5[2)]	10	V
C_{ps}	Coupling capacitance primary secondary		12		pF
MTBF	Mean Time Between Failure T_a = 40°C		2,0		10^6 h
w	weight		45		g

This technical information specifies semiconductor devices but promises no characteristics. No warranty or guarantee expressed or implied is made regarding delivery, performance or suitability.

 © by SEMIKRON

SKHI 22 A / B (R) ...



SEMIDRIVER™

Hybrid Dual IGBT Driver

SKHI 22 A / B (R)

Preliminary Data

Features

- Double driver for halfbridge IGBT modules
- SKHI 22A is compatible to old SKHI 22
- SKHI 22B has additional functionality
- CMOS compatible inputs
- Short circuit potection by V_{CE} monitoring and switch off
- Drive interlock top / bottom
- Isolation by transformers
- Supply undervotage protection (13 V)
- Error latch / output

Typical Applications

- Driver for IGBT modules in bridge circuits in choppers, inverter drives, UPS and welding inverters

1) see fig. 6

2) At R_{CE} = 18 kΩ, C_{CE} = 330 pF

Absolute Maximum Ratings

Symbol	Conditions	Values	Units
V_S	Supply voltage prim.	18	V
V_{iH}	Input signal volt. (High) SKHI 22A	V_S + 0,3	V
	SKHI 22B	5 + 0,3	V
$Iout_{PEAK}$	Output peak current	8	A
$Iout_{AVmax}$	Output average current	40	mA
f_{max}	max. switching frequency	50	kHz
V_{CE}	Collector emitter voltage sense across the IGBT	1200	V
dv/dt	Rate of rise and fall of voltage secondary to primary side	50	kV/µs
V_{isolIO}	Isolation test voltage input - output (2 sec. AC)	2500	Vac
V_{isol12}	Isolation test voltage output 1 - output 2 (2 sec. AC)	1500	V
R_{Gonmin}	Minimum rating for R_{Gon}	3	Ω
$R_{Goffmin}$	Minimum rating for R_{Goff}	3	Ω
$Q_{out/pulse}$	Max. rating for output charge per pulse	4[1]	µC
T_{op}	Operating temperature	- 40 ... + 85	°C
T_{stg}	Storage temperature	- 40 ... + 85	°C

Characteristics T_a = 25 °C, unless otherwise specified

Symbol	Conditions	min.	typ.	max.	Units
V_S	Supply voltage primary side	14,4	15	15,6	V
I_{SO}	Supply current primary side (no load)		80		mA
	Supply current primary side (max.)			290	mA
V_i	Input signal voltage SKHI 22A on/off		15 / 0		V
	SKHI 22B on/off		5 / 0		V
V_{iT+}	Input threshold voltage (High) SKHI 22A	10,9	11,7	12,5	V
	SKHI 22B	3,5	3,7	3,9	V
V_{iT-}	Input threshold voltage (Low) SKHI 22A	4,7	5,5	6,5	V
	SKHI 22B	1,5	1,75	2,0	V
R_{in}	Input resistance SKHI 22A		10		kΩ
	SKHI 22B		3,3		kΩ
$V_{G(on)}$	Turn on gate voltage output		+ 15		V
$V_{G(off)}$	Turn off gate voltage output		- 7		V
R_{GE}	Internal gate-emitter resistance		22		kΩ
f_{ASIC}	Asic system switching frequency		8		MHz
$t_{d(on)IO}$	Input-output turn-on propagation time	0,85	1	1,15	µs
$t_{d(off)IO}$	Input-output turn-off propagation time	0,85	1	1,15	µs
$t_{d(err)}$	Error input-output propagation time		0,6		µs
$t_{pERRRESET}$	Error reset time		9		µs
t_{TD}	Top-Bot Interlock Dead Time SKHI 22A	3,3		4,3	µs
	SKHI 22B	no interlock		4,3	µs
V_{CEsat}	Reference voltage for V_{CE}-monitoring		5[2]	10	V
C_{ps}	Coupling capacitance primary secondary		12		pF
MTBF	Mean Time Between Failure T_a = 40°C		2,0		10^6 h
w	weight		45		g

This technical information specifies semiconductor devices but promises no characteristics. No warranty or guarantee expressed or implied is made regarding delivery, performance or suitability.

© by SEMIKRON

SKHI 22 A / B H4 (R) ...



SEMIDRIVER™

Hybrid Dual IGBT Driver

SKHI 22 A / B H4 (R)

Preliminary Data

Features

- Double driver for halfbridge IGBT modules
- SKHI 22A H4 is compatible to old SKHI 22 H4
- SKHI 22B H4 has additional functionality
- CMOS compatible inputs
- Short circuit protection by V_{CE} monitoring and switch off
- Drive interlock top / bottom
- Isolation by transformers
- Supply under voltage protection (13V)
- Error latch / output

Typical Applications

- Driver for IGBT modules in bridge circuits in choppers, inverter drives, UPS and welding inverters
- DC bus voltage up to 1200 V

1) see fig. 6

2) At R_{CE} = 36 kΩ, C_{CE} = 470 pF, R_{VCE} = 1 kΩ

Absolute Maximum Ratings

Symbol	Conditions	Values	Units
V_S	Supply voltage prim.	18	V
V_{iH}	Input signal volt. (High) SKHI 22A H4	V_S + 0,3	V
	SKHI 22B H4	5 + 0,3	V
$Iout_{PEAK}$	Output peak current	8	A
$Iout_{AVmax}$	Output average current	40	mA
f_{max}	max. switching frequency	50	kHz
V_{CE}	Collector emitter voltage sense across the IGBT	1700	V
dv/dt	Rate of rise and fall of voltage secondary to primary side	50	kV/µs
V_{isolIO}	Isolation test voltage input - output (2 sec. AC)	4000	Vac
V_{isol12}	Isolation test voltage output 1 - output 2 (2 sec. AC)	1500	V
R_{Gonmin}	Minimum rating for R_{Gon}	3	Ω
$R_{Goffmin}$	Minimum rating for R_{Goff}	3	Ω
$Q_{out/pulse}$	Max. rating for output charge per pulse	4[1]	µC
T_{op}	Operating temperature	- 40 ... + 85	°C
T_{stg}	Storage temperature	- 40 ... + 85	°C

Characteristics T_a = 25 °C, unless otherwise specified

Symbol	Conditions	min.	typ.	max.	Units
V_S	Supply voltage primary side	14,4	15	15,6	V
I_{SO}	Supply current primary side (no load)		80		mA
	Supply current primary side (max.)			290	mA
V_i	Input signal voltage SKHI 22A H4 on/off		15 / 0		V
	SKHI 22B H4 on/off		5 / 0		V
V_{iT+}	Input threshold volt. (High) SKHI 22A H4	10,9	11,7	12,5	V
	SKHI 22B H4	3,5	3,7	3,9	V
V_{iT-}	Input threshold volt. (Low) SKHI 22A H4	4,7	5,5	6.5	V
	SKHI 22B H4	1,5	1,75	2.0	V
R_{in}	Input resistance SKHI 22A H4		10		kΩ
	SKHI 22B H4		3,3		kΩ
$V_{G(on)}$	Turn on gate voltage output		+ 15		V
$V_{G(off)}$	Turn off gate voltage output		- 7		V
R_{GE}	Internal gate-emitter resistance		22		kΩ
f_{ASIC}	Asic system switching frequency		8		MHz
$t_{d(on)IO}$	Input-output turn-on propagation time	0,85	1	1,15	µs
$t_{d(off)IO}$	Input-output turn-off propagation time	0.85	1	1,15	µs
$t_{d(err)}$	Error input-output propagation time		0,6		µs
$t_{pERRRESET}$	Error reset time		9		µs
t_{TD}	Top-Bot Interl. Dead Time SKHI 22A H4	3,3		4,3	µs
	SKHI 22B H4	no interlock		4,3	µs
V_{CEsat}	Reference voltage for V_{CE}-monitoring		5[2]	10	V
C_{ps}	Coupling capacitance primary secondary		12		pF
MTBF	Mean Time Between Failure T_a = 40°C		2,0		10^6 h
w	weight		45		g

This technical information specifies semiconductor devices but promises no characteristics. No warranty or guarantee expressed or implied is made regarding delivery, performance or suitability.

 © by SEMIKRON

External Components

Component	Function	Recommended Value
R_{CE}	Reference voltage for V_{CE}-monitoring $V_{CEstat}(V) = \frac{10 \cdot R_{CE}(k\Omega)}{10 + R_{CE}(k\Omega)} - 1{,}4$ (1) with R_{VCE} = 1kΩ (1700V IGBT): $V_{CEstat}(V) = \frac{10 \cdot R_{CE}(k\Omega)}{10 + R_{CE}(k\Omega)} - 1{,}8$ (1.1)	10kΩ < R_{CE} < 100kΩ 18kΩ for SKM XX 123 (1200V) 36kΩ for SKM XX 173 (1700V)
C_{CE}	Inhibit time for V_{CE} - monitoring $t_{min} = \tau_{CE} \cdot \ln\left[\frac{15 - V_{CEstat}(V)}{10 - V_{CEstat}(V)}\right]$ (2) $\tau_{CE}(\mu s) = C_{CE}(nF) \cdot \frac{10 \cdot R_{CE}(k\Omega)}{10 + R_{CE}(k\Omega)}$ (3)	C_{CE} < 2,7nF 0,33nF for SKM XX 123 (1200V) 0,47nF for SKM XX 173 (1700V) 0,5µs < t_{min} < 10µs
R_{VCE}	Collector series resistance for 1700V IGBT-operation	1kΩ / 0,4W
R_{ERROR}	Pull-up resistance at error output $\frac{U_{Pull-Up}}{R_{ERROR}} < 15mA$	1kΩ < R_{ERROR} < 10kΩ
R_{GON}	Turn-on speed of the IGBT [4]	R_{GON} > 3Ω
R_{GOFF}	Turn-off speed of the IGBT [5]	R_{GOFF} > 3Ω

[4] Higher resistance reduces free-wheeling diode peak recovery current, increases IGBT turn-on time.
[5] Higher resistance reduces turn-off peak voltage, increases turn-off time and turn-off power dissipation

PIN array

Fig. 2 shows the pin arrays. The input side (primary side) comprises 10 inputs (SKHI 22A / 21A 8 inputs), forming the interface to the control circuit (see fig.1).

The output side (secondary side) of the hybrid driver shows two symmetrical groups of pins with 4 outputs, each forming the interface to the power module. All pins are designed for a grid of 2,54 mm.

Primary side PIN array

PIN No.	Designation	Explanation
P14	GND / 0V	related earth connection for input signals
P13	V_S	+ 15V ± 4% voltage supply
P12	V_{IN1}	switching signal input 1 (TOP switch) positive 5V logic (for SKHI22A /21A, 15V logic)
P11	free	not wired
P10	/ERROR	error output, low = error; open collector output; max 30V / 15mA (for SKHI22A /21A, internal 10kΩ pull-up resistor versus V_S)
P9	TDT2	signal input for digital adjustment of interlocking time; **SKHI22B: to be switched by bridge to GND (see fig. 3)** **SKHI22A /21A: to be switched by bridge to V_S**
P8	V_{IN2}	switching signal input 2 (BOTTOM switch); positive 5V logic (for SKHI22A /21A, 15V logic)
P7	GND / 0V	related earth connection for input signals
P6	SELECT	signal input for neutralizing locking function; to be switched by bridge to GND
P5	TDT1	signal input for digital adjustment of locking time; to be switched by bridge to GND

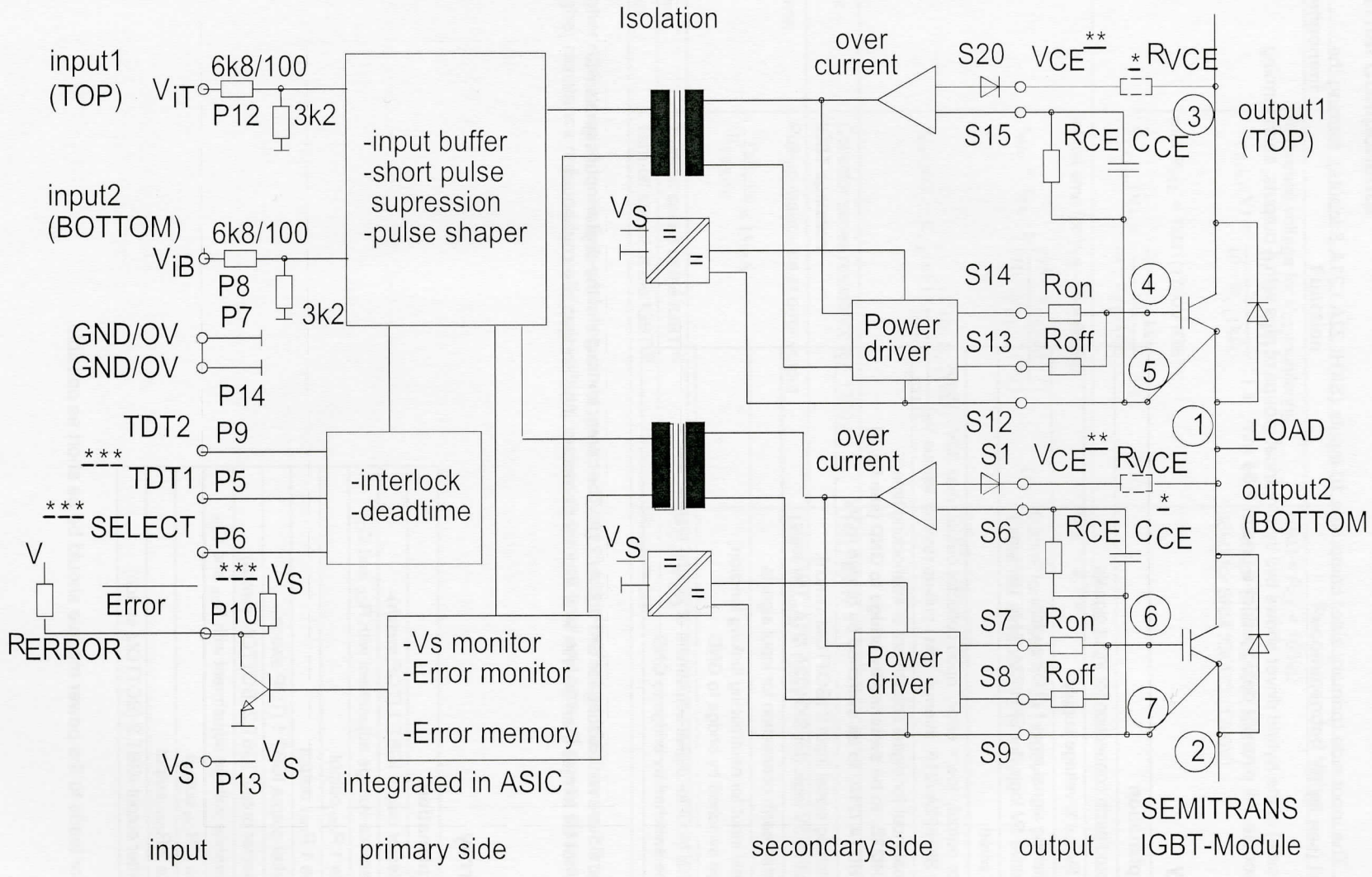
ATTENTION: Inputs P6 and P5 are not existing for SKHI 22A/ 21A. The contactor tracks of the digital input signals P5/ P6/ P9 must not be longer than 20 mm to avoid interferences, if no bridges are connected.

Secondary side PIN array

PIN No.	Designation	Explanation
S20	V_{CE1}	collector output IGBT 1 (TOP switch)
S15	C_{CE1}	reference voltage adjustment with R_{CE} and C_{CE}
S14	G_{ON1}	gate 1 R_{ON} output
S13	G_{OFF1}	gate 1 R_{OFF} output
S12	E1	emitter output IGBT 1 (TOP switch)
S1	V_{CE2}	collector output IGBT 2 (BOTTOM switch)
S6	C_{CE2}	reference voltage adjustment with R_{CE} and C_{CE}
S7	G_{ON2}	gate 2 R_{ON} output
S8	G_{OFF2}	gate 2 R_{OFF} output
S9	E2	emitter output IGBT 2 (BOTTOM switch)

ATTENTION: The connector leads to the power module should be as short as possible.

© by SEMIKRON 12-10-2006



* When SKHI22B is driving 1700V IGBTs, a 1kΩ / 0,4W R_{VCE}-resistor must be connected in series to the V_{CE} input.
** The VCE-terminal is to be connected to the IGBT collector C. If the V_{CE}-monitoring is not used, connect S1 to S9 or S20 to S12 respectively.
*** Terminals P5 and P6 are not existing for SKHI22A/21A; internal pull-up resistor exists in SKHI22A/21A only.
1-7 Connections to SEMITRANS GB-module

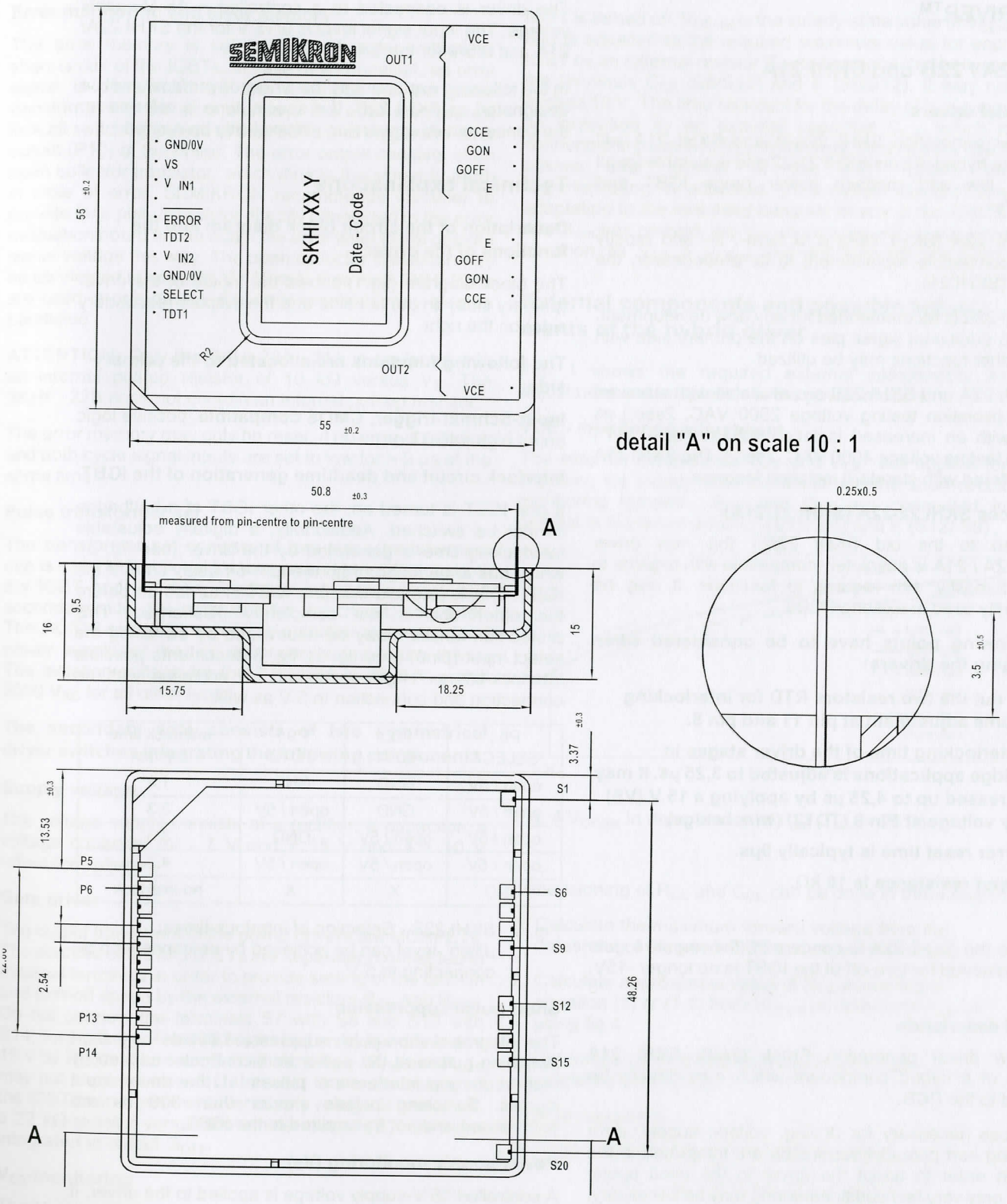


Fig. 2 Dimension drawing and PIN array (P5 and P6 are not existing for SKHI22A/21A)

SEMIDRIVER™

SKHI 22A / 22B und SKHI 21A

Hybrid dual drivers

The driver generation SKHI 22A/B and SKHI 21A will replace the hybrid drivers SKHI 21/22 and is suitable for all available low and medium power range IGBT and MOSFETs.

The SKHI 22A (SKHI 21A) is a form-, fit- and mostly function-compatible replacement to its predecessor, the SKHI 22 (SKHI 21).

The SKHI 22B is recommended for any new development. It has two additional signal pins on the primary side with which further functions may be utilized.

The SKHI 22A and SKHI 22B are available with standard isolation (isolation testing voltage 2500 VAC, 2sec.) as well as with an increased isolation voltage (type "H4") (isolation testing voltage 4000 VAC, 2sec.). The SKHI 21A is only offered with standard isolation features.

Differences SKHI 22-22A (SKHI 21-21A)

Compared to the old SKHI 22/21 the new driver SKHI 22A / 21A is absolutely compatible with regards to pins and mostly with regards to functions. It may be equivalently used in existing PCBs.

The following points have to be considered when exchanging the drivers:

- **Leave out the two resistors RTD for interlocking dead time adjustment at pin 11 and pin 9.**
- **The interlocking time of the driver stages in halfbridge applications is adjusted to 3,25 µs. It may be increased up to 4,25 µs by applying a 15 V (VS) supply voltage at Pin 9 (TDT2) (wire bridge)**
- **The error reset time is typically 9µs.**
- **The input resistance is 10 kΩ.**

As far as the SKHI 22A is concerned, the negative gate voltage required for turn-off of the IGBT is no longer -15V, but -7V.

General description

The new driver generation SKHI 22A/B, SKHI 21A consists of a hybrid component which may directly be mounted to the PCB.

All devices necessary for driving, voltage supply, error monitoring and potential separation are integrated in the driver. In order to adapt the driver to the used power module, only very few additional wiring may be necessary.

The forward voltage of the IGBT is detected by an integrated short-circuit protection, which will turn off the module when a certain threshold is exceeded.

In case of short-circuit or too low supply voltage the integrated error memory is set and an error signal is generated.

The driver is connected to a controlled + 15 V-supply voltage. The input signal level is 0/15 V for the SKHI 22A/ 21A and 0/5 V for the SKHI 22B.

In the following explanations the whole driver family will be designated as SKHI 22B. If a special type is referred to, the concerned driver version will explicitly be named.

Technical explanations[1]

Description of the circuit block diagram and the functions of the driver

The block diagram (fig.1) shows the inputs of the driver (primary side) on the left side and the outputs (secondary side) on the right.

The following functions are allocated to the primary side:

Input-Schmitt-trigger, CMOS compatible, positive logic (input high = IGBT on)

Interlock circuit and deadtime generation of the IGBT

If one IGBT is turned on, the other IGBT of a halfbridge cannot be switched. Additionally, a digitally adjustable interlocking time is generated by the driver (see fig. 3), which has to be longer than the turn-off delay time of the IGBT. This is to avoid that one IGBT is turned on before the other one is not completely discharged. This protec-tion-function may be neutralized by switching the select input (pin6) (see fig. 3). fig. 3 documents possible interlock-times. "High" value can be achieved with no connection and connection to 5 V as well.

P6 ; SELECT	P5 ; TDT1	P9 ; TDT2	interlock time t_{TD} /µs
open / 5V	GND	GND	1,3
open / 5V	GND	open / 5V	2,3
open / 5V	open / 5V	GND	3,3
open / 5V	open / 5V	open / 5V	4,3
GND	X	X	no interlock

Fig. 3 SKHI 22B - Selection of interlock-times: „High"-level can be achieved by no connection or connecting to 5 V

Short pulse suppression

The integrated short pulse suppression avoids very short switching pulses at the power semiconductor caused by high-frequency interference pulses at the driver input signals. Switching pulses shorter than 500 ns are suppressed and not transmitted to the IGBT.

Power supply monitoring (V_S)

A controlled 15 V-supply voltage is applied to the driver. If it falls below 13 V, an error is monitored and the error output signal switches to low level.

1.The following descriptions apply to the use of the hybrid driver for IGBTs as well as for power MOSFETs. For the reason of shortness, only IGBTs will be mentioned in the following. The designations "collector" and "emitter" will refer to IGBTs, whereas for the MOSFETs "drain" and "source" are to be read instead.

Error monitoring and error memory

The error memory is set in case of under-voltage or short-circuit of the IGBTs. In case of short-circuit, an error signal is transmitted by the V_{CE}-input via the pulse transformers to the error memory. The error memory will lock all switching pulses to the IGBTs and trigger the error output (P10) of the driver. The error output consists of an open collector transistor, which directs the signal to earth in case of error. SEMIKRON recommends the user to provide for a pull-up resistor directly connected to the error evaluation board and to adapt the error level to the desired signal voltage this way. The open collector transistor may be connected to max. 30 V / 15 mA. If several SKHI 22Bs are used in one device, the error terminals may also be paralleled.

ATTENTION: Only the SKHI 22A / 21A is equipped with an internal pull-up resistor of 10 kΩ versus V_S. The SKHI 22B does not contain an internal pull-up resistor.

The error memory may only be reset, if no error is pending and both cycle signal inputs are set to low for > 9 µs at the same time.

Pulse transformer set

The transformer set consists of two pulse transformers one is used bidirectional for turn-on and turn-off signals of the IGBT and the error feedback between primary and secondary side, the other one for the DC/DC-converter. The DC/DC-converter serves as potential-separation and power supply for the two secondary sides of the driver. The isolation voltage for the "H4"-type is 4000 V_{AC} and 2500 V_{AC} for all other types.

The secondary side consists of two symmetrical driver switches integrating the following components:

Supply voltage

The voltage supply consists of a rectifier, a capacitor, a voltage controller for - 7 V and + 15 V and a + 10 V reference voltage.

Gate driver

The output transistors of the power drivers are MOSFETs. The sources of the MOSFETs are separately connected to external terminals in order to provide setting of the turn-on and turn-off speed by the external resistors R_{ON} and R_{OFF}. Do not connect the terminals S7 with S8 and S13 with S14, respectively. The IGBT is turned on by the driver at + 15 V by R_{ON} and turned off at - 7 V by R_{OFF}. R_{ON} and R_{OFF} may not chosen below 3 Ω. In order to ensure locking of the IGBT even when the driver supply voltage is turned off, a 22 kΩ-resistor versus the emitter output (E) has been integrated at output G_{OFF}.

V_{CE}-monitoring

The V_{CE}-monitoring controls the collector-emitter voltage V_{CE} of the IGBT during its on-state. V_{CE} is internally limited to 10 V. If the reference voltage V_{CEref} is exceeded, the IGBT will be switched off and an error is indicated. The reference voltage V_{CEref} may dynamically be adapted to the IGBTs switching behaviour. Immediately after turn-on of the IGBT, a higher value is effective than in the steady state. This value will, however, be reset, when the IGBT is turned off. V_{CEstat} is the steady-state value of V_{CEref} and is adjusted to the required maximum value for each IGBT by an external resistor R_{CE} to be connected between the terminals C_{CE} (S6/S15) and E (S9/S12). It may not exceed 10 V. The time constant for the delay of V_{CEref} may be increased by an external capacitor C_{CE}, which is connected in parallel to R_{CE}. It controls the time tmin which passes after turn-on of the IGBT before the V_{CE}-monitoring is activated. This makes possible any adaptation to the switching behavior of any of the IGBTs. After t_{min} has passed, the V_{CE}-monitoring will be triggered as soon as $V_{CE} > V_{CEref}$ and will turn off the IGBT.

External components and possible adjustments of the hybrid driver

Fig. 1 shows the required external components for adjustment and adaptation to the power module.

VCE - monitoring adjustment

The external components R_{CE} and C_{CE} are applied for adjusting the steady-state threshold and the short-circuit monitoring dynamic. R_{CE} and C_{CE} are connected in parallel to the terminals C_{CE} (S15/ S6) and E (S12/ S9).

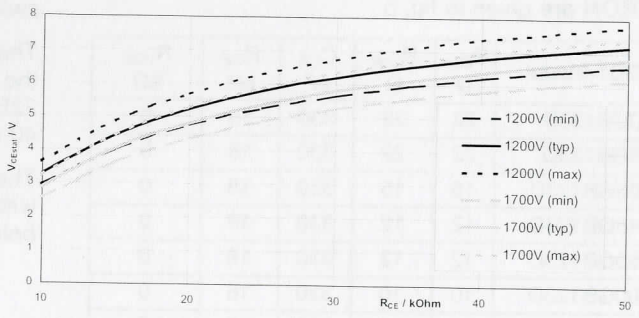


Fig. 4 V_{CEstat} in dependence of R_{CE} (T_{amb} = 25°C)

Dimensioning of R_{CE} and C_{CE} can be done in three steps:

1. Calculate the maximum forward voltage from the datasheet of the used IGBT and determine V_{CEstat}
2. Calculate approximate value of R_{CE} according to equation (1) or (1.1) from V_{CEstat} or determine R_{CE} by using fig.4.
3. Determine t_{min} and calculate C_{CE} according to equations (2) and (3).

Typical values are

for 1200 V IGBT: V_{CEstat} = 5 V; t_{min} = 1,45 µs,
R_{CE} = 18 kΩ, C_{CE} = 330 pF

for 1700 V IGBT: V_{CEstat} = 6 V; t_{min} = 3 µs,
R_{CE} = 36 kΩ, C_{CE} = 470 pF

Adaptation to 1700 V IGBT

When using 1700 V IGBTs it is necessary to connect a 1 kΩ / 0,4 W adaptation resistor between the V_{CE}-terminal (S20/ S1) and the respective collector.

Adaptation to error signal level

An open collector transistor is used as error terminal, which, in case of error, leads the signal to earth. The signal has to be adapted to the evaluation circuit's voltage level by means of an externally connected pull-up resistor. The maximum load applied to the transistor shall be 30 V / 15 mA.

As for the SKHI 22A / 21A a 10 kΩ pull-up resistor versus V_S (P13) has already been integrated in the driver.

IGBT switching speed adjustment

The IGBT switching speed may be adjusted by the resistors R_{ON} and R_{OFF}. By increasing R_{ON} the turn-on speed will decrease. The reverse peak current of the free-wheeling diode will diminish. SEMIKRON recommends to adjust R_{ON} to a level that will keep the turn-on delay time $t_{d(on)}$ of the IGBT < 1 µs.

By increasing R_{OFF} the turn-off speed of the IGBT will decrease. The inductive peak overvoltage during turn-off will diminish.

The minimum gate resistor value for R_{OFF} and R_{ON} is 3 Ω. Typical values for R_{ON} and R_{OFF} recommended by SEMIKRON are given in fig. 5

SK-IGBT-Modul	R_{Gon} Ω	R_{Goff} Ω	C_{CE} pF	R_{CE} kΩ	R_{VCE} kΩ
SKM 50GB123D	22	22	330	18	0
SKM 75GB123D	22	22	330	18	0
SKM 100GB123D	15	15	330	18	0
SKM 145GB123D	12	12	330	18	0
SKM 150GB123D	12	12	330	18	0
SKM 200GB123D	10	10	330	18	0
SKM 300GB123D	8,2	8,2	330	18	0
SKM 400GA123D	6,8	6,8	330	18	0
SKM 75GB173D	15	15	470	36	1
SKM 100GB173D	12	12	470	36	1
SKM 150GB173D	10	10	470	36	1
SKM 200GB173D	8,2	8,2	470	36	1

Fig. 5 Typical values for external components

Interlocking time adjustment

Fig. 3 shows the possible interlocking times between output1 and output2. Interlocking times are adjusted by connecting the terminals TDT1 (P5), TDT2 (P9) and SELECT (P6) either to earth/ GND (P7 and P14) according to the required function or by leaving them open.

A typical interlocking time value is 3,25 µs (P9 = GND; P5 and P6 open). For SKHI 22A / 21A the terminals TDT1 (P5) and SELECT (P6) are not existing. The interlocking time has been fixed to 3,25 µs and may only be increased to 4,25 µs by connecting TDT2 (P9) to V_S (P13).

ATTENTION: If the terminals TDT1 (P5), TDT2 (P9) and SELECT (P6) are not connected, eventually connected track on PC-board may not be longer than 20 mm in order to avoid interferences.

SEMIKRON recommends to start-up operation using the values recommended by SEMIKRON and to optimize the values gradually according to the IGBT switching behaviour and overvoltage peaks within the specific circuitry.

Driver performance and application limits

The drivers are designed for application with halfbridges and single modules with a maximum gate charge Q_{GE} < 4 µC (see fig. 6).

The charge necessary to switch the IGBT is mainly depending on the IGBT's chip size, the DC-link voltage and the gate voltage.

This correlation is also shown in the corresponding module datasheet curves.

It should, however, be considered that the SKHI 22B is turned on at + 15 V and turned off at - 7 V. Therefore, the gate voltage will change by 22 V during every switching procedure.

Unfortunately, most datasheets do not indicate negative gate voltages. In order to determine the required charge, the upper leg of the charge curve may be prolonged to + 22 V for determination of approximate charge per switch.

The medium output current of the driver is determined by the switching frequency and the gate charge. For the SKHI 22B the maximum medium output current is $Iout_{AVmax}$ < ± 40 mA.

The maximum switching frequency f_{MAX} may be calculated with the following formula, the maximum value however being 50 kHz due to switching reasons:

$$f_{MAX}(kHz) = \frac{4 \cdot 10^4}{Q_{GE}(nC)}$$

Fig. 6 shows the maximum rating for the output charge per pulse for different gate resistors.

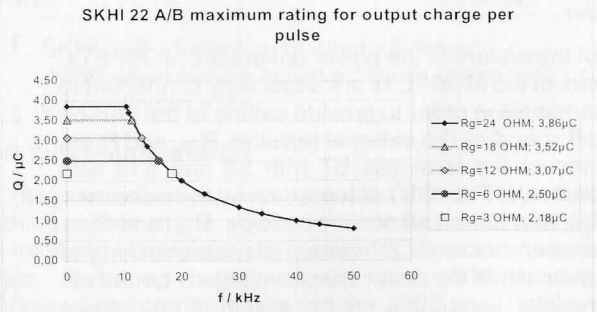


Fig. 6 Maximum rating for output charge per pulse

Further application notes

The CMOS-inputs of the hybrid driver are extremely sensitive to over-voltage. Voltages higher than V_S + 0,3 V or below – 0,3 V may destroy these inputs. Therefore, control signal over-voltages exceeding the above values have to be avoided.

Please provide for static discharge protection during handling. As long as the hybrid driver is not completely assembled, the input terminals have to be short-circuited.

Persons working with CMOS-devices have to wear a grounded bracelet. Any synthetic floor coverings must not be statically chargeable. Even during transportation the input terminals have to be short-circuited using, for example, conductive rubber. Worktables have to be grounded. The same safety requirements apply to MOSFET- and IGBT-modules!

The connecting leads between hybrid driver and the power module should be as short as possible, the driver leads should be twisted.

Any parasitic inductances within the DC-link have to be minimized. Over-voltages may be absorbed by C- or RCD-snubbers between the main terminals for PLUS and MINUS of the power module.

When first operating a newly developed circuit, SEMIKRON recommends to apply low collector voltage and load current in the beginning and to increase these values gradually, observing the turn-off behaviour of the free-wheeling diode and the turn-off voltage spikes generated accross the IGBT. An oscillographic control will be necessary. In addition to that the case temperature of the module has to be monitored. When the circuit works correctly under rated operation conditions, short-circuit testing may be done, starting again with low collector voltage.

It is important to feed any errors back to the control circuit and to switch off the device immediately in such events. Repeated turn-on of the IGBT into a short circuit with a high frequency may destroy the device.

Mechanical fixing on PCB:

In applications with mechanical vibrations (vehicles)[2] do not use a ty-rap for fixing the driver, but - after soldering and testing - apply special glue. Recommended types: CIBA GEIGY XP 5090 + 5091; PACTAN 5011; WACKER A33 (ivory) or N199 (transparent), applied around the case edge (forms a concave mould). The housing may not be pressed on the PCB; do not twist the PCB with the driver soldered on, otherwise the internal ceramics may crack. The driver is not suitable for big PCBs.

Proven, within the scope of the product qualification, was the use of the driver with the printed circuit board SKPC 2006 (L x B x H = 97,0 x 67,5 x 1,5 mm). During the test, the driver was stuck with glue on the printed circuit board. Based on this information the technical conclusion arises, that in an application with big printed circuit boards, this board must be supported and reinforced in the area of the driver.

If a PCB is directly plugged to IGBT modules, the PCB has to be fixed to the heat sink by thread bolts.

The temperature of the solder must not exceed 265℃, and solder time must not exceed 4 seconds. The ambient temperature must not exceed the specified maximum storage temperature of the driver.
The driver is not suited for hot air reflow or infrared reflow soldering processes.

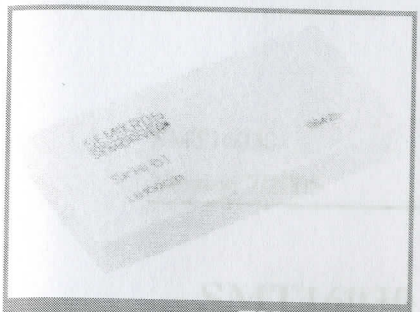
All electrical and mechanical parameters should be validated by user´s technical experts for each application.

For further details please contact SEMIKRON.

2.tested acceleration (x; y; z-axis): 20-100 Hz: 1,5 g; shock: 5 g

This technical information specifies devices but promises no characteristics. No warranty or guarantee expressed or implied is made regarding delivery, performance or suitability.

Appendices E: SKHI61 data sheet



SEMIDRIVER™

Sixpack IGBT and MOSFET Driver

SKHI 61 (R)

Features

- CMOS-compatible input buffers at V_{DD}=5V
- Short-circuit protection by V_{CE}-monitoring and Soft-turn-Off
- Drive interlock top/bottom
- Signal transmission by opto-couplers
- Supply undervoltage protection (13V)
- Error latch / output

Typical Applications

- Driver for IGBT and MOSFET modules in three-phase-bridge circuits, inverter drives, UPS-facilities, etc.

1) At T_a < -25°C the current consumption can be 1,6 times the rated maximum current for the first three operating minutes.

Absolute Maximum Ratings

Symbol	Conditions	Values	Units
V_S	Supply voltage primary	15,6	V
V_{iH}	Input signal voltage	V_S + 0,3	V
$Iout_{PEAK}$	Output peak current	2	A
$Iout_{AVmax}$	Output average current (T_a = 85 °C)	20	mA
f_{max}	Max. switching frequency (C_{GE} < 9nF)	50	kHz
V_{CE}	Collector emitter voltage sense across the IGBT (for 1200V-IGBTs)	900	V
dv/dt	Rate of rise and fall of voltage (secondary to primary side)	15	kV/µs
V_{isolIO}	Isolation test voltage input - output (2 sec. AC)	2500	V
V_{isol12}	Isolation test voltage output 1 - output 2 (2 sec. AC)	1500	V
R_{Gonmin}	Minimum rating of R_{Gon}	10	Ω
$R_{Goffmin}$	Minimum rating for R_{Goff}	10	Ω
$Q_{out/pulse}$	Max. rating for gate T_a = 85 °C	0,7	µC
	charge per pulse T_a = 55 °C	1	µC
T_{op}	Operating temperature	- 40 ... + 85	°C
T_{stg}	Storage temperature	- 40 ... + 85	°C

Characteristics T_a = 25°C, unless otherwise specified

Symbol	Conditions	min.	typ.	max.	Units
V_S	Supply voltage primary	14,4	15,0	15,6	V
I_{SO} 1)	Supply current no load	160		200	mA
	primary side normal op.			450	mA
V_{iT+}	Input threshold voltage (High)	4,0			V
V_{iT-}	Input threshold voltage (LOW)			1,5	V
R_{in}	Input resistance		60		kΩ
$V_{G(on)}$	Turn on gate voltage output		14,9		V
$V_{G(off)}$	Turn off gate voltage output		-6,5		V
R_{GE}	Internal gate-emitter resistance		20		kΩ
f_{ASIC}	ASIC system switching frequency		8		MHz
$td(on)_{IO}$	Input-output turn-on propagation time	0,3	0,45	0,6	µs
$td(off)_{IO}$	Input-output turn-off propagation time	0,3	0,45	0,6	µs
$t_{d(err)}$	Error input-output propagation time	1,15	1,3	1,5	µs
$t_{pERRRESET}$	Error memory reset time	7	15	27	µs
t_{TD}	Interlock dead time adjustable	no interlock		4,1	µs
V_{CEstat}	Reference voltage for V_{CE}-monitoring		5,8		V
t_{blank}	Blanking time		3,5		µs
C_{ps}	Coupling capacitance primary-secondary		40		pF
MTBF	Mean Time Between Failure T_a = 40°C		1		10^6 h
w	weight		95		g
H x B x T	Dimensions		20x57x114		mm

This technical information specifies semiconductor devices but promises no characteristics. No warranty or guarantee expressed or implied is made regarding delivery, performance or suitability.

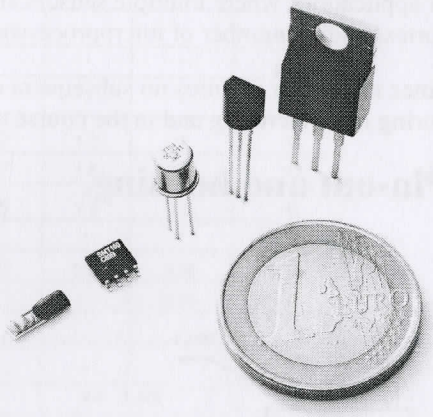
© by SEMIKRON

Appendices F: SMT16030 digital temperature sensor

SMT16030 DIGITAL TEMPERATURE SENSOR

Features

Absolute accuracy ± 0.7 °C
Linear output within 0.2 °C
Resolution better then 0.005 °C
Duty Cycle output
Calibrated on chip
TTL, CMOS compatible
Temperature range 175 °C (-45 to +130 °C)
Directly connectable to data input of microprocessor
Easy multiplexing of multiple sensors



Typical applications

Heater systems
Measuring instruments
Washing machines
Overheating protection
Appliances

Introduction

The Smartec temperature sensor is a sophisticated full silicon temperature sensor with a digital output. The one wire output (duty-cycle modulated) can be directly connected to all kinds of micro-controllers without the need of A/D conversion. The temperature range is –45 °C to 150 °C. The high resolution (< 0.005 °C) makes the sensor useful for high precision applications. The sensor is available in various housings like T018, T092, T0220 and for high volume production in SOIC. Special housing can be manufactured on request.

Product highlights

The SMART TEMPERATURE SENSOR features a duty-cycle modulated square wave output voltage with linear response to temperatures in the -45 °C to +130 °C range. The absolute accuracy is better than 1.2 °C. In the range from -30 to +100 °C absolute accuracy is better than 0.7 °C, while the linearity is better than 0.2 °C (Model TO18).

SMARTEC B.V, Delpratsingel 26
4811 AP Breda, The Netherlands

WWW.SMARTEC.NL
Tel: +31(0)765205353

The SMART TEMPERATURE SENSOR is calibrated during test and burn-in of the chip. The integrated modulator ensures the sensor unit can communicate effectively with low-cost microcontrollers without the need of (onboard) A/D converters or an Xtal controlled oscillator.

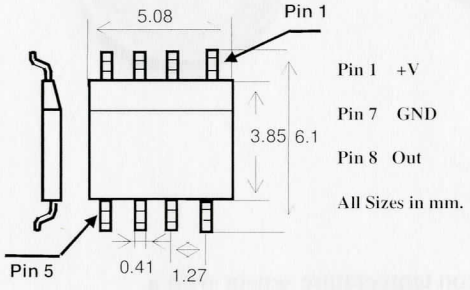
The SMART TEMPERATURE SENSOR combines digital output and on-chip calibration to ensure major cost reductions and performance-related advantages.

In applications where multiple sensors are used, easy multiplexing can be obtained by using a corresponding number of microprocessor inputs or by using low cost digital multiplexers.

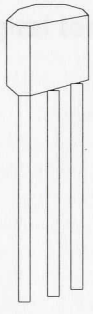
Since the sensor requires no subsequent calibration, optimal cost savings are recorded both during manufacturing and in the course of after-sales servicing.

Pin-out and housing.

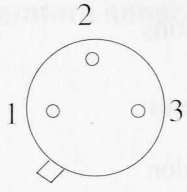
SOIC-8



TO92



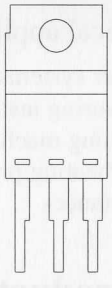
TO18



bottom view

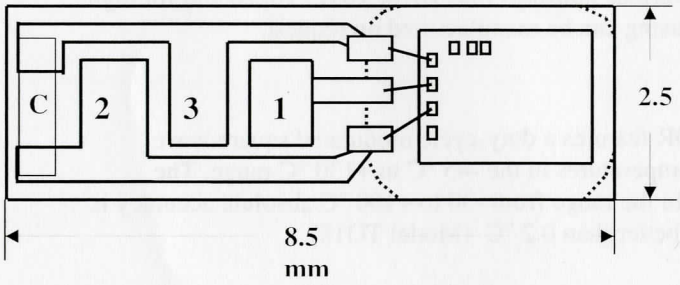
1 Output
2 + Vcc
3 GND

TO220



metal backplate = GND

HEC housing



C = 100 nF
(between Vcc and GND)

Pin 1 Output
Pin 2 + Vcc
Pin 3 GND

SMARTEC B.V, Delpratsingel 26
4811 AP Breda, The Netherlands

WWW.SMARTEC.NL
Tel: +31(0)765205353

Specifications

Parameters	TO18 min	TO18 typ	TO18 max	TO92 max [1]	TO220 Max	HEC max	SOIC-8 max	Units
Supply voltage[2]	4.75	5	7.2	*	*	*	*	V.
Supply current	160		200	*	*	*	*	µA.
temperature range[3]	-45	-	130	*	*	*	*	°C
Total accuracy[4]	-30 + 100 °C		0.7	1.2	1.7	1.5	1	°C
	-45 + 130 °C		1.2	2	1.7	1.5	1.5	°C
Non linearity[5]			0.2	0.4	0.5	1.0	1.0	°C
Supply voltage sensitivity			0.1	*	*	*	*	°C/V
Repeatability			0.1	0.2	0.2	0.2	0.05	°C
Long term Drift			0.05	-	-	-	0.05	°C
Operating temperature	-45		130	*	*	*	*	°C
Storage temperature	-50		150	*	*	*	*	°C

Output

- duty cycle	=0.320+0.00470*t (t=temperature in C)							
- frequency	1	-	4	*	*	*	*	Khz
- noise			0.005	*	*	*	*	°C
- impedance			200	*	*	*	*	Ohm
- short circuit	infinite maximum current applied 40 mA							

1 * All not mentioned specifications are the same as for TO18
2 Case connected to ground
3 The SMT 30-160-18 can be used from -65 to +160 °C for a short period without physical damage to the device. The specified accuracy applies only to the rated performance temperature range.
4 Total accuracy includes all errors.
5 Applicable from -30 to +100 °C

SMARTEC B.V, Delpratsingel 26
4811 AP Breda, The Netherlands
WWW.SMARTEC.NL
Tel: +31(0)765205353

Product description

The SMT160-30 is a three terminal integrated temperature sensor, with a duty-cycle output. Two terminals are used for the power supply of 5 Volts and the third terminal carries the output signal. A duty cycle modulated output is used because this output is interpretable by a micro-processor without A-D converter, while the analogue information is still available. The SMT160-30 (TO18 model) has an overall accuracy of 0.7 °C in the range from -30 C to +100 °C and an accuracy of 1.2 °C from -45 to +130 °C. This makes the sensor especially useful in all applications where "human" (climate control, food processing etc.) conditions are to be controlled. Due to its very high resolution (< 0.005K) this sensor is especially suited for applications where very accurate measurements are needed.

The CMOS output of the sensor can handle cable length up to 20 meters. This makes the SMT160-30 very useful in remote sensing and control applications.

Understanding the specifications.

It is important to understand the meaning of the various specifications and their effects on accuracy. The SMT160-30 is basically a bipolar temperature sensor, with accurate electronics to convert the sensor signal into a duty cycle. During production the devices are calibrated.

The output signal

The output is a square wave with a well-defined temperature-dependent duty cycle. The duty cycle of the output signal is linearly related to the temperature according to the equation:

$$D.C. = 0.320+0.00470*t$$

D.C. = duty cycle
t = Temperature in °C

A simple calculation shows that - for instance- at 0 °C:

D.C.= 0.320 or 32.0 % and at 130 °C

D.C.= 0.931 or 93.1 %

In the output frequency of the sensor there is no temperature information, only the duty cycle contains temperature information in accordance to the formula given above. The output signal may show low frequency jitter or drift. Therefore most oscilloscopes and counters are not suited for verifying the accuracy of these sensors. The temperature information contained in the duty-cycle value, however, is guaranteed to be accurate within the values specified for each model (housing).

SMARTEC B.V, Delpratsingel 26
4811 AP Breda, The Netherlands

WWW.SMARTEC.NL
Tel: +31(0)765205353

Total accuracy

The mentioned equation is the nominal one. The maximum deviation from the nominal equation is defined as total accuracy. With temperatures above 100 °C the accuracy decreases.

Non linearity

Non-linearity as it applies to the SMT160-30 is the deviation from the best-fit straight line over the whole temperature range. For the temperature range of -30 °C to +100 °C the non-linearity is less than 0.2 °C (TO18).

Long-term drift

This drift strongly depends on the operating condition. At room temperature the drift is very low (< 0.05 °C). However at higher temperatures the drift will be worse, mainly because of changes in mechanical stress. This drift is partly irreversible and causes non-ideal repeatability and long-term effects. At temperatures above 100 °C (but in the operating range) a long-term drift better than 0.1 °C is to be expected.

Noise

The resolution is better than 0.005 °C. The standard deviation of the noise level (measured over a 20 ms. period) is below this 0.005 °C.

Time constants

The time constant of the sensor is measured under different circumstances.

To compare this with other types of sensors the same kind of measurements were done. The time constant is defined as the time required to reach 63% of an instantaneous temperature change.

The figures mentioned below are difficult to measure; an accuracy of around 5 % is a reasonable estimation. These figures only apply to the sensor built in a TO-18 housing and not the TO-92, the TO220 nor the naked chip. The values found only depend on the physical parameters of the measurement setup.

SMARTEC B.V, Delpratsingel 26
4811 AP Breda, The Netherlands
WWW.SMARTEC.NL
Tel: +31(0)765205353

condition	timeconstant (s) (TO18)
mounted in an alu block of a certain temperature (mean value of different measurements)	0.6
in a bath filled with oil that was stirred (mean value of different measurements)	1.4
Moving air with a speed of about 3 m/s	
- without heatsink	13.5
- with heatsink	5
Non moving air	
-without heatsink	60
-with heatsink	100

Overview of time constants in different conditions

General operation

A simple way of measuring a duty cycle is to use a microcontroller. The sensor output can be directly connected to a microcontroller input. The microcontroller can determine the duty-cycle value by sampling the sensor output. If the microcontroller is not fast enough to determine the temperature accurately enough within one sensor output cycle, the sampling can be extended over multiple periods. This method has the advantage to filter out noise. From the theory of signal processing it can be derived that there is a fixed ratio between the sensors signal frequency, the sampling rate and the sampling noise. This sampling noise limits the accuracy and amounts to:

$$T_{error} = 200 * t_s / sqrt(6 * t_m * t_p)$$

T_{error} = measurement error (= standard deviation of the sampling noise)
t_s = microcontrollers sampling rate
t_m = total measurement time
t_p = output signal periodicity of the sensor

Microcontrollers can sample at a high frequency so with a simple program it is possible to measure the sensor's duty cycle within 50 ms and a resolution of .01 °C.

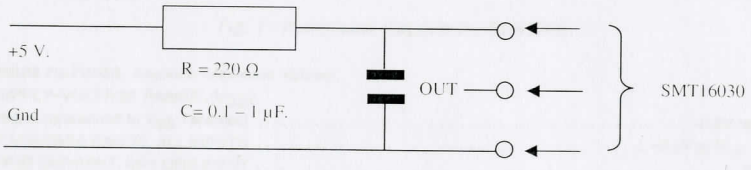
SMARTEC B.V, Delpratsingel 26
4811 AP Breda, The Netherlands
WWW.SMARTEC.NL
Tel: +31(0)765205353

NOTE:

The above mentioned error is NOT related to the intrinsic accuracy of the sensor. It just tells us what happens to the accuracy (standard deviation) of the measurement of a digital signal, when that signal is being sampled by a microcontroller.

About noise protection and how to prevent damage caused by a wrong power supply polarity.

The Smartec SMT16030 is based on a free running oscillator. Periodic spikes on the power supply line may make the oscillator synchronise, resulting in a false temperature reading. To overcome this problem it is advised to put a filter in the power supply line of the sensor. It is suggested to use a low pass RC filter as given below. An additional advantage also is the power supply polarity protection of the sensor. The resistor of 220 Ohm limits the current through the sensor to about 25 mA. At this current the sensor will survive a possible wrong power supply polarity. The software can detect the presence of the output signal and therefore a proper connection of the sensor. See below for a suggested diagram.



Power line noise filtering and polarity damage protection

For more information about how to measure duty cycles by means of a microcontroller, please refer to our application notes, available for download at our website WWW.SMARTEC.NL.

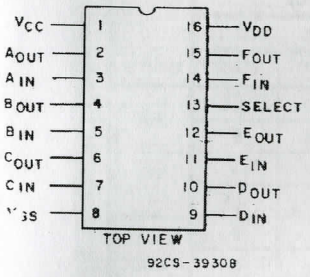
SMARTEC B.V, Delpratsingel 26
4811 AP Breda, The Netherlands

WWW.SMARTEC.NL
Tel: +31(0)765205353

Appendices G: CD4504B Cmos hex level shifter

TEXAS INSTRUMENTS
Data sheet acquired from Harris Semiconductor
SCHS069D – Revised November 2004

CD4504B Types



TERMINAL ASSIGNMENT

CMOS Hex Voltage-Level Shifter for TTL-to-CMOS or CMOS-to-CMOS Operation

High-Voltage Types (20-Volt Rating)

Features:

- *Independence of power-supply sequence considerations–V_{CC} can exceed V_{DD}; input signals can exceed both V_{CC} and V_{DD}*
- *Up and down level-shifting capability*
- *Shiftable input threshold for either CMOS or TTL compatibility*
- *Standardized symmetrical output characteristics*
- *100% tested for quiescent current @ 20 V*
- *Maximum input current of 1 μA at 18 V over full package-temperature range; 100 nA at 18 V and 25° C*
- *5 V, 10 V, and 15 V parametric ratings*
- *Meets all requirements of JEDEC Standard No. 13B, "Standard Specifications for Description of 'B' Series CMOS Devices"*

■ CD4504B hex voltage level-shifter consists of six circuits which shift input signals from the V_{CC} logic level to the V_{DD} logic level. To shift TTL signals to CMOS logic levels, the SELECT input is at the V_{CC} HIGH logic state. When the SELECT input is at a LOW logic state, each circuit translates signals from one CMOS level to another.

The CD4504B types are supplied in 16-lead hermetic dual-in-line ceramic packages (F3A suffix), 16-lead dual-in-line plastic packages (E suffix), 16-lead small-outline packages (M, M96, and MT suffixes), and 16-lead thin shrink small-outline packages (PW and PWR suffixes).

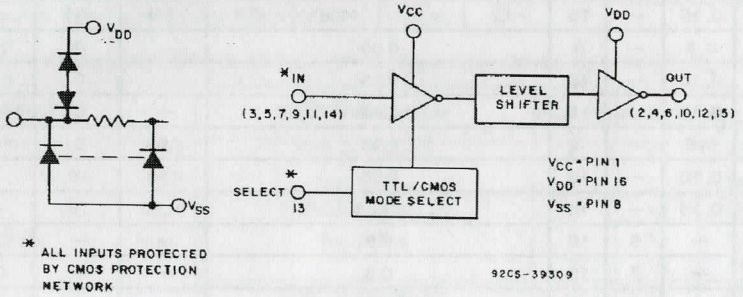


Fig. 1 - Functional diagram for CD4504B.

MAXIMUM RATINGS, *Absolute-Maximum Values:*

DC SUPPLY-VOLTAGE RANGE, (V_{DD})
Voltages referenced to V_{SS} Terminal) ..... -0.5V to +20V
INPUT VOLTAGE RANGE, ALL INPUTS ..... -0.5V to V_{CC} +0.5V
DC INPUT CURRENT, ANY ONE INPUT ..... ±10mA
POWER DISSIPATION PER PACKAGE (P_D):
For T_A = -55°C to +100°C 500mW
For T_A = +100°C to +125°C ..... Derate Linearity at 12mW/°C to 200mW
DEVICE DISSIPATION PER OUTPUT TRANSISTOR
FOR T_A = FULL PACKAGE-TEMPERATURE RANGE (All Package Types) 100mW
OPERATING-TEMPERATURE RANGE (T_A) ..... -55°C to +125°C
STORAGE TEMPERATURE RANGE (T_{stg}) ..... -65°C to +150°C
LEAD TEMPERATURE (DURING SOLDERING):
At distance 1/16 ± 1/32 inch (1.59 ± 0.79mm) from case for 10s max ..... +265°C

Copyright © 2004, Texas Instruments Incorporated

V_{GEN}

STATIC ELECTRICAL CHARACTERISTICS

CHARACTERISTIC		CONDITIONS V_O (V)	V_{IN} (V)	V_{CC} (V)	V_{DD} (V)	LIMITS AT INDICATED TEMPERATURES (°C) -55	-40	+85	+125	+25 MIN	+25 TYP	+25 MAX	UNITS
Quiescent Device Current, I_{DD} Max and I_{CC} in CMOS-CMOS Mode		—	0, 5	5	5	1.5	1.5	1.5	1.5	—	0.02	1.5	mA
		—	0, 10	5	10	2	2	2	2	—	0.02	2	
		—	0, 15	5	15	4	4	120	120	—	0.02	4	μA
		—	0, 20	5	20	20	20	600	600	—	0.04	20	
Quiescent Device Current, I_{CC} Max TTL-CMOS Mode		—	0, 5	5	5	5	5	6	6	—	2.5	5	mA
		—	0, 10	5	10	5	5	6	6	—	2.5	5	
		—	0, 15	5	15	5	5	6	6	—	2.5	5	
Output Low (Sink) Current, I_{OL} Min		0.4	0.5	—	5	0.64	0.61	0.42	0.36	0.51	1	—	mA
		0.5	0, 10	—	10	1.6	1.5	1.1	0.9	1.3	2.6	—	
		1.5	0, 15	—	15	4.2	4	2.8	2.4	3.4	6.8	—	
Output High (Source) Current, I_{OH} Min		4.6	0, 5	—	5	-0.64	-0.61	-0.42	-0.36	-0.51	-1	—	
		2.5	0, 5	—	5	-2	-1.8	-1.3	-1.15	-1.6	-3.2	—	
		9.5	0, 10	—	10	-1.6	-1.5	-1.1	-0.9	-1.3	-2.6	—	
		13.5	0, 15	—	15	-4.2	-4	-2.8	-2.4	-3.4	-6.8	—	
Output Voltage: Low-Level, V_{OL} Max		—	0, 5	—	5	0.05				—	0	0.05	V
		—	0, 10	—	10	0.05				—	0	0.05	
		—	0, 15	—	15	0.05				—	0	0.05	
Output Voltage: High-Level, V_{OH} Min		—	0, 5	—	5	4.95				4.95	5	—	
		—	0, 10	—	10	9.95				9.95	10	—	
		—	0, 15	—	15	14.95				14.95	15	—	
Input Low Voltage, V_{IL} Max Note 1	TTL-CMOS	1	—	5	10	0.8				—	—	0.8	
	TTL-CMOS	1	—	5	15	0.8				—	—	0.8	
	CMOS-CMOS	1	—	5	10	1.5				—	—	1.5	
	CMOS-CMOS	1.5	—	5	15	1.5				—	—	1.5	
	CMOS-CMOS	1.5	—	10	15	3				—	—	3	
Input High Voltage, V_{IH} Min Note 1	TTL-CMOS	9	—	5	10	2				2	—	—	
	TTL-CMOS	13.5	—	5	15	2				2	—	—	
	CMOS-CMOS	9	—	5	10	3.5				3.5	—	—	
	CMOS-CMOS	13.5	—	5	15	3.5				3.5	—	—	
	CMOS-CMOS	13.5	—	10	15	7				7	—	—	
Input Current, I_{IN} Max		—	0, 18	—	18	±0.1	±0.1	±1	±1	—	$\pm 10^{-5}$	±0.1	μA

Note 1: Applies to the 6 input signals. For mode control (P13), only the CMOS-CMOS ratings apply.

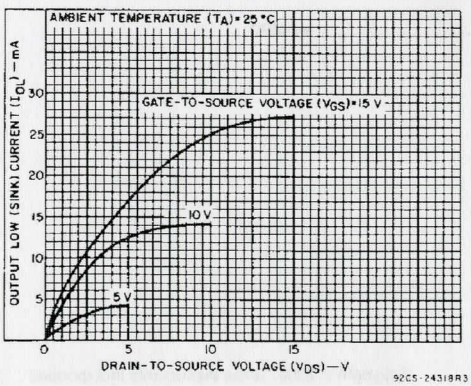


Fig. 2 - Typical output low (sink) current characteristics.

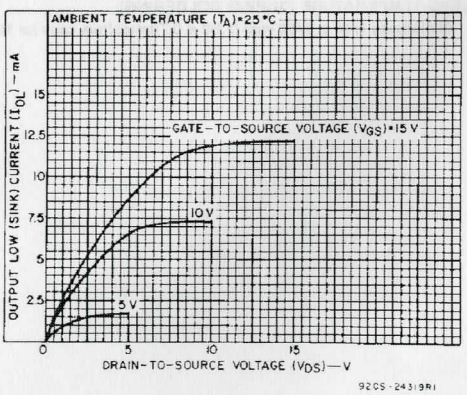


Fig. 3 - Minimum output low (sink) current characteristics.

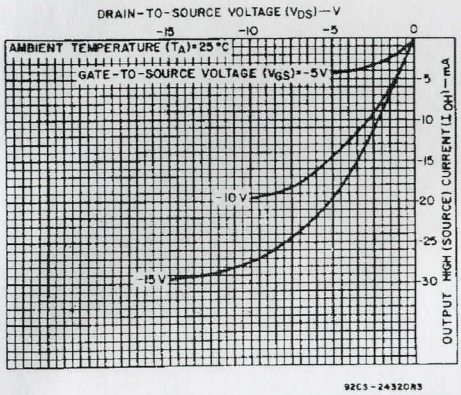


Fig. 4 - Typical output high (source) current characteristics.

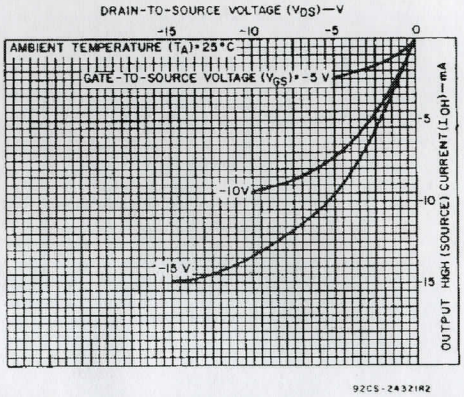


Fig. 5 - Minimum output high (source) current characteristics.

RECOMMENDED OPERATING CONDITIONS

For maximum reliability, nominal operating conditions should be selected so that operation is always within the following ranges:

CHARACTERISTIC	V_{DD} (V)	LIMITS		UNITS
		Min.	Max.	
Supply-Voltage Range (For T_A = Full Package-Temperature Range)	—	5	18	V

DYNAMIC ELECTRICAL CHARACTERISTICS, At T_A = 25°C; Input t_r,t_f = 20 ns, C_L = 50 pF, R_L = 200 Ω

CHARACTERISTIC		SHIFTING MODE	VCC (V)	VDD (V)	LIMITS TYP.	LIMITS MAX.	UNITS
Propagation Delay: High-to Low,	t_{PHL}	TTL to CMOS $V_{DD} > V_{CC}$	5	10	140	280	ns
			5	15	140	280	
		CMOS to CMOS $V_{DD} > V_{CC}$	5	10	120	240	
			5	15	120	240	
			10	15	70	140	
		CMOS to CMOS $V_{CC} > V_{DD}$	10	5	275	550	
			15	5	275	550	
			15	10	70	140	
Low-to-High,	t_{PLH}	TTL to CMOS $V_{DD} > V_{CC}$	5	10	140	280	
			5	15	140	280	
		CMOS to CMOS $V_{DD} > V_{CC}$	5	10	120	240	
			5	15	120	240	
			10	15	70	140	
		CMOS to CMOS $V_{CC} > V_{DD}$	10	5	200	400	
			15	5	200	400	
			15	10	60	120	
Transition Time,	t_{THL},t_{TLH}	All Modes		5	100	200	
				10	50	100	
				15	40	80	
Input Capacitance,	C_{IN}	Any Input			5	7.5	pF

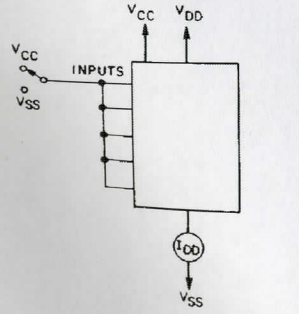


Fig. 6 - Quiescent device current.

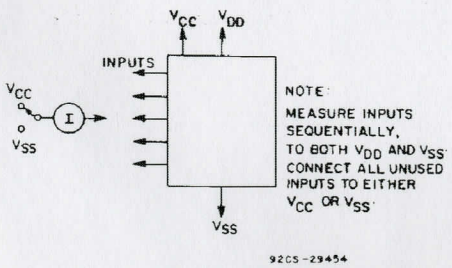


Fig. 7 - Input current.

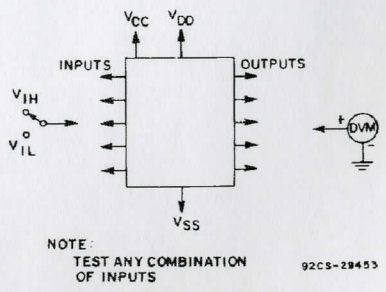


Fig. 8 - Input voltage.